NASA-CR-72883
WANL-TNR-228

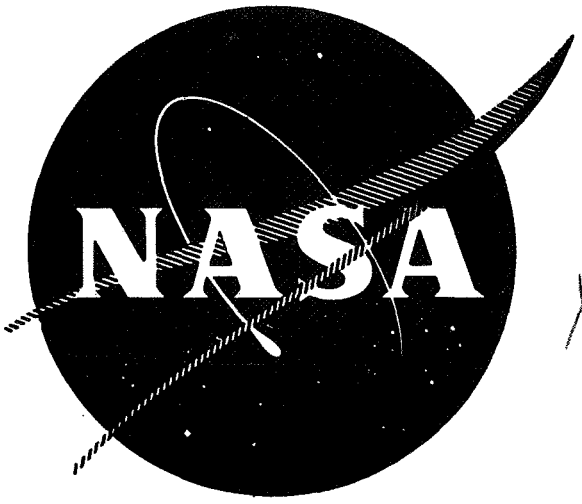

DEVELOPMENT OF DUCTILE HIGH STRENGTH CHROMIUM ALLOYS

by

A. M. Filippi

Westinghouse Astronuclear Laboratory

Prepared for

National Aeronautics and Space Administration

NASA- Lewis Research Center

Contract NAS 3-12427

William D. Klopp, Project Manager

Astronuclear Laboratory

NASA-CR-72883
WANL-TNR-228

FINAL REPORT

DEVELOPMENT OF DUCTILE HIGH-STRENGTH CHROMIUM ALLOYS

by

A. M. FILIPPI

WESTINGHOUSE ASTRONUCLEAR LABORATORY
P. O. Box 10864
Pittsburgh, Pennsylvania 15236

prepared for

NATIONAL AERONAUTICS AND SPACE ADMINISTRATION

November 26, 1970

Contract NAS 3-12427

NASA Lewis Research Center
Cleveland, Ohio
William D. Klopp, Project Manager

FOREWORD

The work described herein was performed at the Astronuclear Laboratory, Westinghouse Electric Corporation, under NASA Contract NAS 3-12427. Mr. W. D. Klopp, Refractory Metals Section, NASA-Lewis Research Center, functioned as Project Manager.

The author wishes to acknowledge four people for outstanding assistance on this program. They are: Mr. R. W. Conlin for x-ray diffraction and microprobe analysis, Mr. R. L. Berrier for melting, heat treating, and general project coordination, Mr. A. R. Keeton for design of the vacuum system and electrical controls associated with the induction melting equipment, and Dr. G. Komenetz for designing and building the induction melt coil and capacitor system to match the available 960 cycle motor generator power.

ABSTRACT

Chromium alloys strengthened solely by a group IV B or V B metal carbide or boride precipitate were examined to define phase stability up to ~2900°F (~1866°K)* and identify the most potent strengtheners. Carbides and borides of zirconium and hafnium were the least effective strengtheners, and those of tantalum most effective. Columbium and titanium compounds displayed a strengthening effect somewhat between these extremes. As fabricated alloys, reduced >90% from ingot to rod at ~2100°F (~1422°K), ranged in tensile strength at 2100°F from ~10 ksi (69 MN/m^2) for the compositions Cr-.5Hf-.5C (a/o) and Cr-.5Zr-.5C, to ~55 ksi (380 MN/m^2) for Cr-.5Cb-.5B and Cr-.5Ta-.5B. Ductile-brittle transformations of the alloys occurred from 100°F to 700°F (311 to 644°K) and were directly related to strength. Rupture life at 2100°F (1422°K) was typically <25 hours for alloys tested at 15 ksi (104 MN/m^2) in the as fabricated condition and <15 hours for tests at 12 ksi (83 MN/m^2) on recrystallized material. A major improvement in rupture strength at 2100°F (1422°K) was obtained by heat treating several alloys which displayed the following phase transformation behavior.

$$Cr + MC \xrightarrow[(\sim 1422^\circ K)]{\sim 2100^\circ F} Cr + MC + Cr_{23}C_6 \xrightarrow[(\sim 1755^\circ K)]{\sim 2700^\circ F} (Cr, M) + Cr_{23}C_6$$

$$Cr + MxBy \xrightarrow[(<1422^\circ K)]{<2100^\circ F} Cr + MxBy + Cr_4B \xrightarrow[(\sim 1755^\circ K)]{\sim 2700^\circ F} (Cr, M) + Cr_4B$$

Heat treatment consisted of first annealing above 2700°F (1755°K) followed by rapid cooling to form and retain the $Cr_{23}C_6$ or Cr_4B phases. Following this, alloys were aged a short time at 2100°F (1422°K) to begin the carbide or boride interchange reactions, $Cr_{23}C_6 \longrightarrow MC$ and $Cr_4B \longrightarrow MxBy$. In this condition, rupture strengths, on a 100 hour basis at 2100°F (1422°K), of 11.5, 13.0, 15.0, 16.5 and 23.0 ksi (79, 90, 104, 114 and 159 MN/m^2), respectively, were determined for the compositions Cr-.5Ti-.5C (a/o), Cr-.25Ta-.25C, Cr-.5Cb-.5B, Cr-.5Ta-.5C and Cr-.5Ta-.5B. Rupture strength of the latter three solely dispersion strengthened compositions are comparable to or exceed the highest values reported for chromium-base alloys.

*Both Common and the International System of Units (SI Units) are used throughout this report.

TABLE OF CONTENTS

LIST OF FIGURES

LIST OF FIGURES (continued)

LIST OF FIGURES (continued)

LIST OF TABLES

SUMMARY

Chromium alloys containing additions of a single group IV B or V B metal plus carbon or boron to form approximately 0.5 or 1 v/o carbide or boride dispersion were studied to establish temperature and composition dependence of phase stability and mechanical properties. The following phase transformation behavior was observed:

$$Cr + MC \xrightarrow{T_1} Cr + MC + Cr_{23}C_6 \xrightarrow{T_2} (Cr, M) + Cr_{23}C_6$$

$$Cr + MxBy \xrightarrow{T_1} Cr + MxBy + Cr_4B \xrightarrow{T_2} (Cr, M) + Cr_4B$$

$Cr + MB + MB_2$ stable to T_3

T_1	T_2	T_3	Compositions a/o
2300°F** (1533°K)	2700°F		Cr-.5(Ta, Ti or Cb)-.5C*, Cr-.25(Ta or Cb)-.25C*
>2900°F (>1866°K)			Cr-.5(Zr or Hf)-.5C*
<2100°F (<1422°K)	≤2500°F (≤1644°K)		Cr-1Ti-.5B
	<2100°F		Cr-.5Ti-.5B, Cr-.5Ti-.25B
<2100°F	2600°F		Cr-.5Cb-.5B*
<2100°F	2700°F		Cr-.5Ta-1B*
<2100°F	>2700°F		Cr-.5Ta-.5B*
2600°F (1700°K)	>2700°F		Cr-.5(Ta or Cb)-.25B
>2700°F (>1755°K)			Cr-1Cb-.5B
		>2700°F	Cr-.5Zr-.5B, Cr-.5Zr-.25B

*Examined to measure mechanical properties

**Temperature ± 100°F (± 56°K)

Compositions prepared for mechanical property investigation were induction melted as 10 pound heats (4.5 kg), cast into 2.5 inch diameter ingots (6.35 cm), then extruded and swaged to 3/8 inch (.95 cm) test rod at 2100 to 2200°F (1422 to 1477°K). Alloys containing tantalum consistently displayed the best combination of tensile and creep strength. Those alloyed with zirconium and hafnium were poorest in this respect, while alloys containing titanium or columbium displayed a behavior somewhat between the extremes. Ductile-to-brittle transformation temperatures of the as-fabricated alloys varied from approximately 100°F to 700°F (311 to 664°K) and were directly related to strength. Highest tensile strengths at 2100°F (1422°K) were measured on the as-fabricated alloys and ranged from a low of ~10 ksi (~69 MN/m^2) for the Cr-.5(Hf or Zr)-.5C compositions, to ~55 ksi (~380 MN/m^2) for the Cr-.5(Ta or Cb)-.5B compositions. All alloys displayed poor rupture properties at 2100°F (1422°K) when tested in the as-fabricated or simple 1 hour at 2400°F (1589°K) recrystallized conditions. Rupture typically occurred in 25 hours or less at 15 ksi (104 MN/m^2) for as fabricated material and 15 hours or less at 12 ksi (83 MN/m^2) after recrystallization. A dramatic improvement in rupture properties, however, was observed for several alloys heat treated to form $Cr_{23}C_6$ or Cr_4B, then aged for 3 hours at 2100°F (1422°K) prior to testing. Partial solutioning of the $Cr_{23}C_6$ (or Cr_4B) phase and precipitation of the stable group IV B or V B metal carbide (or boride) is brought about by the short aging period prior to testing at 2100°F (1422°K). This carbide (or boride) interchange reaction, which proceeds during rupture testing at 2100°F (1422°K), was found to be a potent strengthener. In this heat treated condition, rupture strengths, on a 100 hour basis at 2100°F (1422°K), of 11.5, 13.0, 15.0, 16.5 and 23.0 ksi (79, 90, 104, 114, 149 MN/m^2), respectively, were determined for the Cr-.5Ti-.5C, Cr-.25Ta-.25C, Cr-.5Cb-.5B, Cr-.5Ta-.5C and Cr-.5Ta-.5B alloys. Rupture strengths of the Cr-.5Ta-.5B, Cr-.5Ta-.5C and Cr-.5Cb-.5B alloys closely approach or exceed the highest values reported for chromium alloys, 16 ksi and 18 ksi (110 and 124 MN/m^2), respectively, for the Cr-4Mo-.6Ta-.4C and Cr-4Mo-.6Cb-.4C compositions.

Achieving this magnitude of rupture strength at 2100°F (1422°K) in chromium solely by dispersion strengthening, i.e., without solid solution addition of molybdenum or tungsten, is noteworthy. Alloying chromium with solid solution additions, especially with molybdenum

or tungsten, is generally accepted as being detrimental to low temperature ductile-brittle behavior.

I. INTRODUCTION

Inherent to chromium are properties which make it a particularly attractive candidate for application in advanced air breathing engines. Its high melting point compared to the super-alloy bases nickel and cobalt, good oxidation resistance relative to the other group VI B and the group V B metals, intermediate density, and high elastic modulus are attributes which suggest a strong potential for such application. To achieve this potential, however, two undesirable characteristics of the element must be overcome. First, strength at elevated temperatures which is low principally due to the body centered cubic structure of chromium must be significantly improved by alloying. Secondly, like many other BCC metals chromium undergoes a transition from ductile-to-brittle behavior which for the pure element occurs in the vicinity of room temperature and should be improved (lowered) or at least maintained unchanged. Unfortunately in this respect, alloying chromium to improve strength at elevated temperatures generally results in an increased ductile-to-brittle transition temperature*, especially when solid solution strengtheners are employed.

A recent study by Ryan[1] has shown that the elevated temperature strength of chromium can be greatly improved without sacrificing low temperature ductility solely by dispersion hardening with group IV B and V B metal monocarbides. For example, 1 v/o TaC, present as fine particles and combined with suitable thermal-mechanical processing, has been shown to enhance substructure stability resulting in an 800°F (1440°K) increase in the one hour re-crystallization temperature of chromium. An increase of the 100 hour rupture strength at 2000°F (1366°K) from 4 ksi to 15 ksi (27.5 to 104 MN/m^2) was obtained as a consequence of this microstructural stability. Most importantly, the TaC strengthened alloy displayed a DBTT in tension similar to that of pure chromium.

The potential for carbide strengthening chromium was extended on this program. Alloys containing either Ta, Cb, Ti, Zr, or Hf plus an equal atomic amount of carbon to combine

*Referred to in latter text as DBTT.

completely with and form approximately 0.5 or 1 v/o of the monocarbide of these metals were studied. The possibility for strengthening chromium by alloying to form borides of these metals was also examined.

Seven carbide and four boride strengthened compositions were prepared as 10 pound ingots (4.5 kg) by induction melting, and fabricated by extrusion and swaging to produce 3/8 inch (.95 cm) diameter test material. Mechanical properties of the study alloys particularly pertinent to their use in air breathing engines were measured. Specifically, data were gathered to measure tensile behavior at 1900°F and 2100°F (1313, 1422°K), stress-rupture properties at 2100°F (1422°K), and temperature dependence of tensile ductility and impact toughness. A major effort on the program also involved the study of what influence heat treatment at 2000°F to 3000°F (1366 to 1973°K) had on precipitate stability, hardness, microstructure, and mechanical properties.

In a related study, the effect of both temperature and composition on boride phase stability in selected boride strengthened alloys was examined. Small 250 gram nonconsumable arc melted heats of ten Cr-Group IV B or V B Metal - B compositions were studied to reveal what boride phases were stable in the temperature range 2100°F to 2700°F (1422 to 1755°K). X-ray diffraction analysis of boride phases extracted from samples of each composition equilibrated in this temperature range then water quenched was used as the principal study tool. Two of the eleven compositions prepared as 10 pound ingots (4.5 kg) and extensively evaluated were chosen from this work.

II. MATERIALS AND EXPERIMENTAL PROCEDURES

Base Material

Electrolytic chromium produced by the Union Carbide Corporation was supplied by NASA for use on the program. Chemical analysis of the material for the content of carbon, oxygen, nitrogen, and common metallic impurities is reported in Table 1. The range shown for carbon, oxygen, and nitrogen contamination represents the extremes of four different analytical samples taken from a 100 pound(45.4kg) lot of electrolytic flake. The degree of variance in the content of these contaminants is believed to reflect a condition to be expected from an electrolytically deposited product.

Alloy Additions

Alloy additions were blended in the form of chips with the chromium flake to make up the desired compositions. Group IV B and V B additions were purchased as sheet and sheared into small pieces suitable for blending. Yttrium, added to the induction melt charge to scavenge impurities, was obtained in ingot form and machined to chips on a lathe*. Boron powder of granular consistency and chunks of graphite were used for alloying with these elements. Commercially pure alloying materials were purchased. This level of purity was considered adequate since compositions studied on the program contained less than 2 a/o total alloying additions; as a consequence, their intrinsic impurity level was dominated by that present in the chromium base material.

Melting and Fabrication

One target on the program was preparation of induction melted alloys having an oxygen plus nitrogen content of 0.104 a/o (300 ppm by weight) or lower. This relatively low contaminant

*It is also generally accepted that a small amount of yttrium present in chromium affords much improved oxidation and nitridation resistance.

Table 1. Analysis of Electrolytic Chromium Flake

Element	PPM by Weight
C	75-172 (.032-.073)[1].
O	<25-55 (<.008-.018)[1].
N	41-91 (.015-.033)[1].
B	<20
Si	<20
Al	<50
Ca	<100
Fe	<50
Mn	<20
Pb	<50
Sn	<20
Mg	<5
Ni	<50
Cu	<5
Ag	<5
Ti	<10
Mo	<20
Zn	<200

[1]. Content in atom percent.

requirement, especially in light of the high melting point and consequent reactivity of chromium with most crucible materials, and the approximately 0.023 to 0.051 a/o level of oxygen plus nitrogen in the starting chromium (refer to Table 1), demanded that an induction melting technique which minimized contamination be used. As a step toward accomplishing this, it was decided that the induction melt charge should be properly alloyed, pre-melted, and homogenized to minimize the melt time, and consequently the degree of contamination introduced during the process. To do this the induction melt charge was first consolidated by nonconsumable arc melting. Eight blends of alloy addition chips plus chromium flake, each weighing 550 grams, were nonconsumable arc melted in 3" diameter (7.6 cm) water cooled copper molds to produce the induction melt charge for one ingot. The chamber preparation and nonconsumable arc melting methods used were identical to those previously shown on similar work to avoid any increase in the level of oxygen or nitrogen contamination[2]. The eight nonconsumable arc melts were assembled for induction melting by simply stacking them one on another inside the melt crucible. Nonconsumable arc melting was also used to prepare 250 gram heats of Cr-Group IV B or V B Metal - B compositions for boride phase stability studies.

Induction melting was performed in a Balzers VSG25 chamber which is designed for handling up to approximately 50 pounds (~25 kg) of steel. A photograph of the facility is shown in Figure 1. Melt power was derived from a 960 cycle motor generator set. A Roots Blower which enabled chamber evacuation to below 1×10^{-2} torr (.21 N/m^2) to be accomplished in less than 5 minutes, greatly shortening the time spent in preparation for melting, a 12" diffusion pump (30 cm), and a DUO 180 mechanical pump comprised the vacuum pumping system. An ultimate vacuum between 1×10^{-5} and 1×10^{-6} torr (1.3×10^{-3} and 1.3×10^{-4} N/m^2) was easily obtained.

The following induction melting procedure aimed at minimizing contamination during this process was used.

1. The melt crucible and surrounding granular ceramic packing material and cement holding it in place within the induction coil were baked to approximately 1600°F (1144°K)

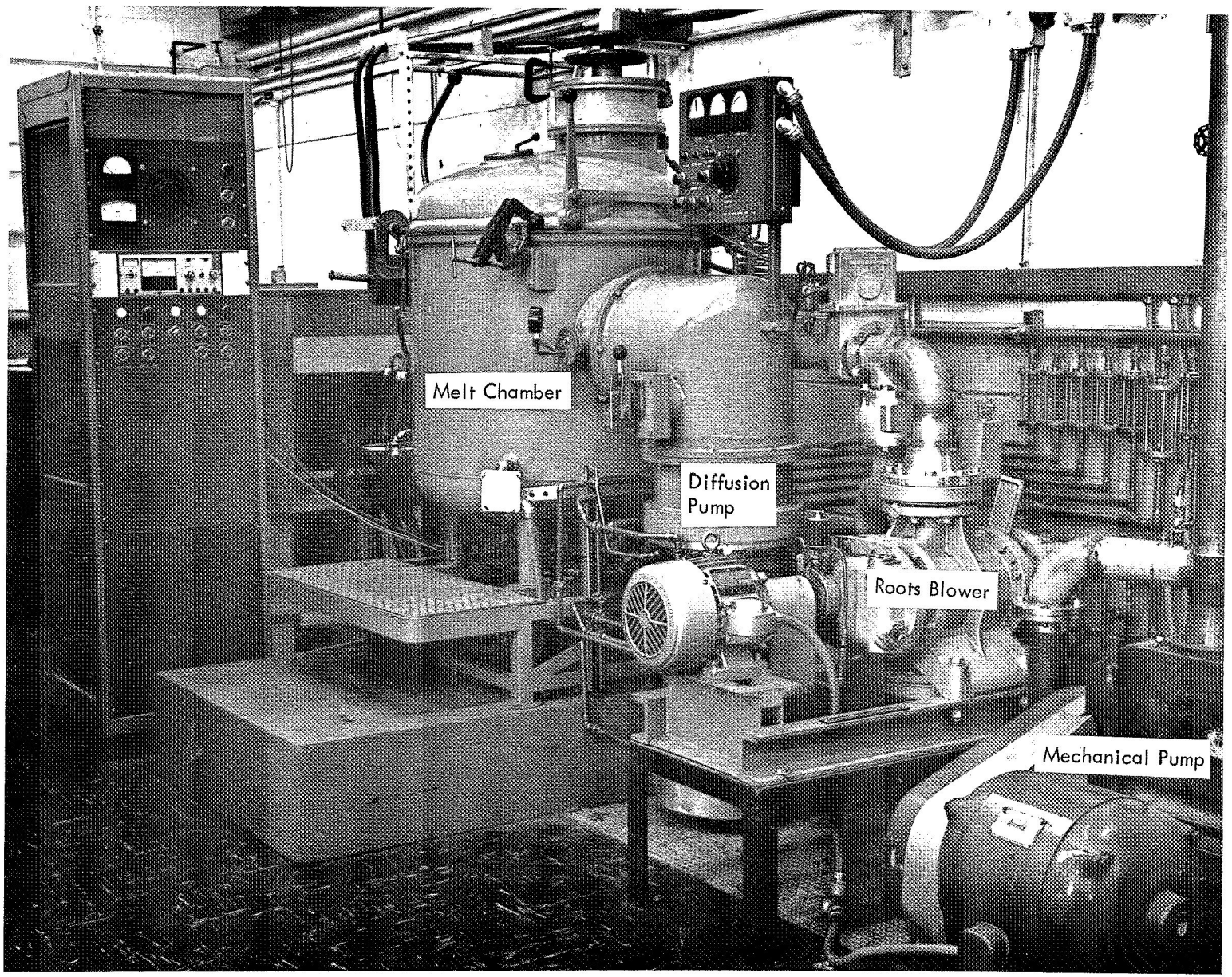

Figure 1. The Induction Melting System

while drawing a vacuum on the melt chamber. This was done by induction heating a pure chromium susceptor placed in the melt crucible. The mold assembly which contained porous ceramic parts and ceramic granules was baked to approximately 900°F (755°K) simultaneous with this operation by a surrounding resistance wire heater. Both melting and mold assemblies were baked under dynamic vacuum until a chamber pressure below 10^{-4} torr (1.3×10^{-2} N/m^2) was reached.

2. The melt crucible and associated surrounding materials were then cooled to room temperature while under dynamic vacuum. Following this, the chamber was filled with argon and quickly opened to replace the pure chromium susceptor with the chromium alloy melt charge, then closed again and evacuated to between 10^{-5} to 10^{-6} torr (1.3×10^{-3} to 1.3×10^{-4} N/m^2). A chamber leak rate was determined at this point, and if found to be lower than 3×10^{-4} torr (4×10^{-2} N/m^2) per minute melting was started. If a higher leak rate was observed, pumping was continued until it was driven to below the 3×10^{-4} torr/minute level. The melt chamber volume of the Balzers VSG25 is 15 cubic feet (.43 m^3).

3. The process of melting commenced with heating the charge to approximately 1600°F (1144°K) while under dynamic vacuum and holding this condition for 1/2 hour. This permitted any moisture, oxygen, or nitrogen, re-adsorbed on the cold melting assembly when the chamber was opened to load the crucible to be driven off. The chamber pressure characteristically increased to between 10^{-4} and 10^{-5} torr (1.3×10^{-2} and 1.3×10^{-3} N/m^2) during this operation.

4. After the charge had been held at 1600°F (1122°K) for 1/2 hour under dynamic vacuum, the chamber was isolated from the pumping system, and argon gas was introduced to a pressure level of 380 torr (5.7×10^4 N/m^2). High purity argon (less than 5 ppm total active impurity content) was used to minimize melt contamination from this source. Power to the induction coil was then increased to the maximum output level of the power source, 55 KW, to facilitate melting in a minimum time. Melting characteristically

began between 8 and 12 minutes after full power application, and the 100% molten stage was achieved 4 to 7 minutes later. Melt power was gradually reduced after melting was first observed to avoid splashing material out of the crucible. Optical pyrometer readings of 100% molten heats maintained at maximum stirring without oversplash indicated a temperature of 3600°F (2255°K) uncorrected for error due to sight port absorption.

5. Ten pound chromium heats (4.5 kg) were melted in yttria stabilized zirconia crucible which by judgment from similar work appeared to be the least contaminating material for induction melting chromium[3,4]. The inside crucible dimensions were 4-1/16 inch diameter by 7-1/4 inch height (10.3 cm x 18.4 cm) yielding a volume 2.4 times that of the 10 pound chromium heats. A new crucible was used for each melt.

6. A 0.29 a/o yttrium metal addition was made to the nonconsumable arc melted charge to combine with and eliminate contaminants introduced by reaction between the molten heat and the yttria stabilized zirconia crucible. A 0.05 a/o residual yttrium content was desired in the ingots. The actual level of yttrium retained was observed to be very sensitive to melt time and ranged from 0.01 to .19 a/o, the higher value being found most consistent with maintaining oxygen plus nitrogen contamination well below the 0.104 a/o (max.) target.

The induction melted heats produced on the program were cast into mold assemblies having a water cooled copper chill at the bottom and zirconia insulation at the side. This arrangement was used to facilitate both axial solidification and a low cooling rate in an attempt to avoid development of a large shrinkage cavity and cracks, common defects in alloyed chromium ingots[2,3].

A drawing showing the cross section of the casting assembly is given in Figure 2. Molten metal was channeled uniformly into the 2-1/2 inch diameter by 9 inch (6.3 cm x 23 cm) high mold cavity through a calcia stabilized zirconia pouring dish. A graphite tube was used to support the

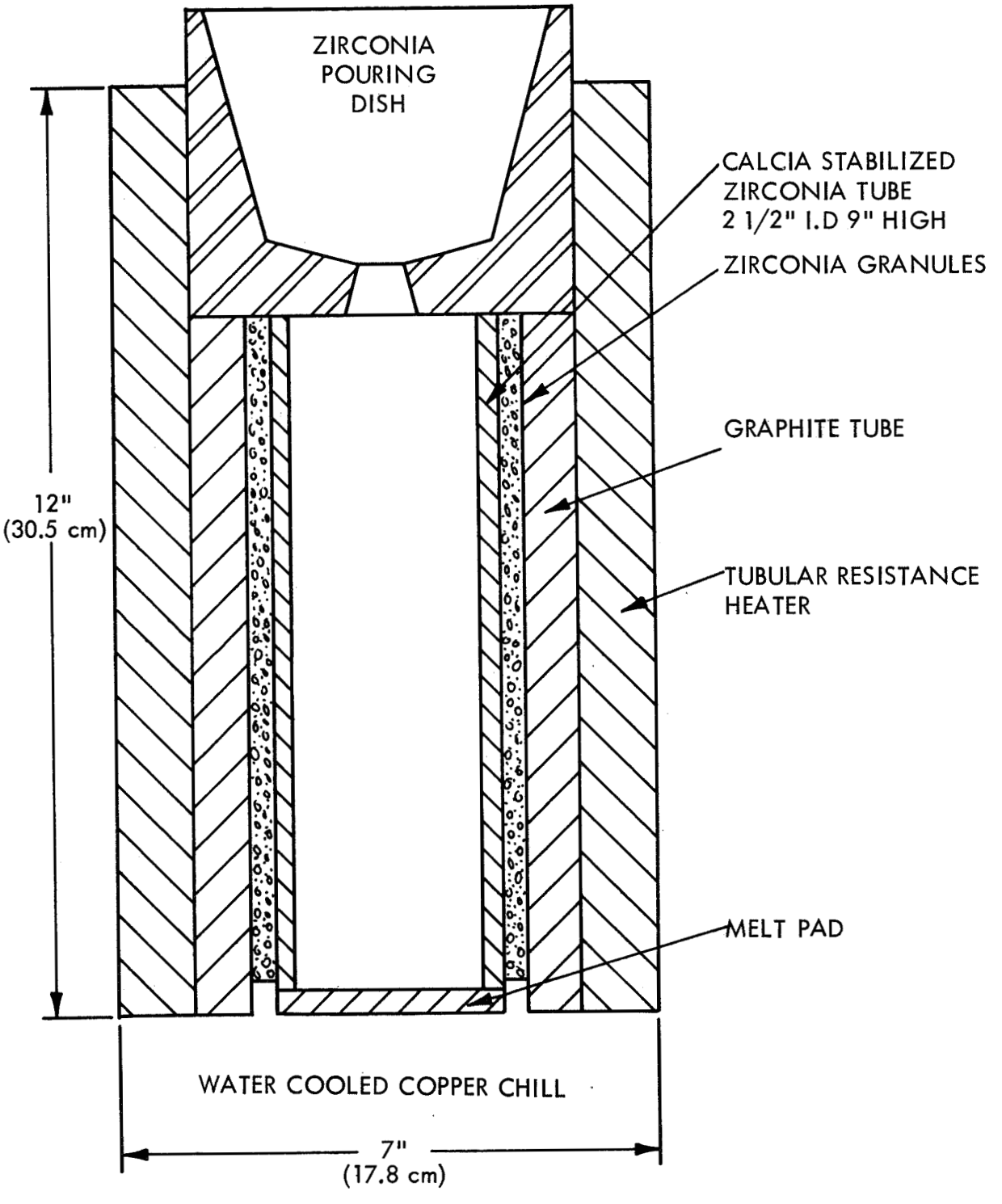

Figure 2. The Casting Assembly

stabilized zirconia mold sleeve and granular back-up material. This was surrounded with a resistance heater used to both drive off atmospheric impurities adsorbed on the mold parts and preheat the assembly to approximately 900°F (755°K) to lessen the ingot cooling rate. A thin pad of the alloy being induction melted was prepared by nonconsumable arc melting and placed at the mold bottom to prevent any surface melting of the copper chill by the sudden impingement of molten metal.

A total of eleven 10 pound (4.54 kg) induction melted ingots were prepared. Nominal and analyzed compositions of the study heats are reported in Table 2. Nominal compositions containing a carbon level equal in atomic percent to that of the metallic alloy constituent were formulated assuming that these additions would completely combine to form a monocarbide precipitate phase. Of these compositions, those containing 0.5 a/o metallic alloying element would yield approximately 1 v/o precipitate, and those containing 0.25 a/o metal addition 0.5 v/o precipitate, as calculated from the densities of the respective monocarbides. Complete combination of the boron and alloying metal addition in the boride strengthened alloys would yield 1 v/o monoboride or diboride phase.

The time period 100% molten material was held prior to pouring was varied on the first four program alloy heats induction melted (IM-5 through 8) to define its relationship to residual yttrium content and oxygen plus nitrogen contaminant levels. The first heat, IM-5, was held molten for five minutes before pouring, while IM-6, 7 and 8 were held in this state for successively longer times up to eleven minutes. Oxygen plus nitrogen content on IM-5, 6 and 7 fell within the 0.104 a/o target, and the desired residual yttrium level was closely approached on IM-6 and IM-7. Very little yttrium was retained in IM-8 resulting in a high, 0.390 a/o, oxygen level. Nitrogen content did not reach a serious level on any of these heats.

Analysis of the melt and chemistry data obtained on IM-5 through 8 indicated a 6 to 8 minute holding period prior to pouring might yield a suitable balance between the residual yttrium

Table 2. Analysis of Induction Melted Alloys[1].

Heat No.	Nominal Composition a/o	Analyzed Composition a/o	Impurity Content[2]. a/o O	a/o N
IM-5	Cr-.5Ta-1B-.05Y	Cr-.48Ta-1.36B-.19Y	.0395	.0368
IM-6	Cr-.5Ta-.5C-.05Y	Cr-.44Ta-.53C-.08Y	.0490	.0244
IM-7	Cr-.5Ti-.5C-.05Y	Cr-.50Ti-.52C-.04Y	.0580	.0170
IM-8	Cr-.5Hf-1B-.05Y	Cr-(.44Hf)-1.21B-.01Y	.3900	.0135
IM-9	Cr-.5Cb-.5C-.05Y	Cr-.50Cb-.57C-.08Y	.130 (.100)	.0255
IM-10	Cr-.25Cb-.25C-.05Y	Cr-.26Cb-.30C-.03Y	.155 (.146)	.0199
IM-11	Cr-.25Ta-.25C-.05Y	Cr-.27Ta-.28C-.05Y	.062 (.062)	.0207
IM-12	Cr-.5Zr-.5C-.05Y	Cr-(.39Zr)-(.52C)-(.18Y)	(.0322)	(.0104)
IM-13	Cr-.5Hf-.5C-.05Y	Cr-(.44Hf)-(.57C)-(.16Y)	(.0226)	(.0072)
IM-14	Cr-.5Cb-.5B-.05Y	Cr-(.40Cb)-(.37B)-(.14Y)	(.0500)	(.0300)
IM-15	Cr-.5Ta-.5B-.05Y	Cr-(.51Ta)-(.39B)-(.09Y)	(.0470)	(.0280)

[1]. Results given in parenthesis represent analysis of bar extruded from the induction melted ingots. Other results are ingot top analysis.

[2]. Target: $O + N \leq 0.104$ a/o.

level and the oxygen plus nitrogen contaminant content and this control was imposed on heats IM-9 through 11. The residual yttrium level met exactly or closely approached the 0.05 a/o nominal content on these heats, but oxygen plus nitrogen contamination slightly exceeded the 0.104 a/o target on IM-9 and 10. Again, as found for heat IM-5 through IM-8, contamination with oxygen was most serious. It was concluded from this that a 6 to 8 minute molten state holding period was too long to properly balance the residual yttrium and contaminant levels. A more conservative 3 to 5 minute molten state holding time was used on heats IM-12 through 15 and the oxygen plus nitrogen levels were maintained below the 0.104 a/o target, but this was achieved at the expense of retaining approximately two to four times the desired yttrium content.

The results of chemical analysis definitely show that oxygen contamination can become serious when too low a residual yttrium level is reached. Nitrogen contamination, on the other hand, had little relationship to yttrium content. The melt crucible which reacts slightly with the molten heat is believed to be the source of oxygen contamination, and the likely reaction by which yttrium in the charge eliminates this impurity is:

$$2\underline{Y} + 3\underline{O} \longrightarrow Y_2O_3\,(s)$$

An equilibrium was probably established for this scavenging reaction during the time period over which the charge was held molten prior to pouring. Since the levels of dissolved reactants would be low the equilibrium constant for the reaction can be written in terms of yttrium and oxygen concentrations, i.e.,

$$Ke = \frac{1}{[\underline{Y}]^2\,[\underline{O}]^3}$$

or

$$\underline{Y} = \frac{1}{Ke^{1/2}\,[\underline{O}]^{3/2}}$$

It follows that maintaining oxygen at a low level demands a high yttrium content. Furthermore, and most important, achieving both low oxygen and yttrium in induction melted chromium, which was a target of the program, appears to be thermodynamically inconsistent.

A typical 10 pound (4.54 kg) induction melted ingot is shown in Figure 3. The shrinkage cavities in the ingots were found to vary between 3 and 4 inches (7.6 and 10.2 cm) in depth indicating heating the casting assembly to 900°F (755°K) did not significantly reduce the solidification rate from the side wall. Several ingots were x-ray examined with the results showing that portion of the ingot below the shrinkage void to be entirely free of cracks.

All ingots were cut across at the bottom of the shrinkage cavity, and the sound portion separated was machined to 2-1/4 inch diameter. They were then clad in 3/8 inch (.95 cm) wall thickness carbon steel pipe for extrusion. Extrusion was performed in the Westinghouse operated facility at Wright Patterson Air Force Base. The billets were all extruded through an 8.4 to 1 area reduction to 1.02 inch (2.6 cm) diameter bar at 2100°F (1422°K). Between 25 and 35 inches (.63 and .88 m) of sound material, that remaining after nose and tail extrusion defects were cut off, was obtained on each composition. A photograph showing the length of sound extruded bar prepared on heats IM-5 through 8 is displayed in Figure 4. The bars shown were cut into one-third sections in preparation for swaging to test rod.

Test rod of 3/8 inch diameter (.95 cm) was prepared by swaging. Bars were swaged at 2100°F to 2200°F (1422 to 1477°K) with the co-extruded steel clad on them. Heating was performed in a hydrogen or argon atmosphere, and reductions of 0.04 to 0.08 inch (.10 to .20 cm) in diameter were taken per swaging pass. When processing was completed, the bars were stress relieved for 15 minutes at the swaging temperature.

Hardness of the study alloys in the cast, extruded and swaged conditions is reported in Table 3. Difficulty in extrusion or swaging was not encountered with any composition.

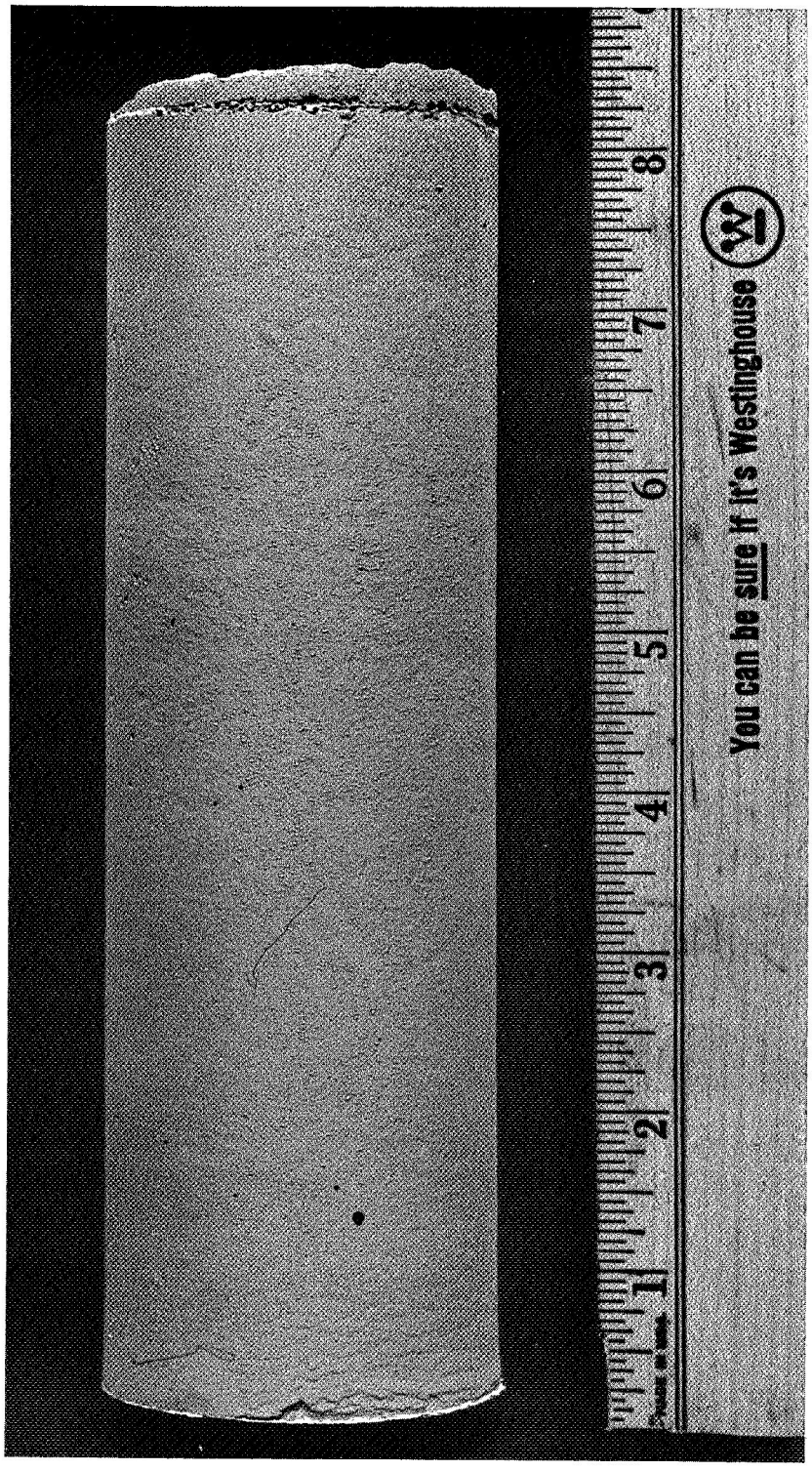

Figure 3. An Induction Melted Ingot

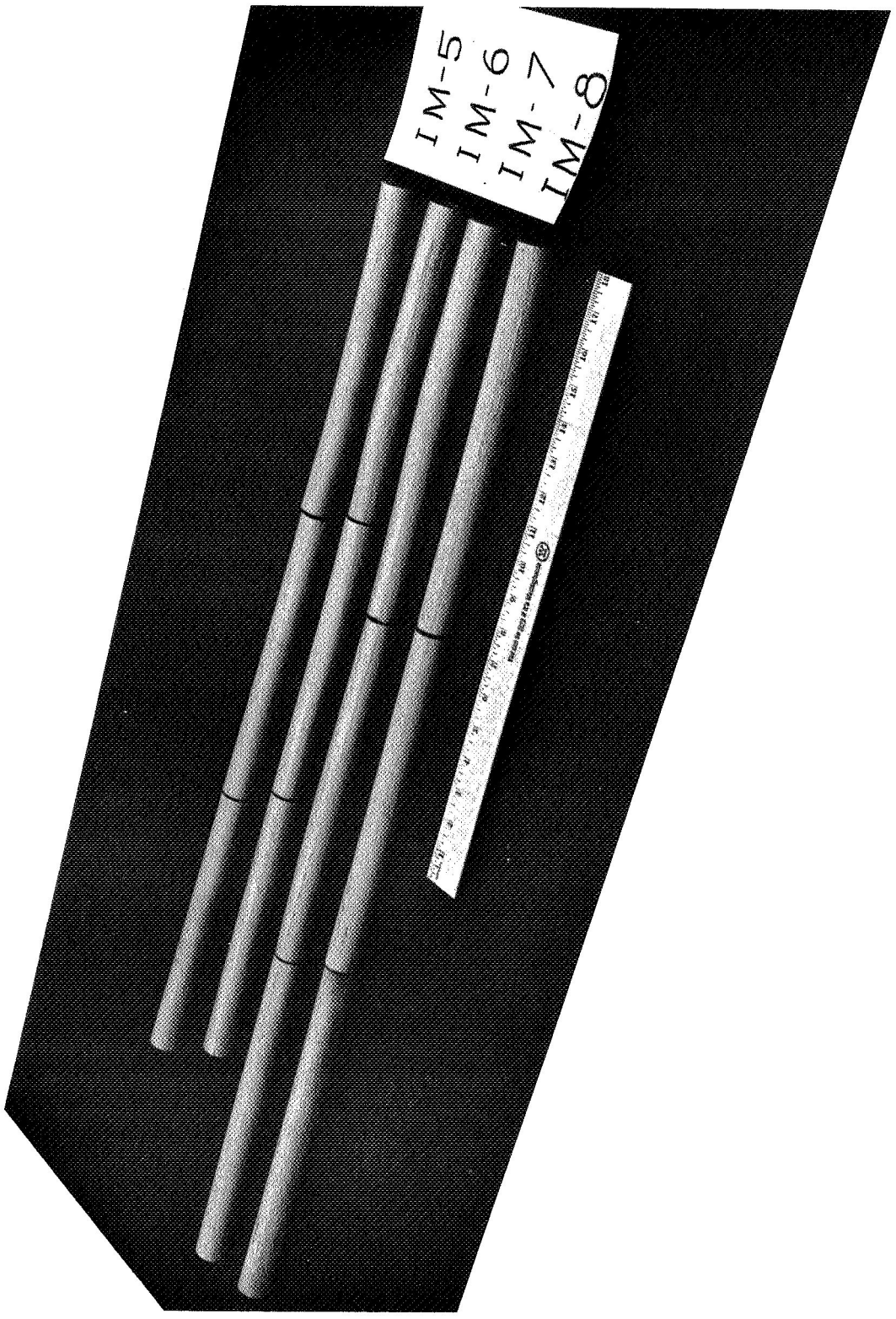

Figure 4. Lengths of Sound Extruded Bar Obtained on Heats IM-5 through 8

Table 3. Effect of Processing on Hardness of the Induction Melted Alloys

Heat No.	Nominal Composition a/o	Diamond Pyramid Hardness, 10 kg Load			Final Microstructural Condition[3.]
		Cast	Extruded[1.]	Swaged[2.]	
IM-5	Cr-.5Ta-1B-.05Y	163	220	276	C. W.
IM-6	Cr-.5Ta-.5C-.05Y	167	205	202	P. C. W.
IM-7	Cr-.5Ti-.5C-.05Y	148	188	180	P. C. W.
IM-8	Cr-.5Hf-1B-.05Y	129	197	145	Rx.
IM-9	Cr-.5Cb-.5C-.05Y	152	215	203	P. C. W.
IM-10	Cr-.25Cb-.25C-.05Y	144	201	193	P. C. W.
IM-11	Cr-.25Ta-.25C-.05Y	148	202	201	P. C. W.
IM-12	Cr.-.5Zr-.5C-.05Y	144	170	154	Rx.
IM-13	Cr-.5Hf-.5C-.05Y	138	165	151	Rx.
IM-14	Cr-.5Cb-.5B-.05Y	173	230	222	C. W.
IM-15	Cr-.5Ta-.5B-.05Y	164	232	256	C. W.

1. 8.4 to 1 area reduction at 2100°F (1422°K)

2. 7.5 to 1 area reduction at 2200°F for IM-5 through 8, and 2100°F for IM-9 through 15 (1422 & 1477°K)

3. C. W. Cold Worked
P. C. W. Partially Cold Worked
Rx. Completely Recrystallized

Property Evaluation

Mechanical Properties

Tensile and stress-rupture data were obtained using a specimen of 1 inch (2.54 cm) gauge length and 3/16 inch (.45 cm) gauge diameter shown in Figure 5. Also displayed in this figure is the micro-izod sample used for impact tests.

Elevated temperature tensile and stress-rupture tests were conducted in a cold wall tantalum resistance heated unit under vacuum of 5×10^{-6} torr (max.) (6.5×10^{-4} N/m^2) measured at temperature. Samples were held at temperature for 1/2 hour before application of load. A 0.03 inch/minute (.076 cm/min) crosshead rate was used on the high temperature tensile tests.

Tests to determine impact and tensile DBTT were performed in air. A crosshead rate of 0.02 inch/minute (.05 cm/min) was used on the tensile tests. Tensile samples were held at temperature for 1/2 hour before testing, while impact samples were tested immediately upon achievement of test temperature. Impact samples were heated with a gas flame while cantelever supported in the test fixture to a temperature roughly 50°F (28°K) above the desired test temperature. The flame was then removed, and when temperature dropped to the test temperature the sample was struck. Temperature was monitored on a digital voltmeter modified to read directly in Fahrenheit degrees when using the output from a copper-constantan thermocouple. The thermocouple was attached to the specimen gauge section.

Heat Treatment

Heat treatments used to establish structural, phase stability, and mechanical property responses described in the first two sections of the Experimental Program and Discussion were performed in a cold wall tantalum element resistance furnace. Samples were hermetically encapsulated in tantalum tubes (tantalum end plugs were electron beam welded to the tubing). Heat treatment was performed under vacuum of between 10^{-5} and 10^{-6} torr (1.3×10^{-3} and 1.3×10^{-4} N/m^2); and when completed, all samples were quenched by introduction of helium. Quenching occurred

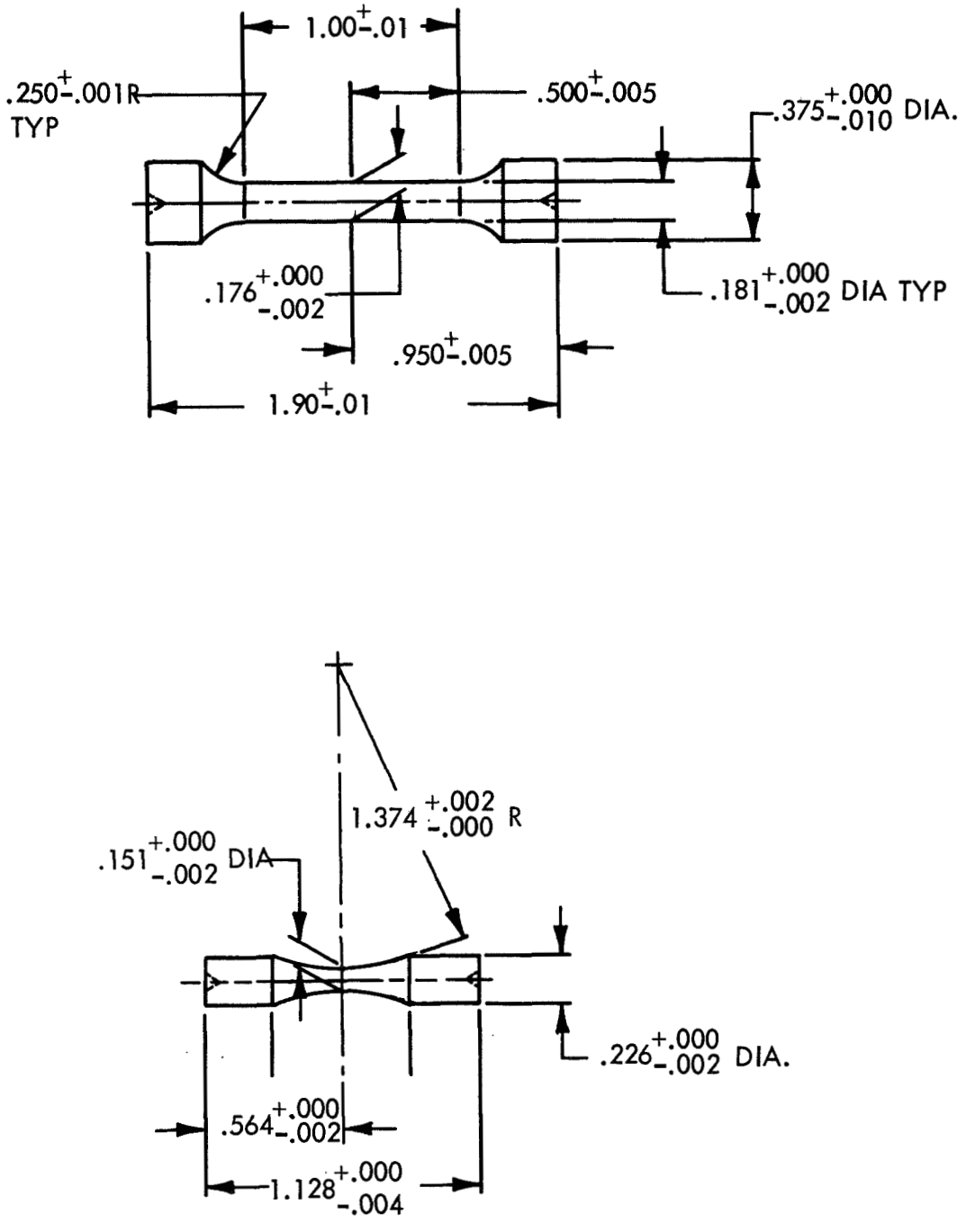

Figure 5. Tensile and Impact Samples Used for Property Evaluations

at rates of 800°F/minute between 2800°F and 2000°F, 400°F/minute between 2000°F and 1800°F, and 200°F/minute between 1800°F and 1700°F (445°K/minute between 1811°K and 1366°K, 221°K/minute between 1366°K and 1255°K, and 111°K/minute between 1255°K and 1200°K). Temperature was measured optically employing techniques to approximate black body conditions.

Equilibration heat treatments used to establish temperature and composition dependence of boride phase stability described in the third part of Experimental Program and Discussion were done in a hydrogen atmosphere furnace. Temperature was measured optically from the sample container. Samples were hermetically encapsulated in molybdenum for these heat treatments. At the completion of heat treatment, these samples were very rapidly quenched by direct immersion in water.

Metallography

Initial steps in sample preparation for microstructural inspection included grinding from 120 through 600 grit paper, and rough polishing on canvas cloth using one micron alumina abrasive. Final preparation was done by acid polishing on Frostmanns cloth, using jewelers rouge abrasive suspended in a weak chromic acid solution. Structure was developed by etching electrolytically in a 5% solution of chromic acid in water.

Phase Identification

Precipitates were extracted from 10 gram samples by matrix dissolution in 300 ml of 10% bromine-methanol solution. Standard Debye x-ray diffraction patterns were obtained on extractions using a 114 mm. Seimens camera and nickel filtered copper radiation.

Extracted phases were also redispersed on carbon replicas and examined by electron microscopy and diffraction on a JEM 6A unit. Samples were prepared by drying drops of precipitate slurry, obtained by ultrasonic dispersion in amyl acetate, on glass slides, then transferring the residue to parlodion and carbon replicas using the standard two stage technique.

Electron microprobe analysis was employed to examine precipitate phases in situ. The work was done on an Applied Research Laboratory Model AMX unit. Metallographically polished and etched samples were examined.

III. EXPERIMENTAL PROGRAM AND DISCUSSION

The results of tests performed on the program and analysis of the data are presented in this section. Data are reported in three categories: The Effect of Fabrication and Heat Treatment on Microstructure, Hardness, and Carbide and Boride Stability; Mechanical Properties of the Carbide and Boride Strengthened Alloys; The Effect of Composition and Temperature on Boride Stability. The evaluation of eleven carbide and boride strengthened alloys fabricated as rod from 10 pound (4.54 kg) induction melted heats is discussed in the first two sections. A separate study of how boride phase stability is affected by both temperature and composition is discussed in the last section. Boride phase stability was evaluated in the study over the temperature range 2100°F to 2700°F (1422 to 1755°K) on ten Cr-Ti, Zr, Ta, or Cb-B compositions.

The Effect of Fabrication and Heat Treatment on Microstructure, Hardness, and Carbide and Boride Stability

Carbide Strengthened Alloys

Microstructures representing the as cast condition of the five nominally Cr-.5 (Ta, Ti, Cb, Zr or Hf)*-.5C alloys are shown in Figure 6. A massive almost continuous grain boundary phase formed in the Cr-.5 (Ta, Ti or Cb)-.5C alloys along with a fine intragranular precipitate. A smaller less continuous grain boundary phase formed in the cast structure of the Cr-.5 (Zr or Hf)-.5C alloys, but intragranular precipitation was not observed. The as cast microstructures of the remaining two carbide strengthened compositions studied on the program, Cr-.25 (Ta or Cb)-.25C, were identical to that displayed by the Cr-.5 (Ta, Ti or Cb)-.5C alloys.

A microstructure identical to that observed on the five Cr-(Ta, Ti or Cb)-C alloys was reported by Filippi for the alloy Cr-.57Ta-.45C-.02Zr in the as cast condition[2]. The grain boundary phase in this alloy was identified as $Cr_{23}C_6$ and the matrix precipitate as TaC. It follows

*For brevity, nominal compositions in atomic percent with yttrium content omitted are used when discussing alloys in the text, and when discussing a set of alloys which are similar in every respect except type of Group IV B or V B alloying element compositions will be noted in this manner. Nominal compositions with yttrium content at the target level, .05 a/o, are used in Tables and Figures.

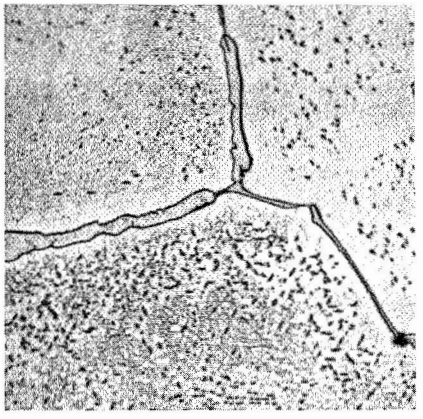

Cr-.5Ta-.5C-.05Y

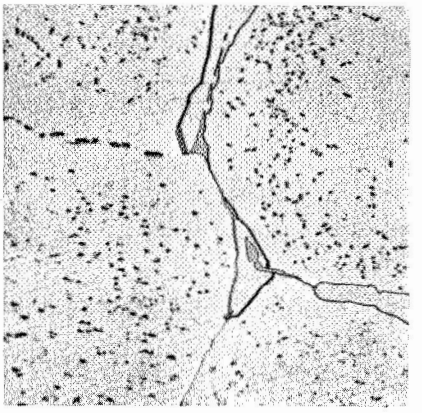

Cr-.5Ti-.5C-.05Y

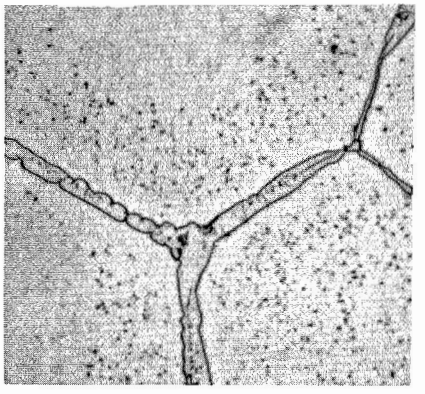

Cr-.5Cb-.5C-.05Y

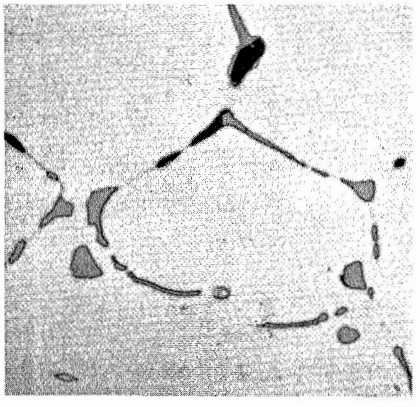

Cr-.5Zr-.5C-.05Y

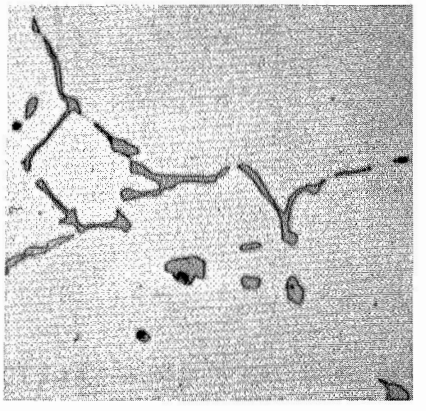

Cr-.5Hf-.5C-.05Y

Figure 6. Microstructures of As Cast Nominally Cr-.5M-.5C-.05Y Alloys 500X

that $Cr_{23}C_6$ is the likely grain boundary phase formed in the Cr-(Ta, Ti or Cb)-C compositions in the as cast condition, while the fine matrix precipitate is the monocarbide of the specific principal metallic alloying addition. Evidence supporting the conclusion that the grain boundary phase formed in these alloys is $Cr_{23}C_6$ was obtained by electron microprobe analysis. Data obtained by this examination are reported in Table 4. Average levels of chromium and each principal metallic alloying addition were measured across intragranular areas and in the grain boundary phase. The intensity of characteristic radiation of a given element is reported as a percentage of that from a pure standard so the values are approximately equivalent to weight percent.

The contents of chromium found in the grain boundary phase of the Cr-(Ta or Cb)-C alloys were similar and very high, but slightly lower than the average value across intragranular areas. These results are consistent with the phase being chromium rich - presumably, therefore, $Cr_{23}C_6$. Some principal metallic element must be in solid solution in the $Cr_{23}C_6$ phase as judged from the small amount detected. The intragranular precipitates observed in the microstructure of these alloys were too fine to permit examination by microprobe analysis.

By comparison, microprobe analysis of the grain boundary phases formed in the as cast Cr-.5(Zr or Hf)-.5C alloys revealed them as rich in the principal metallic alloying element. A small amount of chromium was also detected in the phases. The results suggest monocarbides of zirconium and hafnium containing a small amount of chromium in solid solution are formed in these respective compositions.

Microstructures of the Cr-.5(Ta, Ti, Cb, Zr or Hf)-.5C alloys representing the as fabricated condition are presented in Figure 7. Conversion of the Cr-.5 (Ta, Ti or Cb)-.5C alloys from ingot to rod by extrusion and swaging at 2100 to 2200°F (1422 to 1477°K) resulted in a worked structure containing a few small recrystallized grains. This type of microstructure has been termed partially cold worked in Table 3 where hardness and microstructure characterizing the as fabricated condition of all study alloys are reported. Partially cold worked microstructures were also developed by fabrication in the Cr-.25 (Ta or Cb)-.25C alloys.

Table 4. Microprobe Analysis for Levels of Chromium and Principal Metallic Alloying Additions in the Structure of As Cast Cr-(Ta, Cb, Zr or Hf)-C Alloys

Nominal Compositions a/o	Ratio of Characteristic X-Radiation $\frac{I\ (element)}{I\ (standard)} \times 100$									
	Grain Boundary Phase					Intragranular Area[1]				
	Cr	Ta	Cb	Zr	Hf	Cr	Ta	Cb	Zr	Hf
Cr-.5Cb-.5C-.05Y	91		1			97		3		
Cr-.25Cb-.25C-.05Y	86		1			100		3		
Cr-.25Ta-.25C-.05Y	92	5				100	2			
Cr-.5Zr-.5C-.05Y	9			82		100			2	
Cr-.5Hf-.5C-.05Y	5				88	100				2

[1]. Average concentration across intragranular regions.

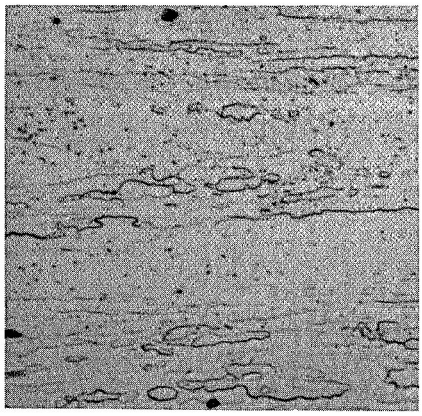

Cr-.5Ta-.5C-.05Y

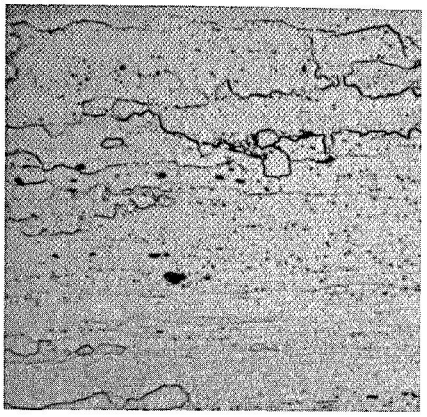

Cr-.5Ti-.5C-.05Y

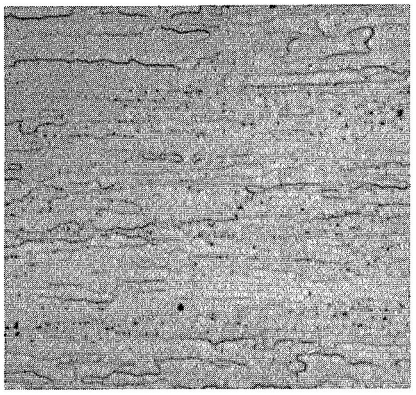

Cr-.5Cb-.5C-.05Y

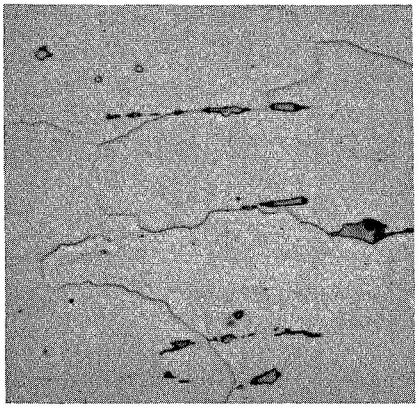

Cr-.5Zr-.5C-.05Y

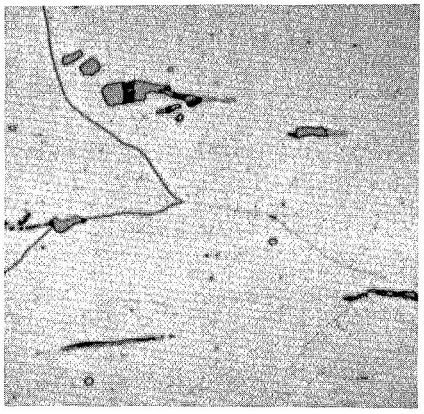

Cr-.5Hf-.5C-.05Y

Figure 7. Microstructures of As Fabricated Nominally Cr-.5M-.5C-.05Y Alloys 500X

By comparison, identical processing of the Cr-.5 (Zr or Hf)-.5C compositions resulted in fully recrystallized microstructures as is obvious in the photomicrographs presented in Figure 7. Examination of the structures suggests that fabrication only fractured and spread along the working direction the ZrC and HfC grain boundary phases present in the as cast alloys. These second phase particles were undoubtedly too large to enhance any stability of a wrought structure at the conditions of fabrication, and fully recrystallized microstructures developed. On the other hand, a fine precipitate, either that present in the as cast condition or an additional amount formed during processing, can be seen in the microstructures of the as fabricated Cr-.5(Ta, Ti or Cb)-.5C alloys, and apparently was effective in impeding the processes of recrystallization. Little of the massive $Cr_{23}C_6$ particles present in the as cast structure of these alloys remained after fabrication indicating appreciable solutioning of this phase occurred.

Photomicrographs characterizing the responses of the compositions Cr-. 5(Zr or Hf)-. 5C to heat treatment for one hour at 2400°F to 2850°F (1589 to 1839°K) are presented in Figure 8. Heat treatment had little influence on the microstructure of these alloys, and after one hour at 2850°F (1839°K) the ZrC and HfC particles present in the structures remained in much the same form as found in the as-fabricated conditions.

In contrast with this, the microstructures of the five Cr-(Ta, Ti or Cb)-C alloys underwent pronounced changes when heat treated at 2400°F (1589°K) and higher. Identical behavior was displayed by these alloys and is characterized in Figure 9 where microstructural changes caused by one hour heat treatment of the Cr-. 5(Ta or Ti)-. 5C compositions at 2400°F to 2850°F (1589 to 1839°K) are shown. Recrystallization is developed by 1 hr/2400°F (1589°K) heat treatment and grains elongated in the direction of work are formed. Presence of a fine intragranular precipitate is also a feature of this annealed condition. Heat treatment for 1 hour at 2600°F (1700°K) results in much the same structure as developed by the 1 hr/2400°F (1589°K) anneal. A major change in microstructure, however, occurs upon heat treatment for 1 hour at 2800°F to 2850°F (1811 to 1839°K). A massive almost continuous grain boundary phase and absence of any obvious intragranular precipitate are observed after annealing at these temperatures.

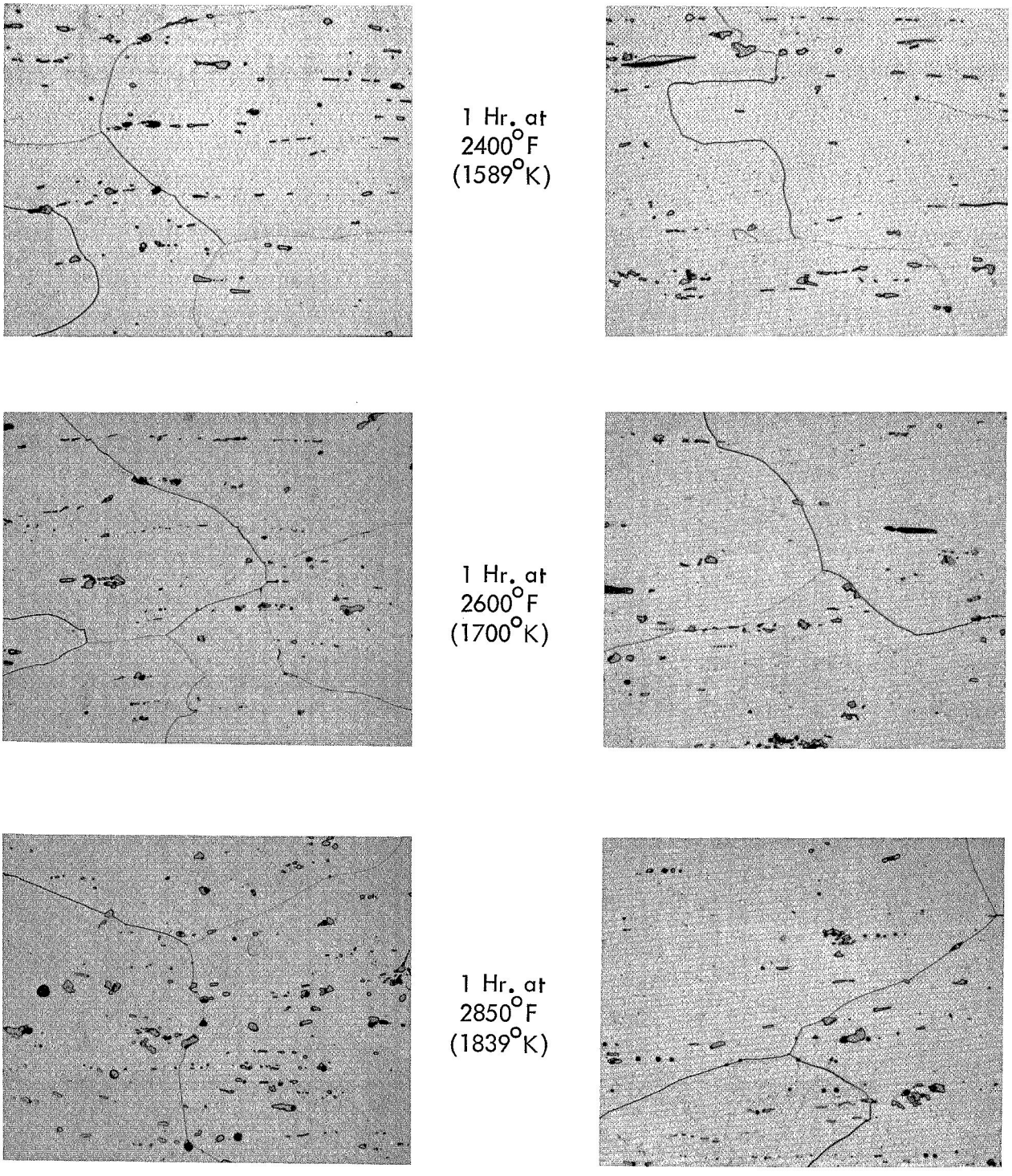

Figure 8. Microstructural Response of Cr-.5Zr-.5C-.05Y (left) and Cr-.5Hf-.5C-.05Y (right) to Heat Treatment for 1 Hour at 2400°F to 2850°F 250X

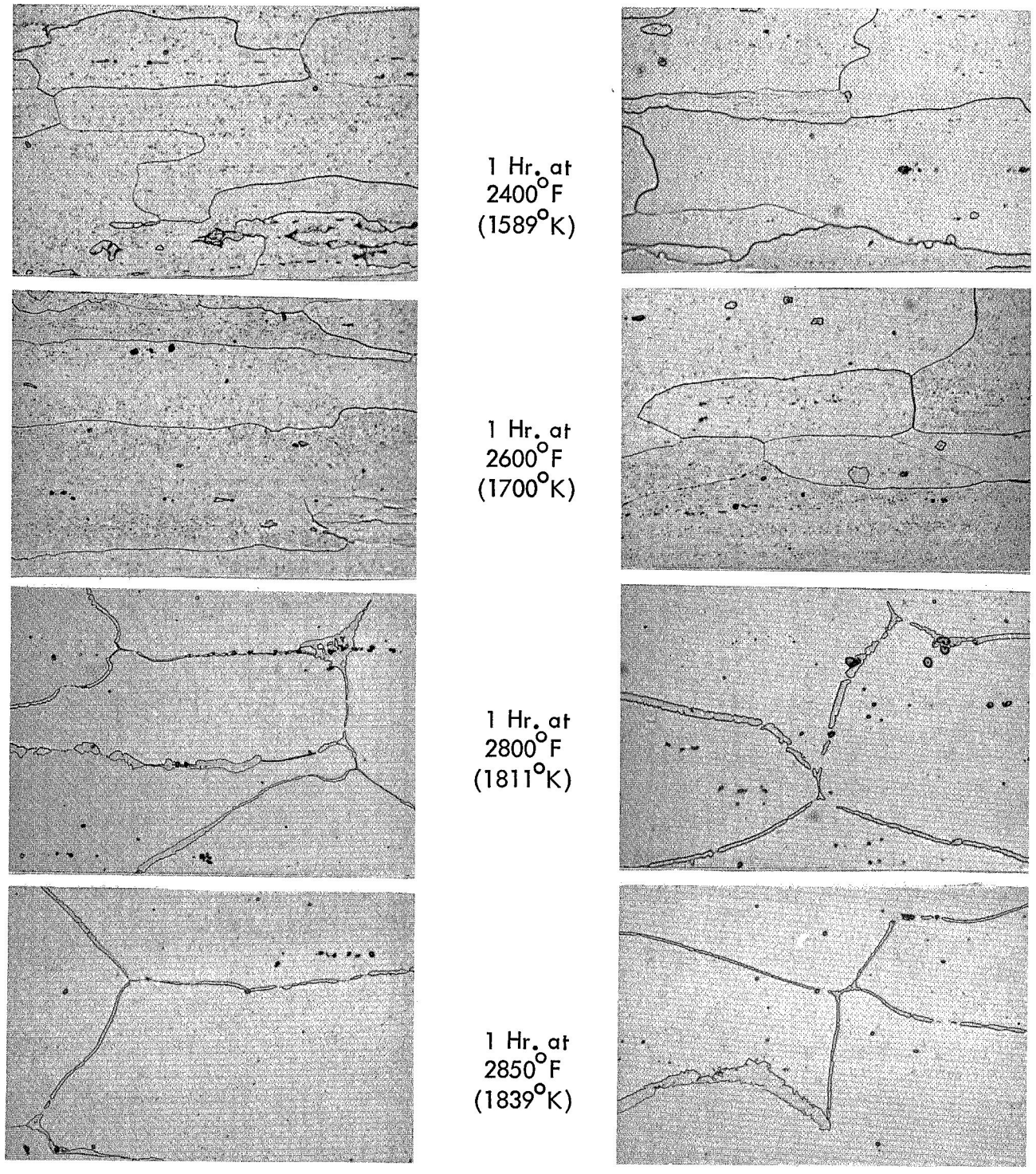

Figure 9. Microstructural Response of Cr-.5Ta-.5C-.05Y (left) and Cr-.5Ti-.5C-.05Y (right) to Heat Treatment for 1 Hour at 2400°F to 2850°F 250X

The carbide particles present in the Cr-.5Ta-.5C alloy in the as fabricated and 1 hr/2400°F, 1 hr/2600°F, and 1 hr/2800°F (1589, 1700, 1811°K) heat treated conditions were extracted and examined by x-ray diffraction. Both TaC and $Cr_{23}C_6$ were identified in the samples representing each alloy condition, but a qualitative judgment made from the x-ray data indicated the amounts of these phases present differed. Graded into strong (S), moderate (M), and weak (W) categories, the amounts of these carbides observed were: as fabricated - TaC (S) $Cr_{23}C_6$ (W), 1 hr/2400°F and 1 hr/2600°F - TaC (S) $Cr_{23}C_6$ (M), 1 hr/2800°F - TaC (W) $Cr_{23}C_6$ (S). This information, interpreted logically rather than literally, indicates that at the temperatures of fabrication, 2100°F to 2200°F (1422 to 1477°K), TaC is the stable carbide phase, while TaC and $Cr_{23}C_6$ are both stable between 2400°F and 2600°F (1589 and 1700°K), and $Cr_{23}C_6$ alone is stable at 2800°F (1811°K). In this interpretation it is assumed that carbide stability changes with temperature in a sequence likely if a simple Cr-Ta-C ternary component system were assumed, i.e., if the presence of any other elements in the alloy, the small amount of yttrium in particular, can be disregarded. Furthermore, the alloy conditions examined certainly did not represent equilibration treatments, and the observation of "weak" amounts of a carbide phase is best ignored since its presence may be due to insufficient holding time-at-temperature, or formation upon cooling due an insufficient quench rate. Because the microstructural changes which occurred as a function of temperature were identical for all the Cr-(Ta, Ti or Cb)-C alloys studied on the program, the phase transformation relationship given below, in which M represents Ta, Ti or Cb, is suggested. Solubility for alloying elements in the carbides and in chromium below T_2 is assumed small and ignored.

$$(Cr)_{matrix} + MC \xrightarrow{T_1} (Cr)_{matrix} + MC + Cr_{23}C_6 \xrightarrow{T_2} (Cr, M)_{matrix} + Cr_{23}C_6$$

$$2200^\circ F \leq T_1 \leq 2400^\circ F \quad (1477^\circ K \leq T_1 \leq 1589^\circ K)$$

$$2600^\circ F \leq T_2 \leq 2800^\circ F \quad (1700^\circ K \leq T_2 \leq 1811^\circ K)$$

Examination of hardness changes caused by heat treatment of the carbide study alloys, reported in Figure 10, lends support to the above phase transformation behavior. Hardness of the Cr-(Ta, Ti or Cb)-C alloys decreased with increasing annealing temperature for the 2100°F to 2400°F (1422 to 1589°K) range as a result of recrystallization. Full recrystallization was apparently obtained in these compositions by one hour heat treatment at 2400°F (1589°K) as

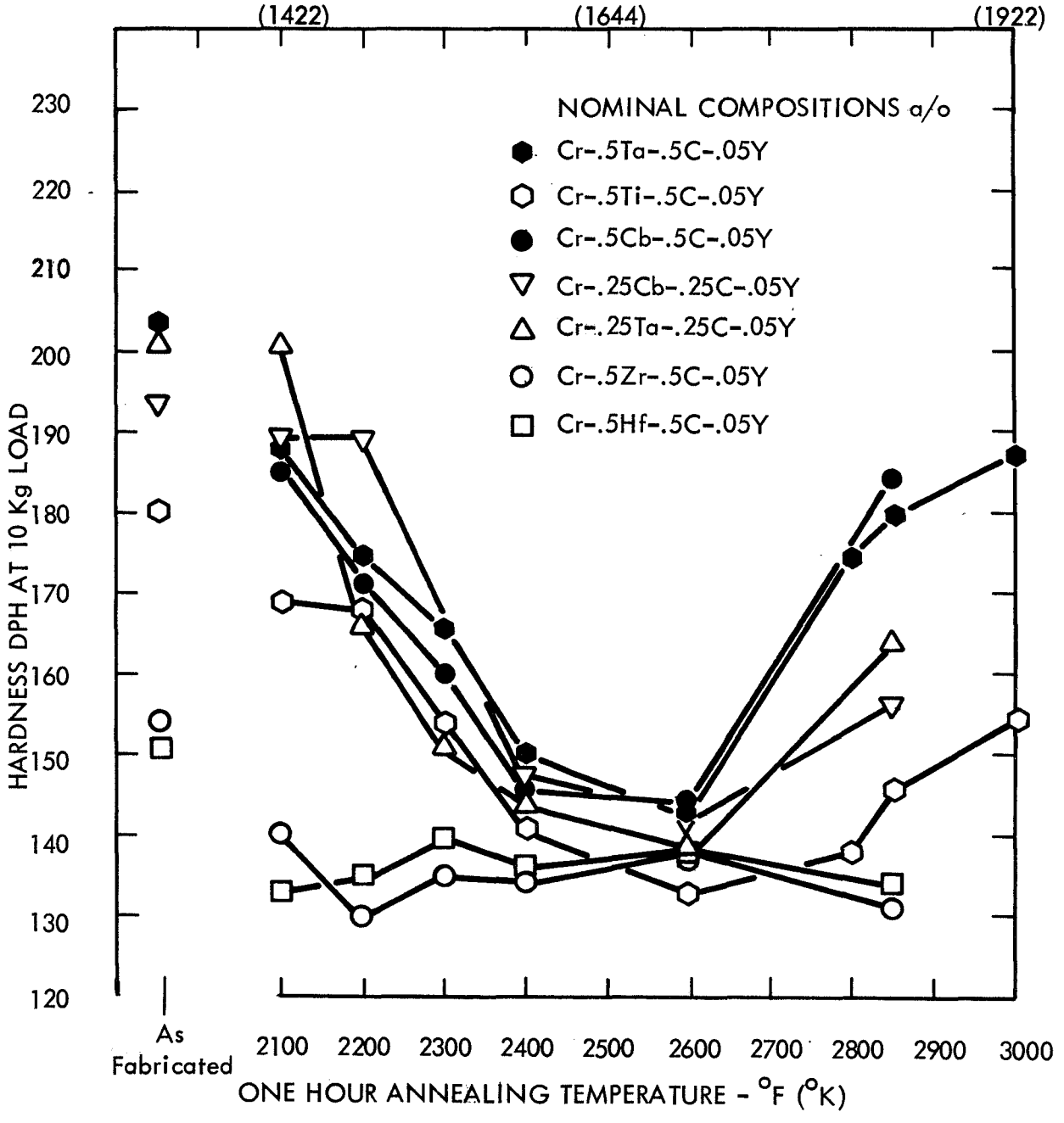

Figure 10. The Effect of Heat Treatment for One Hour at 2100°F to 3000°F on Hardness of the Carbide Study Alloys

judged from the similar hardness level developed after 1 hr/2600°F (1700°K) annealing. Heat treatment at 2400°F (1589°K) was used as a standard recrystallization anneal for evaluation of mechanical properties in this condition. Hardness of the Cr-(Ta, Ti or Cb)-C alloys increased above the 2400°F to 2600°F (1589 to 1700°K) annealed level when annealing was performed at 2800°F (1811°K) or higher. This is consistent with the phase transformation relationship proposed for these alloys because solutioning of the principal metallic alloying additions in the chromium matrix at these temperatures would result in increased hardness.

The Cr-.5(Zr or Hf)-.5C alloys, by comparison, did not display any hardness change upon annealing over the 2100°F to 2850°F (1422 to 1839°K) temperature range. Because these compositions were recrystallized as fabricated, a major decrease in hardness was not noted over the lower half of the annealing temperature range. The lack of a hardness increase upon annealing at 2850°F (1839°K) is conformation of their previously discussed microstructural stability (Figures 6, 7 and 8), particularly in reference to the inocuous effect heat treatment has on the ZrC and HfC phases present in the respective alloys.

The response of carbide stability to heat treatment noted for the Cr-(Ta, Ti or Cb)-C alloys at first appears inconsistent from that anticipated by consideration of carbon solubility in pure chromium. According to Rudy[5], maximum carbon solubility in chromium is approximately 1.3 a/o occurring at 2785 ± 22°F (1803 ± 40°K) the Cr-$Cr_{23}C_6$ eutectic temperature. Since the Cr-(Ta, Ti or Cb)-C alloys studied contained .25 or .50 a/o carbon, it might be implied from this that formation of $Cr_{23}C_6$ by heat treatment at 2800°F or 2850°F (1811 or 1839°K) could only occur through precipitation from solid solution during cooling. However, formation of so massive a grain boundary phase by this diffusion controlled mechanism at the quench rate used on the program (800°F/min. between 2800°F and 2000°F) (1440°K between 1811 and 1366°K) is difficult to rationalize (see photomicrographs in Figure 9). Instead, $Cr_{23}C_6$ is believed thermodynamically stable in the compositions at 2800°F to at least 2850°F (1811 to 1839°K) the highest temperature investigated. This is intended not to dispute the Cr-C phase diagram data, but to emphasize that alloying with tantalum, titanium or columbium must

act to raise the (Cr, C, M) - $(Cr, M)_{23}C_6$ eutectic temperature and decrease carbon solubility. * A representation of the influence these elements are thought to have on the Cr-C system is given in Figure 11.

Evidence that the $Cr_{23}C_6$ carbide did not form in the Cr-(Ta, Ti or Cb)-C alloys by precipitation from solid solution during cooling from 2800°F and 2850°F (1811 and 1839°K) was obtained from examination of the microstructure of the Cr-.5Ta-.5C alloy developed by annealing at these temperatures for an extended time. The microstructure of this alloy developed by annealing for 20 hours at 2850°F (1839°K) is displayed in Figure 12. Particles, star-like in shape, dominate the structure. A very few globular shaped particles are also present. Electron microprobe analysis of the star-like particles revealed them to be rich in chromium at a level slightly below that of the matrix; strong evidence that the phase is $Cr_{23}C_6$. The very few globular particles in the microstructure proved rich in tantalum indicating they are TaC. Formation of particles of these morphologies by precipitation from solid solution during cooling from the 2850°F (1839°K) heat treatment temperature is unlikely. Instead, the microstructure is thought to have formed by separation of the $Cr_{23}C_6$ grain boundary network, which apparently forms early during heat treatment (see Figure 9), into small segments, each segment eventually with time developing a star-like morphology. Movement of grain boundaries by grain growth results in a major portion of the $Cr_{23}C_6$ phase assuming intragranular locations. Similar microstructures were developed by heat treatment for extended times at 2800°F and 2900°F (1811 and 1866°K). Dominance of the microstructure by $Cr_{23}C_6$ particles also confirm the phase transformation relationship proposed for the Cr-(Ta, Ti or Cr)-C alloys, i.e., that basically this carbide alone is stable in these compositions above approximately 2800°F (1811°K).

Measurement of high temperature stress-rupture and tensile properties formed a major part of this program. A description of tensile properties at 1900°F and 2100°F (1311 and 1422°K) and rupture strength at 12 to 15 ksi and 2100°F (83 to 104 MN/M^2 and 1422°K) were of paramount importance to ascertain the potential of the compositions for elevated temperature application.

---

*M = Ta, Ti or Cb in solid solution.

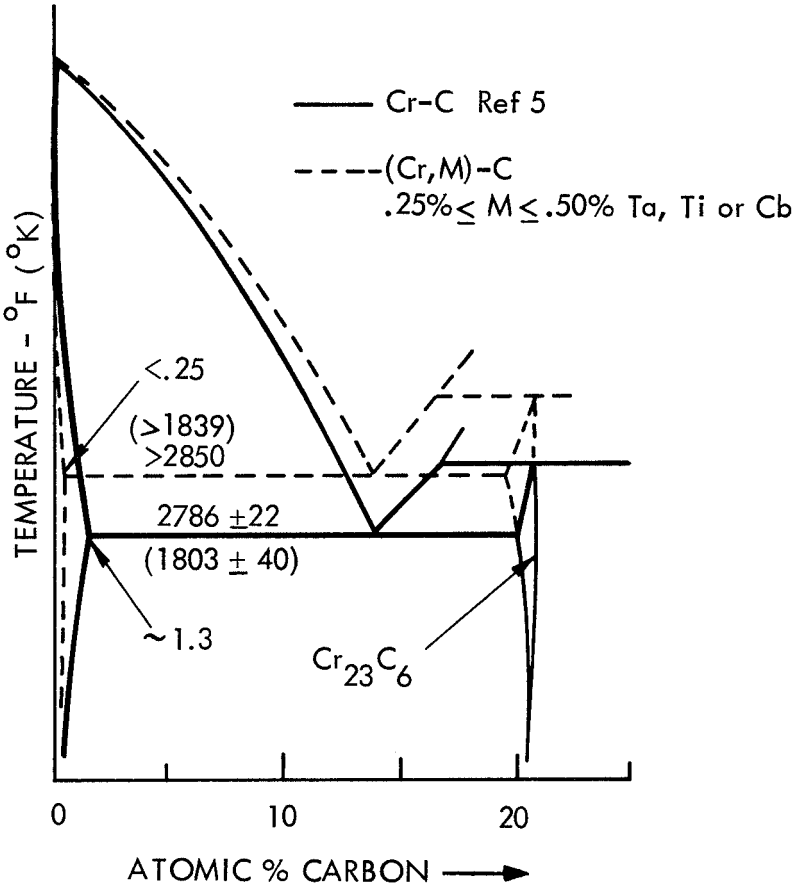

Figure 11. The Influence .25 to .50 a/o Ta, Ti or Cb has on the Cr-C Phase System

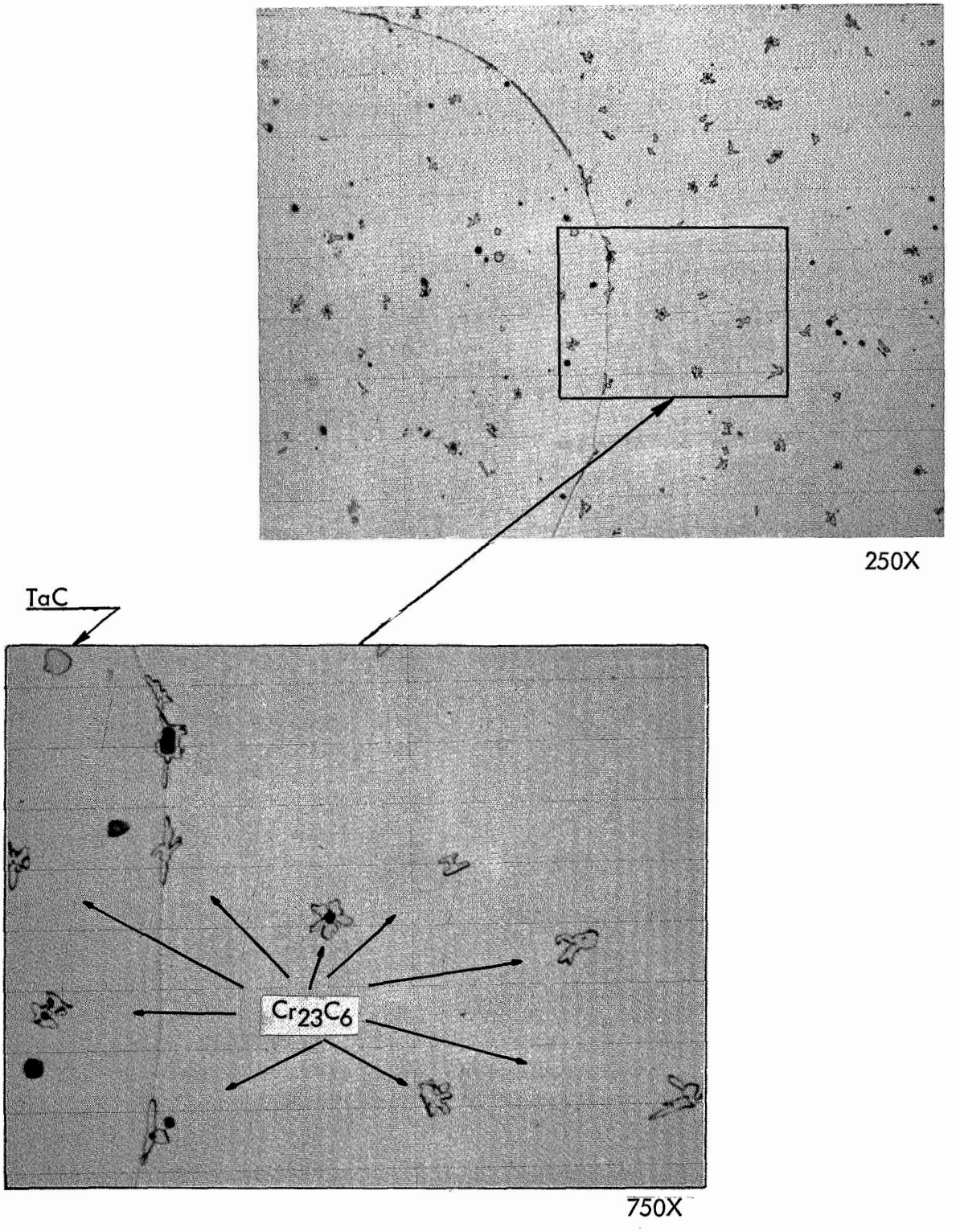

Figure 12. Microstructure of the Cr-.5Ta-.5C-.05Y Alloy Developed by Heat Treatment for 20 Hours at 2850°F (1839°K)

Since dispersion strengthening is the only mechanism likely in the study alloys to be effective at these temperatures, any process which might alter the morphological character and distribution of particles could have a pronounced influence on properaties. Aging to form a monocarbide precipitate in the Cr-(Ta, Ti or Cb)-C compositions after first heat treating to form $Cr_{23}C_6$ was recognized as a treatment which might be effective in this respect. In his investigation of the Mo-1.6Cb-1Ti-.3Zr-.6C alloy, Perkins[6], found that aging the alloy to precipitate CbC after higher temperature heat treatment to form Mo_2C optimized creep strength. He referred to the aging process as a carbide interchange reaction. The responses of hardness and microstructure were observed to judge whether the $Cr_{23}C_6$-to-monocarbide interchange reaction might strengthen the Cr-(Ta, Ti or Cb)-C alloys.

The hardness responses displayed by the Cr-.5(Ta or Ti)-.5C compositions upon aging at 2100°F and 2400°F (1422 and 1589°K) after first heat treating to form the $Cr_{23}C_6$ carbide, are shown in Figures 13 and 14. The results are compared to the hardness of as fabricated material simply annealed at 2100°F (1422°K). Heat treatment at 2900°F (1866°K) for 15 minutes was used to form the $Cr_{23}C_6$ phase.

Hardness of 180 DPH on the Cr-.5Ta-.5C alloy and 150 DPH on the Cr-.5Ti-.5C alloy were measured after formation of $Cr_{23}C_6$ by 2900°F (1866°K) heat treatment. Aging for 1 and 5 hours at 2100°F (1422°K) resulted in marked increases in the hardness of both alloys; and after 100 hours at 2100°F (1422°K), hardness remained above the level obtained after heat treatment to form $Cr_{23}C_6$. By comparison, a pronounced overaged condition was developed by aging for 20 hours at 2400°F (1589°K). Annealing as fabricated material at 2100°F (1422°K) caused hardness to decrease as a result of recrystallization to a level below that attained at this temperature by the carbide interchange process.

The microstructures developed in these alloys by annealing at 2900°F (1866°K) for 15 minutes are shown in Figure 15. Grain boundary precipitation of the $Cr_{23}C_6$ phase is almost continuous, and the structures at magnification of 300X compare well with that developed by annealing for 1 hour at 2800°F to 2850°F (1811 to 1839°K) - see Figure 9. Some fine intragranular precipi-

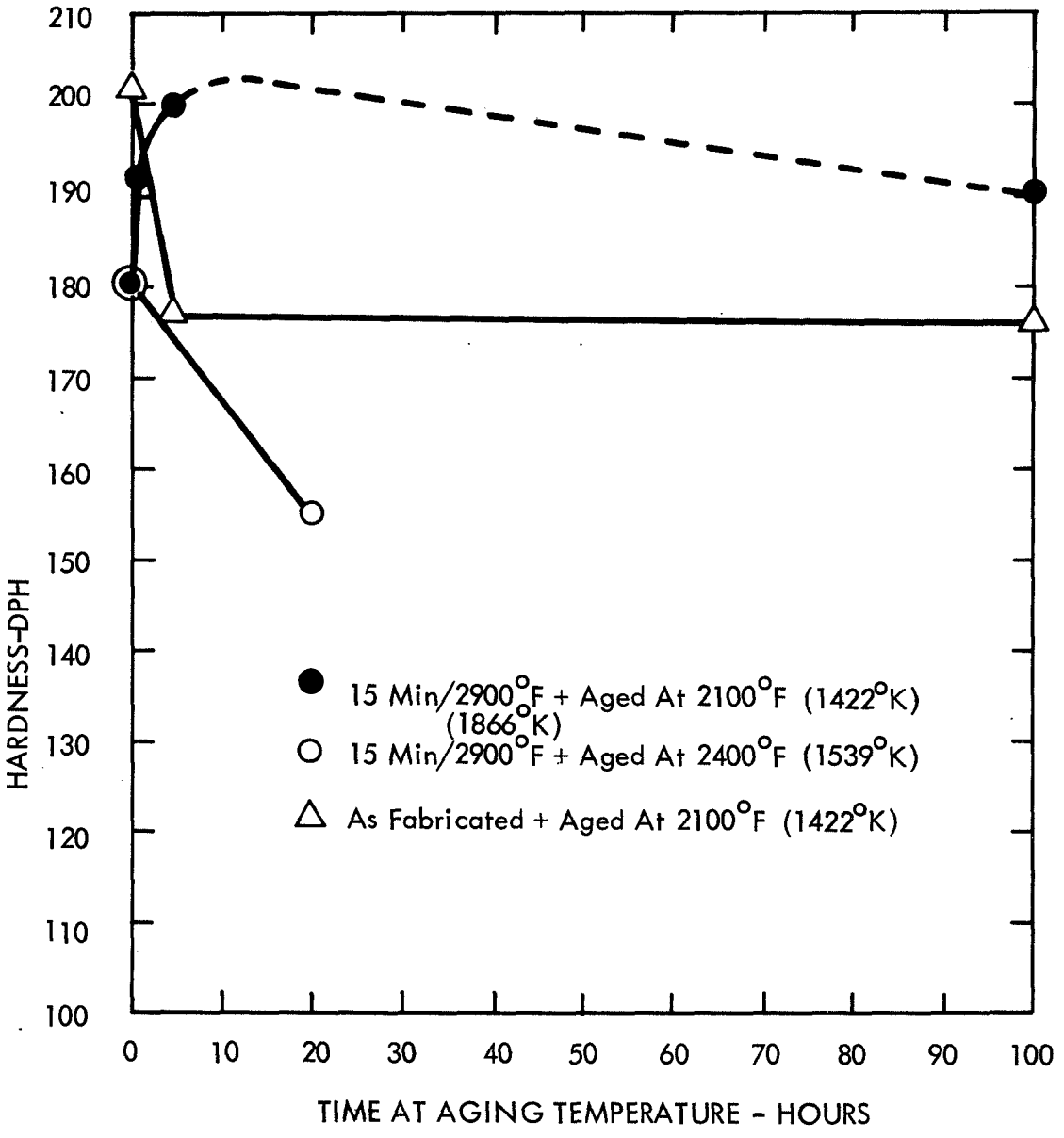

Figure 13. Hardness Response of the Cr-.5Ta-.5C-.05Y Alloy to Simple Annealing at 2100°F and Carbide Interchange Aging at 2100°F and 2400°F

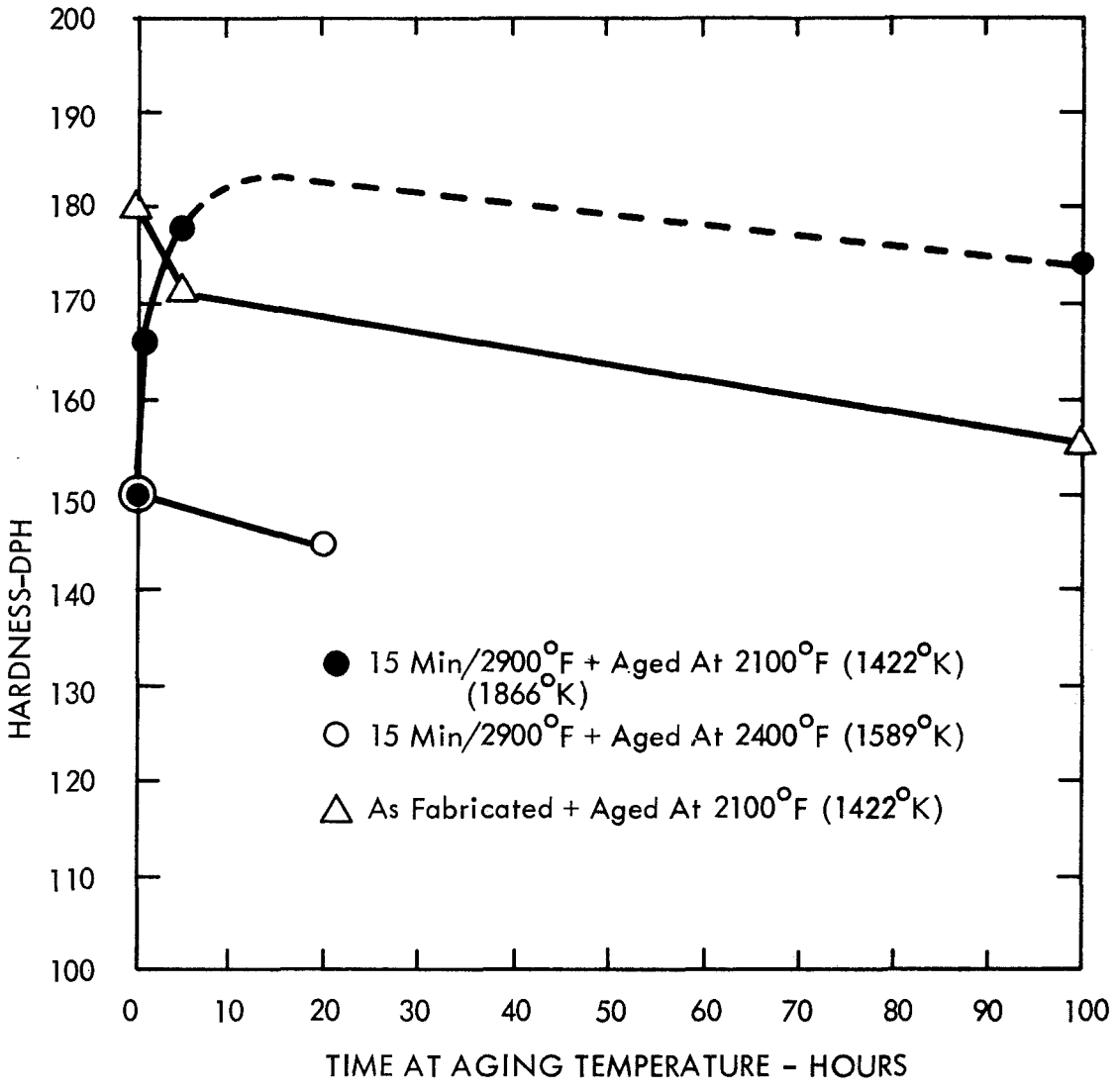

Figure 14. Hardness Response of the Cr-.5Ti-.5C-.05Y Alloy to Simple Annealing at 2100°F and Carbide Interchange Aging at 2100°F and 2400°F

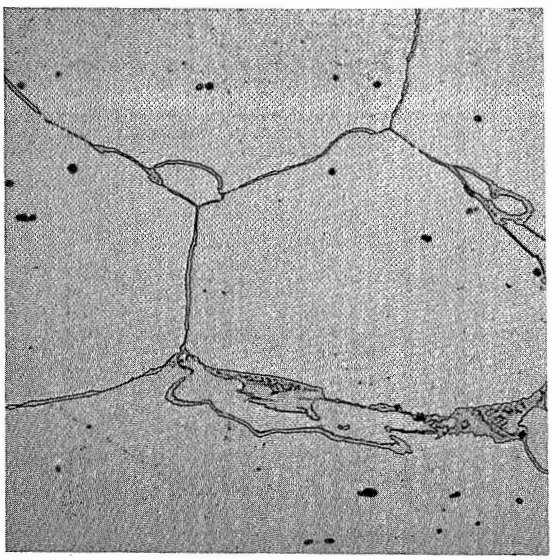

300X

Cr-.5Ta-.5C-.05Y

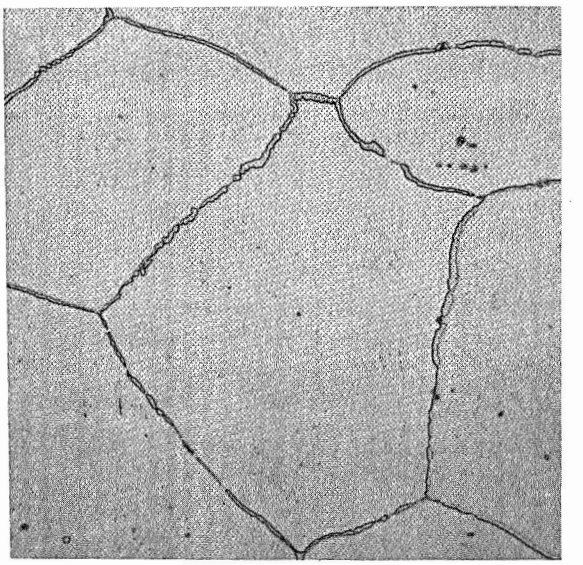

300X

Cr-.5Ti-.5C-.05Y

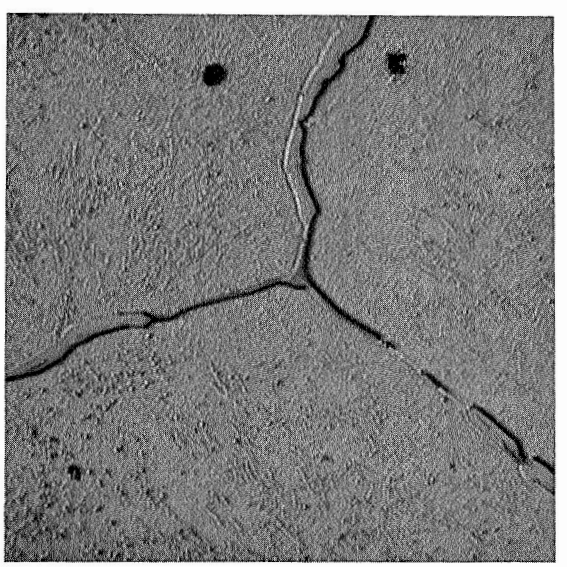

1500X

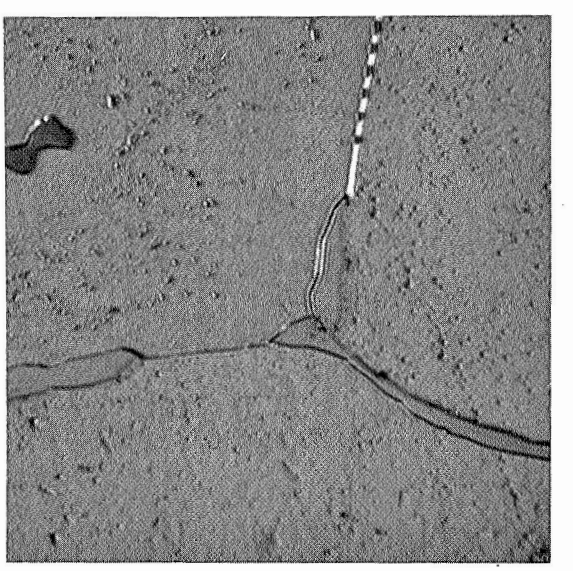

1500X

Figure 15. Microstructures of Alloys Cr-.5Ta-.5C-.05Y and Cr-.5Ti-.5C-.05Y Developed by Heat Treatment for 15 Minutes at 2900°F (1866°K)

tation can be seen in the photomicrographs taken at 1500X. This is probably monocarbide precipitation due to decreasing metal addition and carbon solubilities in the chromium matrix with decreasing temperature.

Photomicrographs showing the condition developed in the Cr-.5(Ta or Ti)-.5C alloys by aging at 2100°F (1422°K) after heat treatment to form the $Cr_{23}C_6$ carbide are presented in Figures 16 and 17. The low magnification (300X) photomicrographs reveal a steady dissolutioning of the $Cr_{23}C_6$ grain boundary phase with aging time to the point where little is remaining after 100 hours. This phase, which is essentially continous in the 15 min/2900°F (1866°K) annealed condition, becomes discontinuous after a few hours of aging at 2100°F (1422°K) as is obvious from the microstructures representing 1 and 5 hours treatment at this temperature. The high magnification (1500X) photomicrographs do not reveal any major change in amount or morphology of the intragranular monocarbide precipitate with aging time of up to 100 hours. Some evidence that intragranular precipitation may favor alignment along certain preferred crystal planes is apparent, but precipitation is generally too random to suggest any definite Widmanstatten relationship.

Photomicrographs of the condition developed in the Cr-.5(Ta or Ti)-.5C compositions by aging for 20 hours at 2400°F (1589°K) after heat treatment to form $C_{23}C_6$ are shown in Figure 18. Monocarbide particles formed by this treatment are larger and more separated as compared to those resulting from aging at 2100°F (1422°K). This condition is consistent with overaging as indicated previously by the marked decrease of hardness to well below the level developed by heat treatment to form the $Cr_{23}C_6$ phase (see Figures 13 and 14).

Hardness changes caused by 2100°F (1422°K) aging after 15 min/2900°F (1866°K) treatment were also examined for the five Cr-.5(Cb, Zr or Hf)-.5C and Cr-.25(Ta or Cb)-.25C composition. The results are presented in Figure 19. The Cr-(Ta or Cb)-C alloys all displayed hardening and overaging as the carbide interchange processes proceeded with time at 2100°F (1422°K). Behavior of the Cr-.5Cb-.5C composition was similar to the Cr-.5Ta-.5C alloy, while that of the Cr-.25Ta-.25C alloy paralleled the Cr-.5Ti-.5C composition (compare with

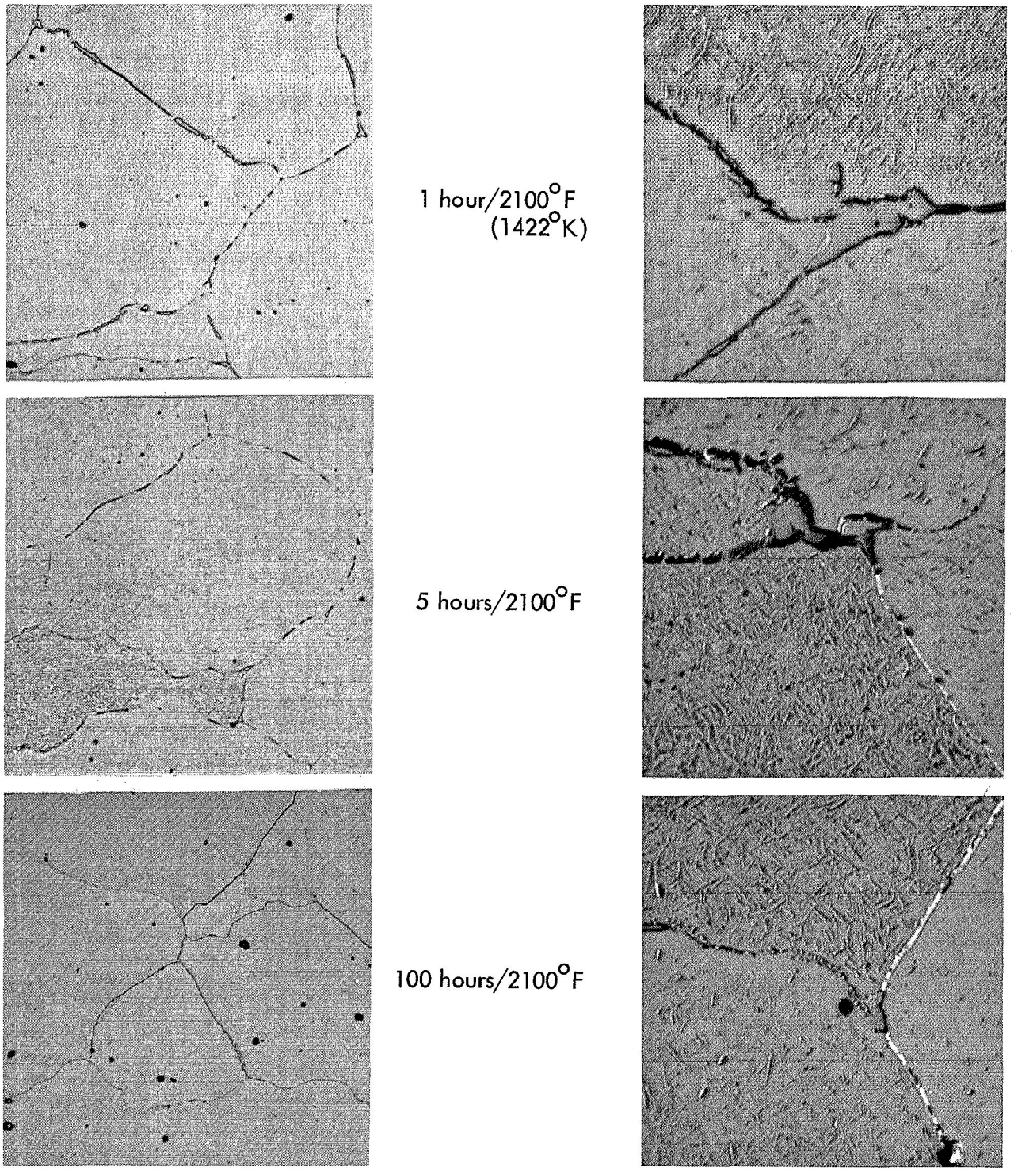

Figure 16. Microstructures of the Cr-.5Ta-.5C-.05Y Alloy Developed by Carbide Interchange Aging at 2100°F after $Cr_{23}C_6$ Formation by 15 Min./2900°F Heat Treatment. Left - 300X. Right - 1500X. (1866°K)

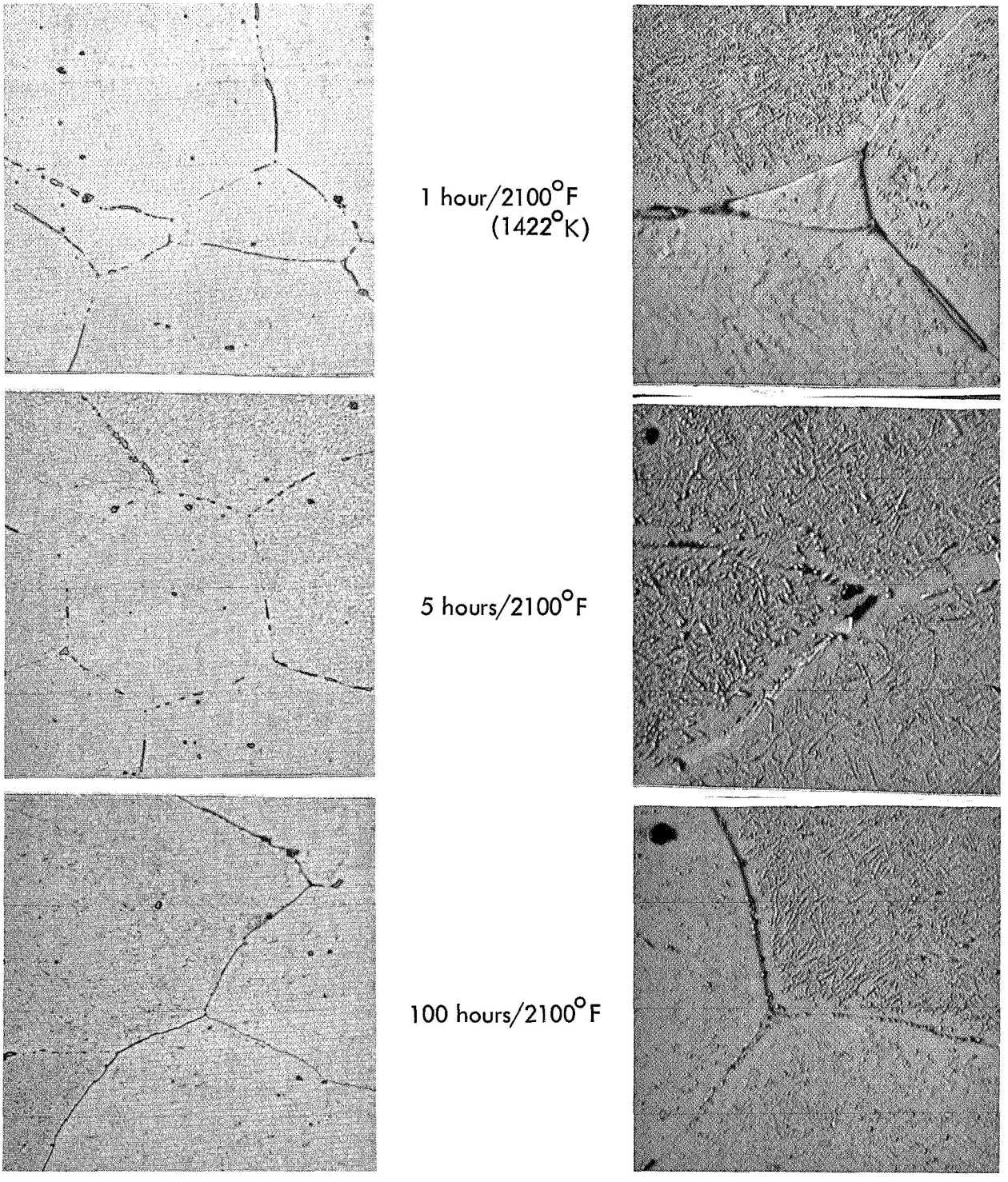

Figure 17. Microstructures of the Cr-.5Ti-.5C-.05Y Alloy Developed by Carbide Interchanging Aging at 2100°F after $Cr_{23}C_6$ Formation by 15 Min./2900°F Heat Treatment. Left - 300X. Right - 1500X. (1866°K)

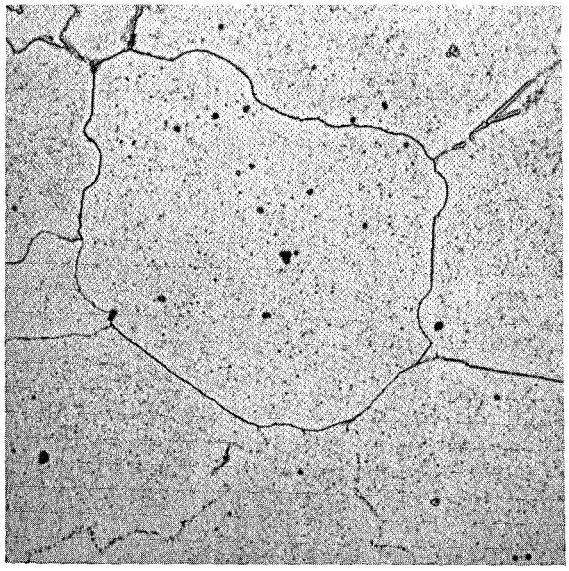

300X

Cr-.5Ta-.5C-.05Y

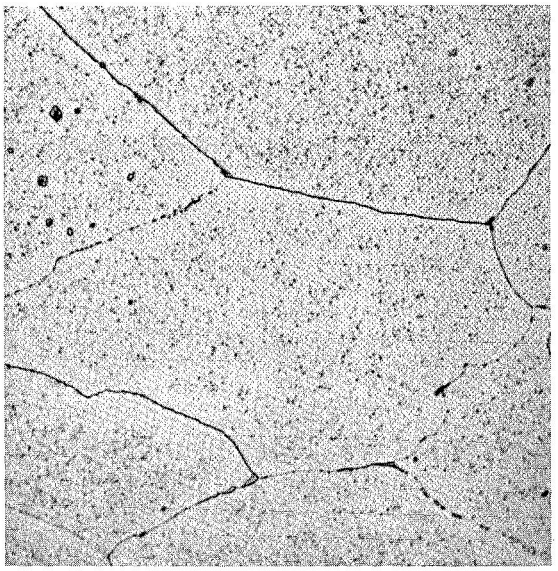

300X

Cr-.5Ti-.5C-.05Y

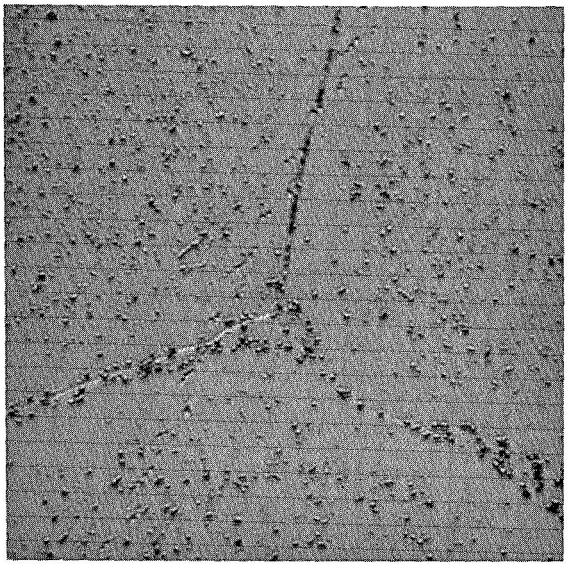

1500X

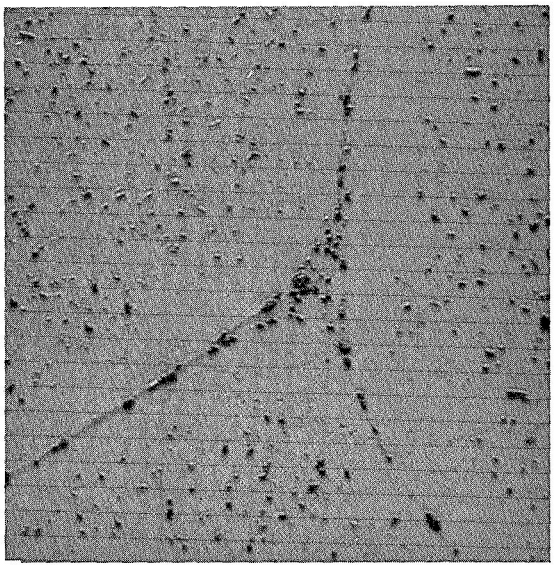

1500X

Figure 18. Microstructures of the Cr-.5Ta-.5C-.05Y and Cr-.5Ti-.5C-.05Y Alloys Developed by Carbide Interchange Aging at 2400°F (1589°K) after $Cr_{23}C_6$ Formation by 15 Min./2900°F (1866°K) Heat Treatment

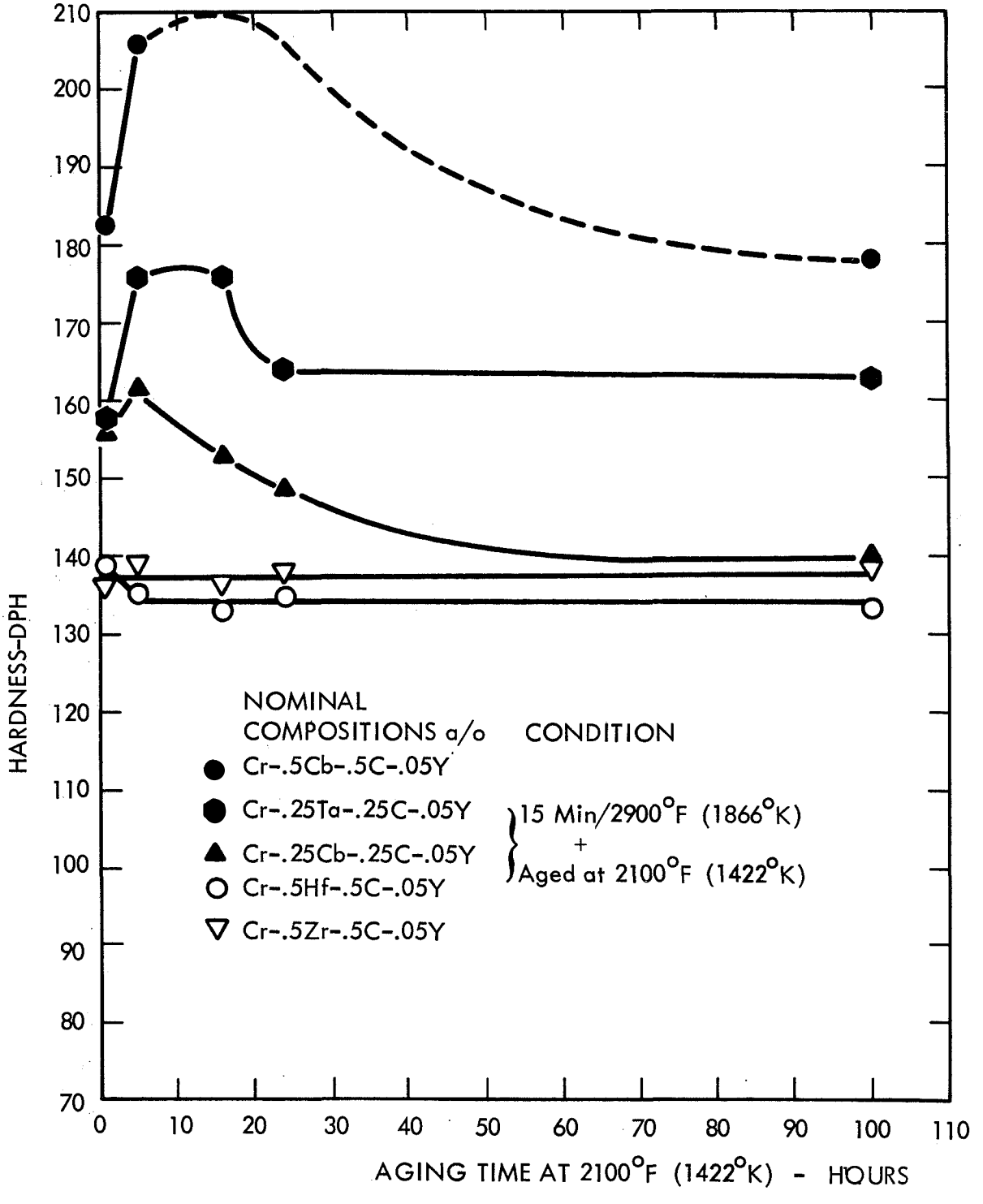

Figure 19. Hardness Response of the Cr-.5(Cb, Hf or Zr)-.5C and Cr-.25(Ta or Cb)-.25C Compositions to Aging at 2100°F after 15 min/2900°F Heat Treatment

Figures 13 and 14. The Cr-.25Cb-.25C alloy by comparison overaged rapidly and fell in hardness to a relatively low level. Response of hardness to aging at 2100°F (1422°K) after 15 min/2900°F (1866°K) heat treatment was not observed on the Cr-.5(Zr or Hf)-.5C compositions. This result would be anticipated since, as previously discussed, large particles of ZrC and HfC remained in the structures of these alloys after heat treatment at 2850°F (1839°K), and annealing just 50°F (28°K) higher would be unlikely to bring about solution treatment or a shift in carbide stability to the $Cr_{23}C_6$ phase.

Precipitate particles of the TaC phase formed in the Cr-.5Ta-.5C alloy at 2100°F (1422°K) by the carbide interchange reaction were extracted and examined by electron microscopy to define their morphology. Electron micrographs of TaC particles developed by 1, 5 and 100 hours of carbide interchange at 2100°F (1422°K) are presented in Figure 20. Difficulty was encountered in locating regions on the microscopy grids where particles were separated sufficiently for photographing. Particles of the phase seemed to be attracted into piles, presumably due to their apparent thin flake-like character, i.e., high surface area. Many particles overlap each other in the photographs presented in Figure 20. A description as thin platelets of no definite shape characterizes the TaC particle morphology representing 1 and 5 hour aging at 2100°F (1422°K). The particles developed by 100 hours at 2100°F (1422°K) were thicker and more disc-like in proportions.

The TaC particles formed in the Cr-.5Ta-.5C alloy by the carbide interchange process at 2100°F (1422°K) obviously defied characterization by size and distribution. However, comparison of particle morphology developed by carbide interchange was made to that found in the alloy after simply annealing at 2100°F (1422°K). Electron micrographs of the TaC phase as extracted from the Cr-.5Ta-.5C alloy annealed for 1, 5 and 100 hours at 2100°F (1422°K) are shown in Figure 21. For the most part, particles developed by these conditions were nearly spheroidal in shape permitting measurement of particle size distribution, results of which are also given in Figure 21. Particles of TaC 0.1 micron in size or smaller formed approximately 85% of the distribution representing a 1 hour anneal at 2100°F (1422°K) and 35% were 0.05 micron or smaller. A similar distribution was measured for precipitates representing 5 hours of

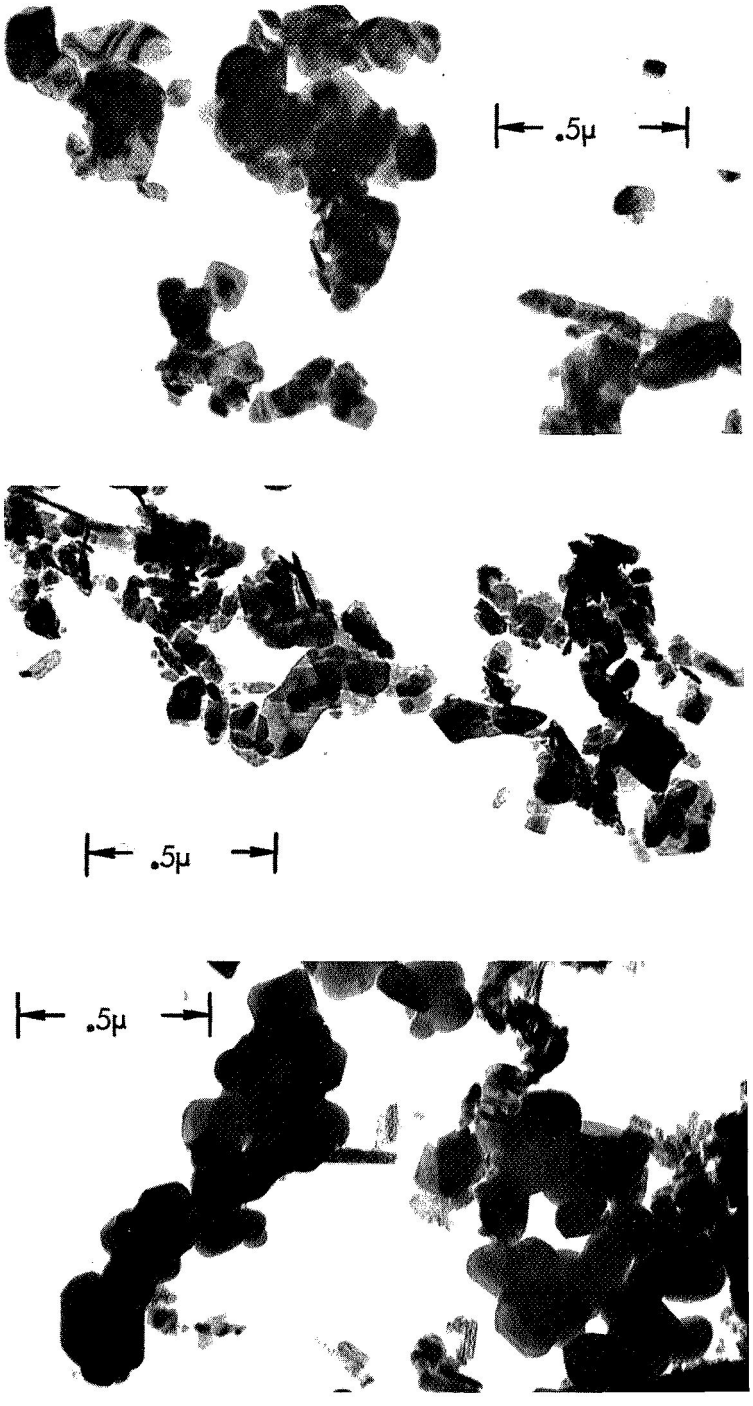

Figure 20. Morphology of Tantalum Carbide Particles Developed in the Cr-.5Ta-.5C-.05Y Alloy by Carbide Interchange Aging at 2100°F after $Cr_{23}C_6$ Formation by 15 Min./2900°F Heat Treatment. 50,000X

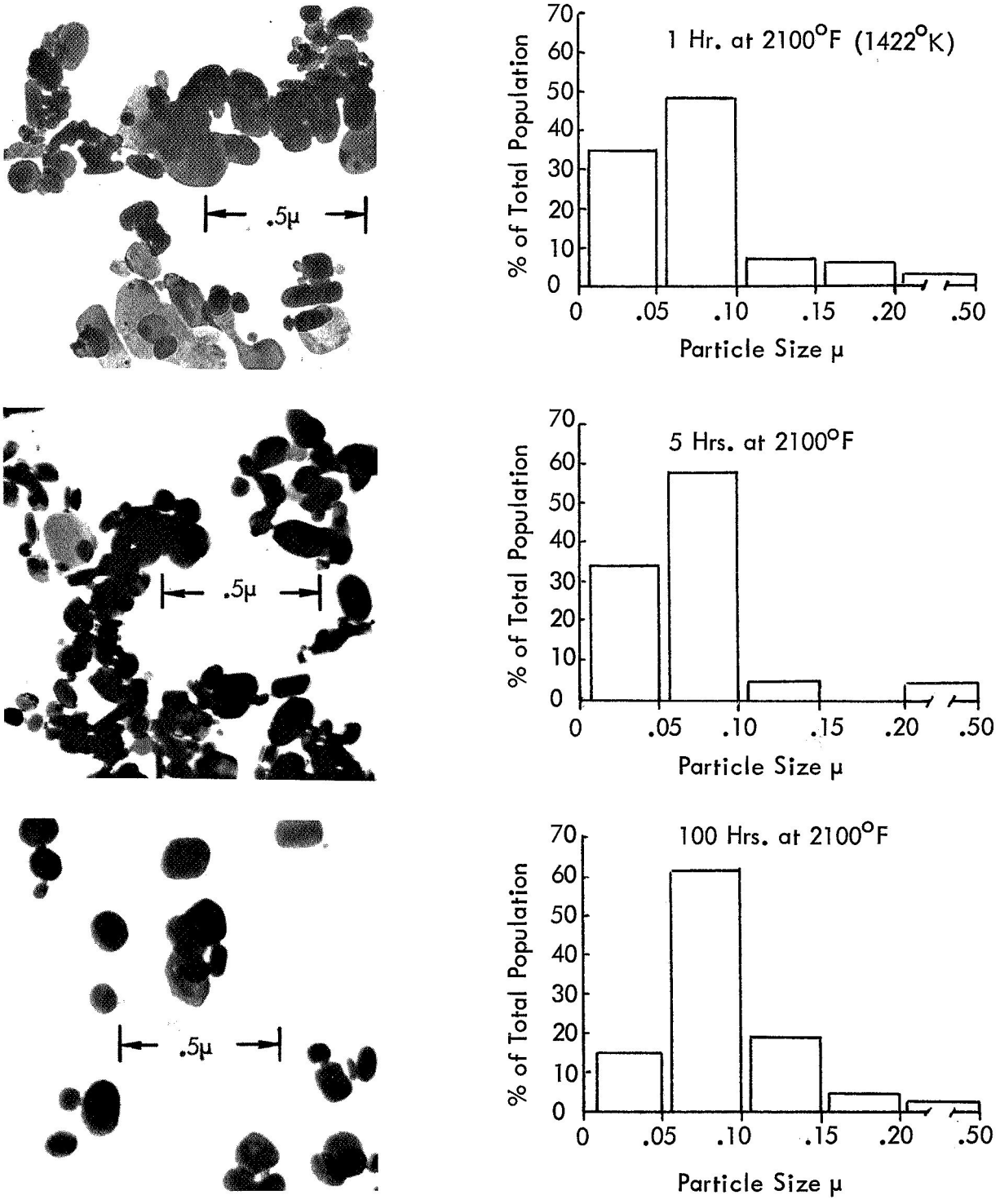

Figure 21. Morphology and Size Distribution of Tantalum Carbide Particles Found in the Cr-.5Ta-.5C-.05Y Alloy after Annealing As Fabricated Material for 1, 5 and 100 Hours at 2100°F. 50,000X Photographed particles not necessarily representative of measured distributions.

annealing at 2100°F (1422°K) - approximately 95% of the particles being smaller than 0.1 micron, and 35% smaller than 0.05 micron. The proportion of particles in the less than 0.05 micron range decreased to 15% after annealing for 100 hours at 2100°F (1422°K) while the percentage in the 0.06 to 0.10 micron range remained much the same as measured for the 1 hour and 5 hour annealed samples. A larger portion of particles in the 0.11 to 0.15 micron range was also found in the sample representing 100 hr/2100°F (1422°K) treatment compared to the 1 hr/2100°F (1422°K) and 5 hr/2100°F (1422°K) conditions.

Particle size and distribution of the TaC phase was also measured in the Cr-.5Ta-.5C alloy for the as fabricated and 1 hr/2400°F (1589°K) recrystallized condition. Much of the mechanical property evaluation of study alloys was performed on samples in these conditions. The results are shown in Figure 22. Approximately 85% of the TaC particles characterizing the as fabricated condition were 0.1 micron or smaller, but about 65% were in the < 0.05 micron range. Annealing for 1 hour at 2400°F (1589°K) decreased the proportion of particles in the < 0.05 micron range to 35% and increased those betwen 0.06 and 0.1 micron to 50%.

Boride Strengthened Alloys

Four boride strengthened compositions, Cr-.5(Ta or Hf)-1B and Cr-.5(Ta or Cb)-.5B, were prepared as 10 pound (4.54 kg) ingots and converted to rod for evaluation of properties. Photomicrographs showing the as cast condition of each composition are given in Figure 23. A massive continuous grain boundary phase formed in the Cr-.5(Ta or Hf)-1B compositions. A smaller somewhat less continuous intergranular phase developed in the Cr-.5(Ta or Cb)-5B alloys. Efforts were not made to identify the intergranular phases. Formation of intragranular precipitation was not obvious in the as cast structure of the boride strengthened alloys.

Photomicrographs of the as fabricated structures of these alloys are displayed in Figure 24. Fabrication by extrusion and swaging at 2100°F to 2200°F (1422 to 1477°K) developed completely wrought microstructures in the Cr-Ta or Cb-B compositions but a fully recrystallized microstructure in the Cr-.5Hf-1B alloy. Significantly higher hardness was developed for the

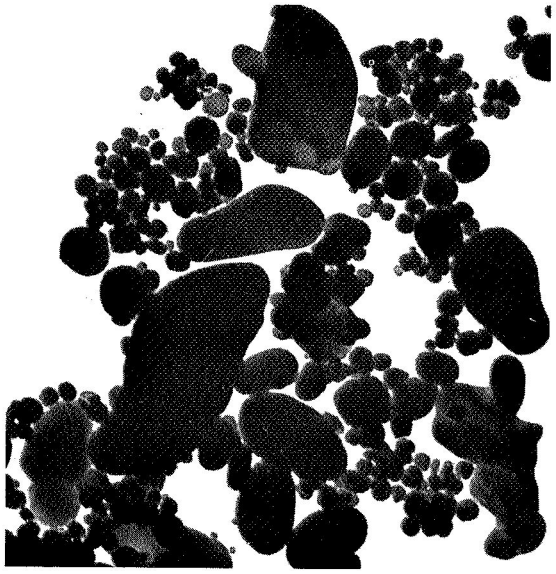

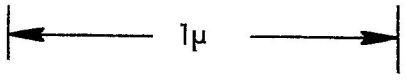

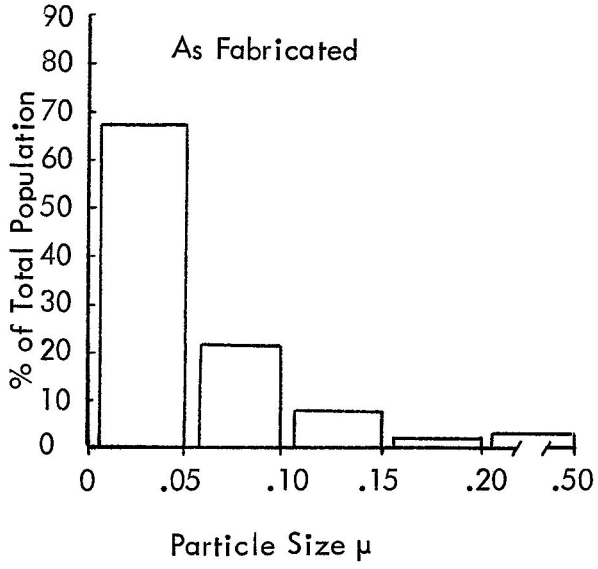

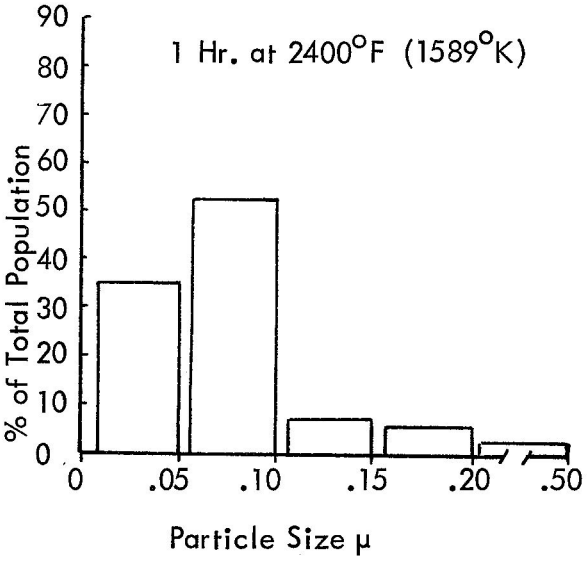

Figure 22. Morphology and Size Distribution of Tantalum Carbide Particles Found in the Cr-.5Ta-.5C-.05Y Alloy in the As Fabricated and 1 Hr./2400°F Recrystallized Conditions. 50,000X Photographed particles not necessarily representative of measured distributions.

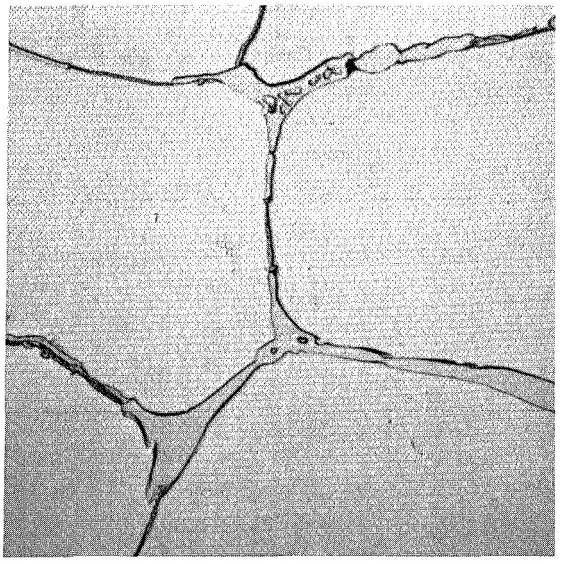

Cr-.5Ta-1B-.05Y

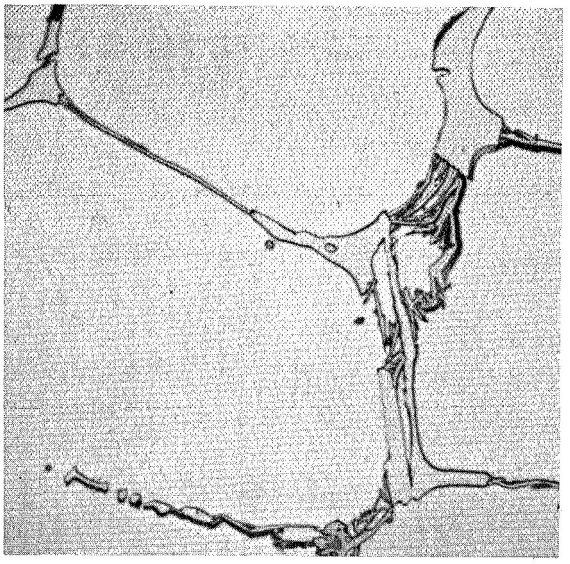

Cr-.5Hf-1B-.05Y

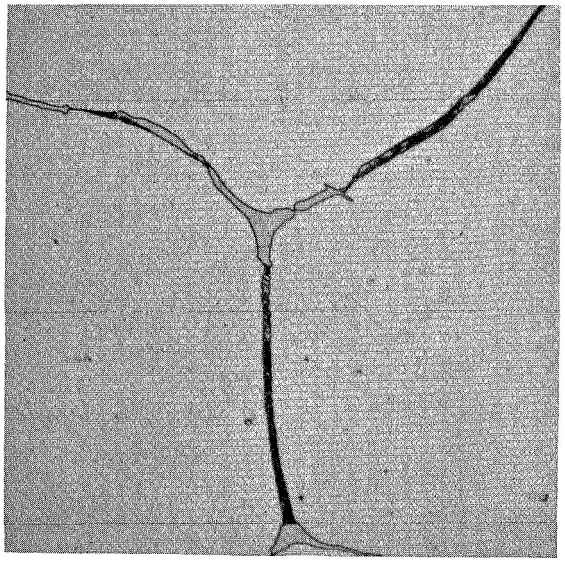

Cr-.5Cb-.5B-.05Y

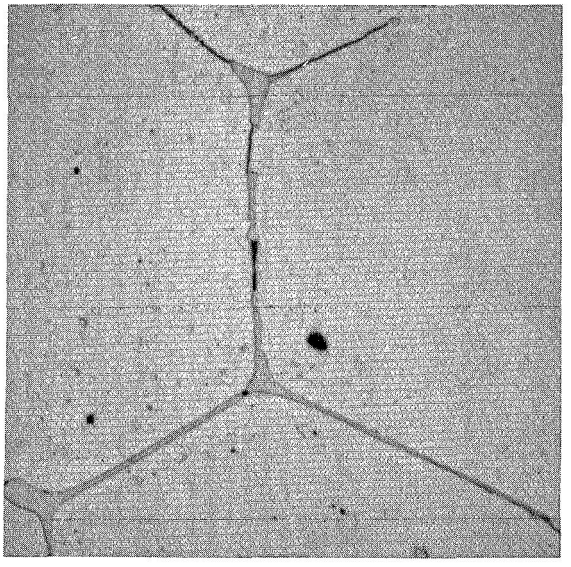

Cr-.5Ta-.5B-.05Y

Figure 23. Microstructures of As Cast Boride Strengthened Alloys 500X

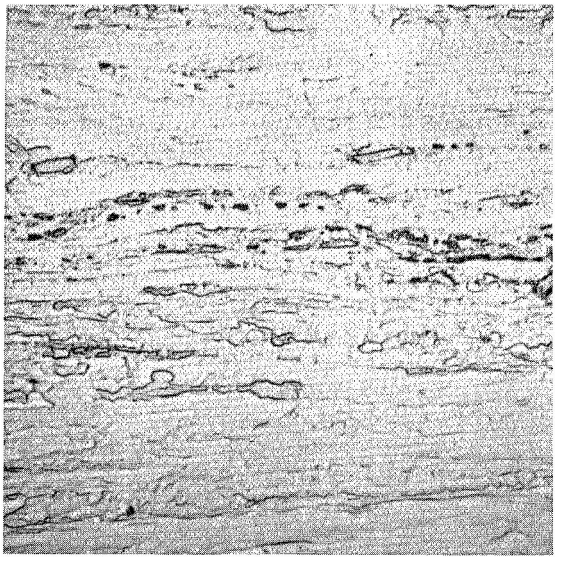

Cr-.5Ta-1B-.05Y

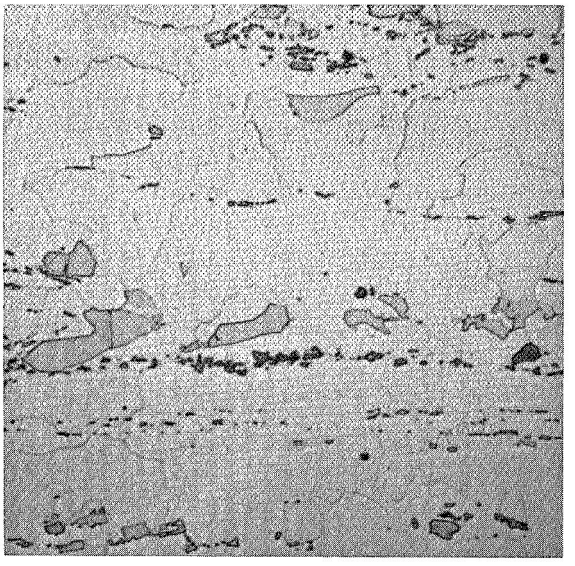

Cr-.5Hf-1B-.05Y

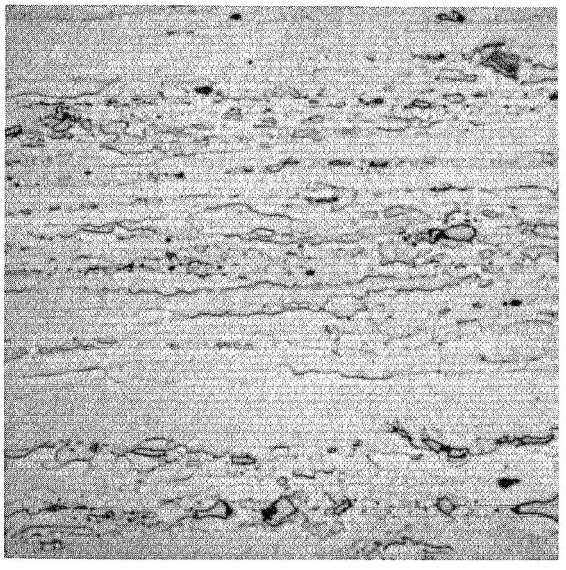

Cr-.5Cb-.5B-.05Y

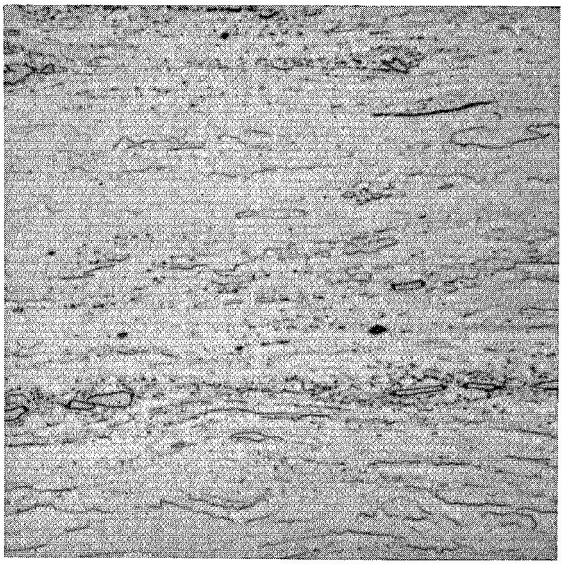

Cr-.5Ta-.5B-.05Y

Figure 24. Microstructures of As Fabricated Boride Strengthened Alloys 500X

as fabricated condition of the Cr-(Ta or Cb)-B compositions than on any of the previously discussed carbide compositions (see Table 3). Some large boride particles which are believed to be remnants of the intergranular phases formed in the as cast condition can be seen in the microstructures representing the as fabricated conditions. An especially large number of these particles were found in the Cr-.5Hf-1B alloy. Small dark grey particles associated together in lines were also found in the microstructure of this alloy. These are believed to be oxide particles, probably HfO_2. This alloy had a high, 0.39 a/o, oxygen content (see Table 2), and as a consequence, oxides of the reactive metal addition would be expected to be present.

Microstructures developed in the Cr-.5(Ta or Hf)-1B compositions by heat treatment for 1 hour at 2400°F to 2860°F (1589 to 1844°K) are shown in Figure 25. Annealing for 1 hour at 2400°F (1589°K) was sufficient to completely recrystallize the Cr-.5Ta-1B alloy. Large second phase particles were found in the microstructure of this composition after annealing at 2400 to 2860°F (1589 to 1844°K). Whether the particles present after heat treatment might be remnants of the original intergranular phase found in the as cast condition, or another phase or phases, could not be deduced from microstructural appearance. The Cr-.5Hf-1B alloy responded to increasing heat treatment temperature in much the same manner except evidence of liquation was noted in 1 hr/2860°F (1844°K) heat treated material. A eutectic-like structure present at grain boundary regions between large particles can be seen in the photomicrograph representing this alloy and condition. Although not obvious in the photomicrograph shown, similar evidence of liquation was also noted after heat treatment at 2860°F (1844°K) in the Cr-.5Ta-1B alloy. The reported Cr-Cr_4B eutectic temperature lies at 2860°F[7], and, as will be discussed next, Cr_4B was observed as a high temperature phase in these alloys.

Precipitates present in the Cr-.5(Ta or Hf)-1B alloys in the as fabricated and 1 hr/2600°F (1700°K) and 1 hr/2800°F (1811°K) annealed conditions were extracted and examined by x-ray diffraction analysis. The boride phases Cr_4B, HfB, and HfB_2 were identified in the samples representing these conditions of the Cr-.5Hf-1B alloy. A small amount of HfO_2 was also detected in these samples resulting undoubtedly from the high oxygen level in the alloy previously mentioned. Stability of three borides is unlikely since, to a first approximation, the alloy is a ternary composition. Because of this result and the major oxygen contamination of the

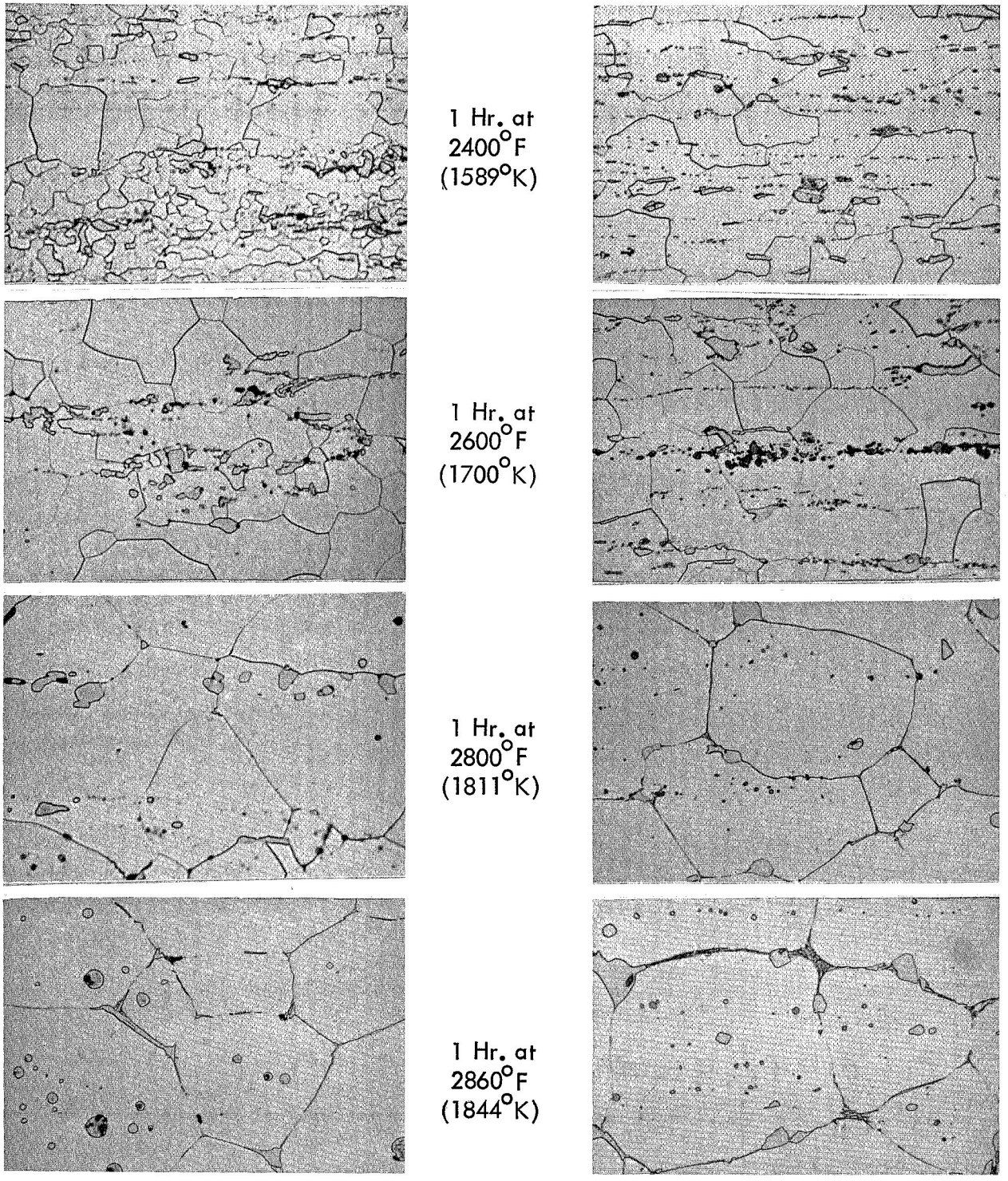

Figure 25. Microstructural Response of Cr-.5Ta-1B-.05Y (left)and Cr-.5Hf-1B-.05Y (right) to Heat Treatment for 1 Hour at 2400°F to 2860°F 250X

alloy, a definitive statement concerning actual phase stability for the Cr-.5Hf-1B alloy cannot be made.

The x-ray diffraction patterns obtained on the boride particles extracted from the Cr-.5Ta-1B alloy in the as fabricated and 1 hr/2600°F (1700°K) conditions were identical but could not be indexed. The diffraction pattern obtained from the sample representing the 1 hr/2800°F (1811°K) condition of this alloy indexed with Cr_4B. These data are reported in Table 5. Diffraction lines corresponding to the Cr_4B phase are present in the patterns representing the as fabricated and 1 hr/2600°F (1700°K) conditions. Attempts made to index the lines of these patterns remaining after eliminating those corresponding to Cr_4B were unsuccessful. Attention is drawn to this set of lines in Table 5. Results of a more detailed examination of how composition and temperature affect boride stability, however, which is discussed in the third part of this report section, suggest that these diffraction lines probably resulted from the presence of a complex tantalum rich boride. This boride will be referred to as the X phase and its diffraction pattern as the X pattern in discussion of boride stability in the Cr-.5(Ta or Cb)-.5B alloys to follow.

Microstructural response of compositions Cr-.5(Ta or Cb)-.5B to heat treatment for 1 hour at 2400°F to 2800°F (1589 to 1811°K) is presented in Figure 26. Heat treatment for 1 hour at 2400°F (1589°K) was sufficient to develop a recrystallized microstructure in both alloys. Heat treatment for 1 hour at 2600°F (1700°K) caused noticeable grain growth over the 1 hr/2400°F (1589°K) condition in the Cr-.5Cb-.5B alloy and development of a few large second phase particles. Very little grain growth over the 1 hr/2400°F (1589°K) level resulted from 1 hr/2600°F (1700°K) heat treatment of the Cr-.5Ta-.5B alloy. The fine intragranular precipitates obvious in the microstructure of the alloy representing 1 hr/2600°F (1700°K) treatment may have restricted grain growth. Microstructures of both alloys in the 1 hr/2800°F (1811°K) condition contained large second phase particles at grain boundaries and intragranular areas.

Table 5. X-ray Diffraction Analysis of Precipitate Phases Representing Three Conditions of the Cr-.5Ta-1B-.05Y Alloy

Diffraction Patterns Observed[1.]						Standard	
As fabricated		1 hr/2600°F		1 hr/2800°F		Calculated Cr_4B Pattern[2.]	
d	I	d	I	d	I	d	I
						3.678	3
						3.579	6
*3.19	W	3.19	W				
						2.949	5
*2.90	W	2.90	W				
*2.62	M-S	2.62	M-S				
*2.52	W	2.52	W				
2.28	M	2.28	M	2.28	M	2.300	36
*2.16	M	2.16	M				
2.10	M	2.10	M	2.10	M	2.108	72
2.03	S	2.03	S	2.03	S	2.044	97
1.96	W	1.96	W	1.95	M-W	1.953	20
*1.86	W	1.86	W			1.845	8
1.82	M	1.82	M	1.81	M	1.826	30
1.65	M	1.65	M	1.65	M	1.649	56
*1.61	W	1.61	W				
*1.43	VW	1.43	VW				
*1.37	VW	1.37	VW				

1. 2600°F = 1700°K
   2800°F = 1811°K
   Many diffraction lines of very weak intensity were observed below d = 1.37. These lines did not provide any additional help in phase identification.

2. E. A. Brandes, B. A. Hatt, Monthly Technical Progress Narrative, Nov. 1969, Contract NASW 1720.

*Denotes diffraction lines believed belonging to a single tantalum rich boride referred to as the X phase in the text.

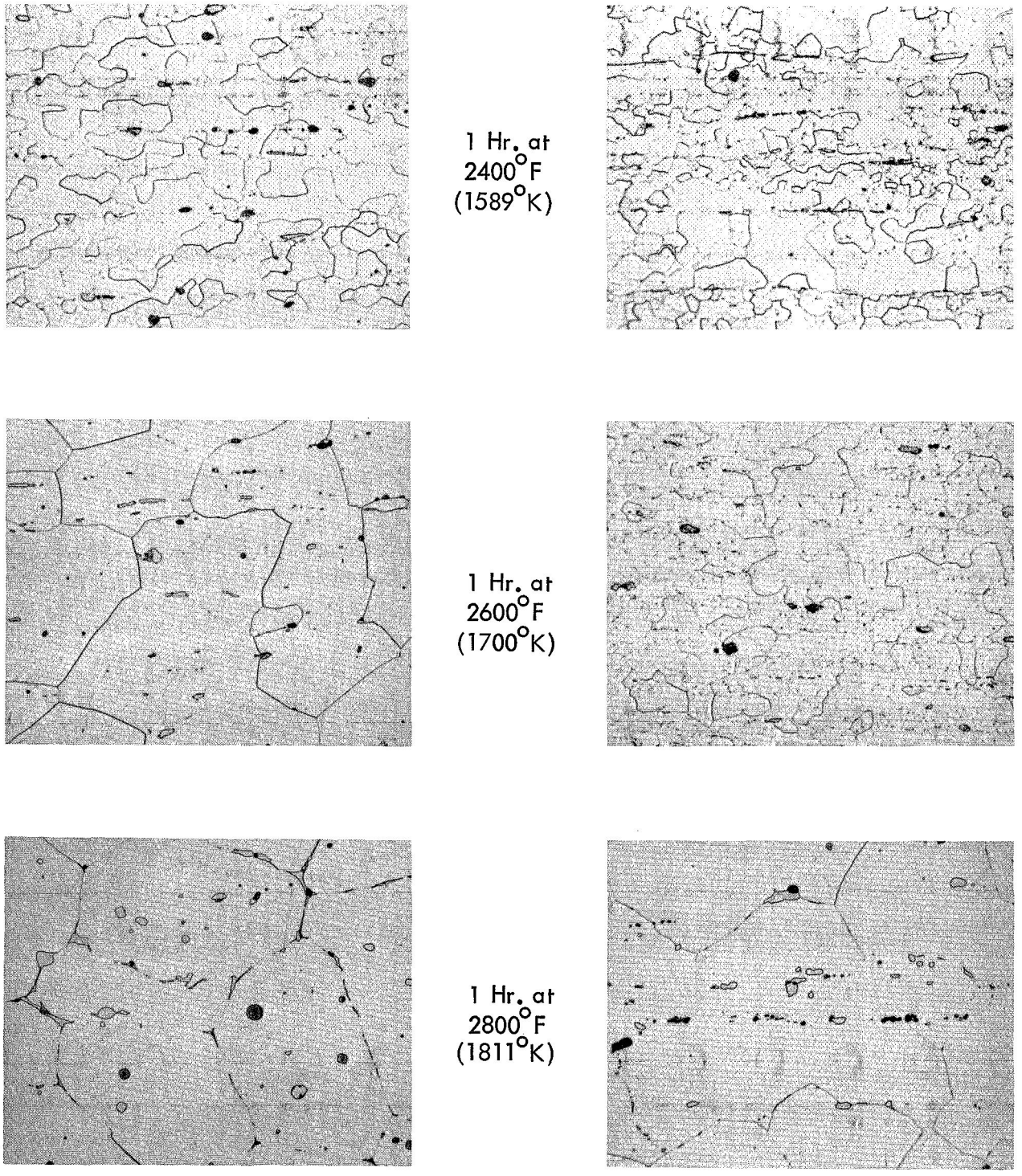

Figure 26. Microstructural Response of Cr-.5Cb-.5B-.05Y (left) and Cr-.5Ta-.5B-.05Y (right) to Heat Treatment for 1 Hour at 2400°F to 2800°F 250X

Boride phase stability over the temperature range 2100°F to 2700°F (1422 to 1755°K) was thoroughly investigated on the Cr-.5(Ta or Cb)-.5B compositions and is discussed in detail in the third part of this report section. In brief, the tantalum rich X phase boride plus Cr_4B were found to be stable over this temperature range in the Cr-.5Ta-.5B alloy. A boride rich in columbium which also gave the X diffraction pattern plus Cr_4B were stable in the Cr-.5Cb-.5B alloy from 2100°F to 2500°F (1422 to 1644°K). Only Cr_4B was stable in this composition at 2700°F (1755°K). These data, combined with the results of boride phase stability obtained on the Cr-.5Ta-1B composition, suggests the following phase transformation relationship in which M is Ta or Cb*.

$$(Cr)_{matrix} + Cr_4B + MxBy\ (X\ phase) \xrightarrow{T} (Cr, M)_{matrix} + Cr_4B$$

$2600°F \leq T \leq 2800°F$ in Cr-.5Ta-1B $\quad (1700°K \leq T \leq 1811°K)$
$2500°F \leq T \leq 2700°F$ in Cr-.5Cb-.5B $\quad (1644°K \leq T \leq 1755°K)$
$T > 2700°F$ in Cr-.5Ta-.5B $\quad T > 1755°K)$

It follows that temperature dependence of boride stability in Cr-(Ta or Cb)-B alloys is analogous to carbide stability in the Cr-(Ta or Cb)-C alloys, i.e., like the carbide compositions the boride compositions containing tantalum or columbium also display a transition in precipitate stability at high temperatures from a Ta or Cb rich compound to a chromium compound. However, development of the Cr_4B phase in these alloys by annealing for 1 hour at temperatures where the compound is stable does not occur by growth of a massive grain boundary precipitate as does formation of $Cr_{23}C_6$ in the carbide alloys. This conclusion is arrived at by noting the second phase morphology in the Cr-.5Ta-1B and Cr-.5Cb-.5B compositions annealed for 1 hour at 2800°F (1811°K) (see Figures 25 and 26). The Cr_4B phase alone was identified in these alloys after 1 hr/2800°F (1811°K) heat treatment, and for the most part it is present in the microstructures as large individual particles.

The response of hardness to one hour heat treatment at 2400°F to 3000°F (1589 to 1972°K) displayed by the boride alloys is reported in Figure 27. Increase of hardness after annealing the Cr-(Ta or Cb)-B compositions at high temperatures is consistent with solid solution hardening

*Solubility for alloying elements in the borides and in chromium below the temperature T is assumed small and ignored.

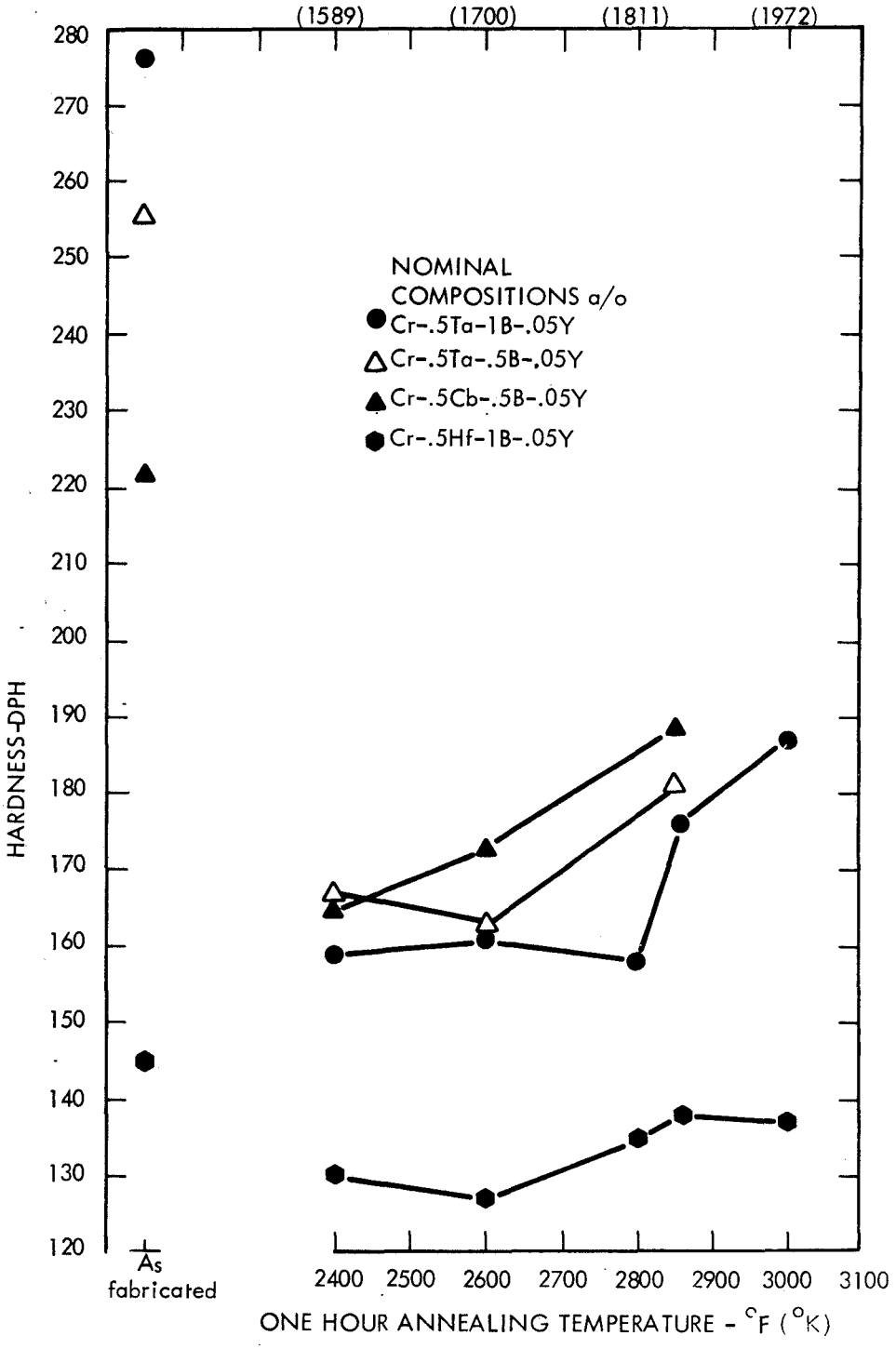

Figure 27. The Effect of Heat Treatment for One Hour at 2400°F to 3000°F on Hardness of the Boride Strengthened Study Alloys

of the chromium matrix by Cb and Ta resulting from $Cr + Cr_4B + MxBy \longrightarrow (Cr, M) + Cr_4B$ transformation. As previously mentioned, this transformation occurs in the Cr-.5Ta-.5B alloy above 2700°F (1755°K). It appears from the increase in hardness of this alloy after annealing at 2800°F (1811°K) that the actual transformation temperature is between 2700°F and 2800°F (1755 and 1811°K). Heat treatment of the Cr-.5Hf-1B composition from 2400 to 3000°F (1589 to 2255°K) did not cause any major change in hardness indicating analogous phase transformations do not occur in this alloy. This behavior is similar to that noted for the Cr-.5Hf-.5C alloy previously discussed, which also did not display a change of carbide stability from HfC to $Cr_{23}C_6$ up to approximately 2850°F (1839°K) the highest temperature investigated.

An examination of the hardness response displayed by the Cr-(Ta or Cb)-B alloys when aged at 2100°F (1422°K) after first heat treating to form Cr_4B was undertaken. A 15 minute anneal at 2800°F (1811°K) was used to form the Cr_4B phase. Results of the study are presented in Figure 28. The Cr-.5Hf-1B alloy was similarly heat treated and used as a control to judge hardness response against.

The Cr-(Ta or Cb)-B alloys displayed hardening and overaging as the boride interchange process proceeded with time at 2100°F (1422°K) in a manner similar to that observed for carbide interchange in the Cr-(Ta, Cb or Ti)-C alloys at this temperature. Peak hardness was greatest for the Cr-.5Cb-.5B alloy although after 50 hours at 2100°F (1422°K) the hardness level of this alloy and the Cr-.5Ta-.5B composition were similar. By comparison, the boride interchange process in the Cr-.5Ta-1B alloy resulted in lowest overall hardness behavior. As would be anticipated from the behavior of boride stability, hardness of the Cr-.5Hf-1B alloy did not respond to aging at 2100°F (1422°K) following 15 min/2800°F (1811°K) heat treatment.

Mechanical Properties of the Carbide and Boride Strengthened Alloys

Mechanical properties of the study alloys were measured to describe tensile and impact ductility at low temperatures, tensile behavior at 1900°F and 2100°F (1311 and 1422°K), and stress rupture behavior at 2100°F (1422°K) under 12, 15 and 17 ksi stress (83, 104 and 118 MN/m^2).

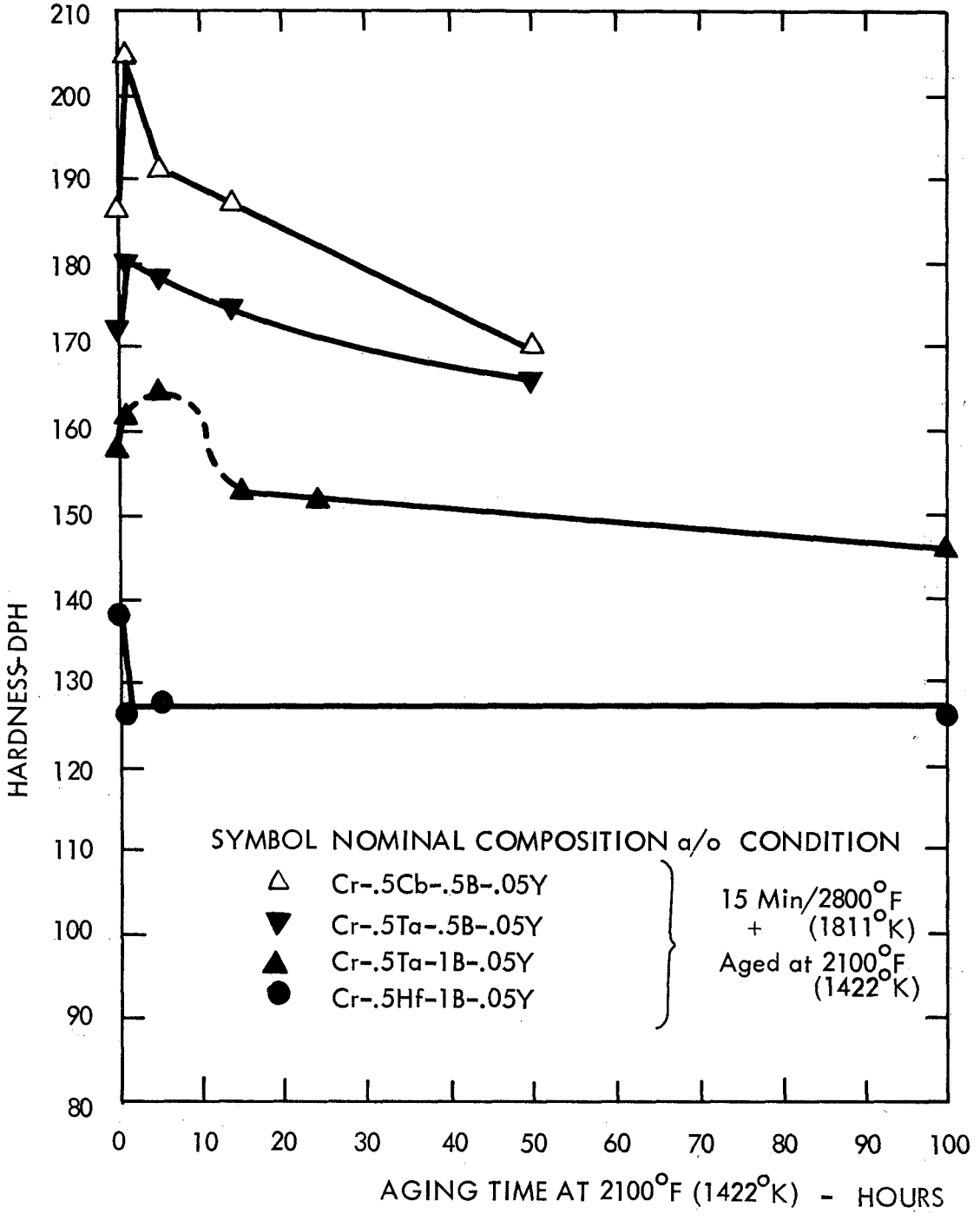

Figure 28. Hardness Response of the Boride Strengthened Alloys to Aging at 2100°F Following 15 min/2800°F Heat Treatment

Discussion of these properties is covered in this section.

Ductile-Brittle Behavior

Specimens were tested as machined, or as annealed after machining, i.e., electropolishing was not employed prior to testing to minimize any detrimental influence surface flaws might have on ductile-brittle behavior. However, specimens were prepared in the machined condition to a diamond polish surface finish of 4 RMS or finer.

The results of tensile tests performed to define a temperature of transition from ductile-to-brittle behavior are reported in Table 6. Impact test data are reported in Table 7. Sufficient information was obtained to establish both a tensile and impact ductile-brittle transition temperature (DBTT) for the as fabricated condition on ten of the eleven alloys studied, and an impact DBTT for these alloys tested in the 1 hr/2400°F (1589°K) heat treated condition. Heat treatment for 1 hour at 2400°F (1589°K) was sufficient to fully recrystallize those alloys left after fabrication with completely or partially cold worked microstructures (see Table 3). A DBTT in tension was also determined for the Cr-.5(Ti or Cb)-.5C alloys in the .25 hr/2800°F (1811°K) + 3 hr/2100°F (1422°K) heat treated condition. Elevated temperature tensile and creep tests were performed on several alloys in this heat treated condition, as a consequence, some measure of its influence on DBTT was made.

Transition temperatures estimated from the tensile and impact data reported in Tables 6 and 7 are summarized in Table 8. Ductile-brittle transition temperature based upon 5% elongation, 5% reduction of area, and 20 in-lbs (32.5 joules) absorbed fracture energy are given.

Tensile DBTT of as fabricated material varied from a low of 110°F (316°K) for the Cr-.5Zr-.5C alloy to a high of 730°F (761°K) for the Cr-.5Ta-.5B alloy. In general, alloys displaying highest as fabricated hardness also displayed the highest DBTT and vise versa. The approximate correlation of material hardness and tensile DBTT is shown in Figure 29 where these properties are plotted.

Table 6. Low Temperature Tensile Behavior of Carbide and Boride Strengthened Alloys (Common Units)

Nominal Composition a/o	Condition[4]	Hardness DPH	Test Temp. °F	.2% Yield ksi	U.T.S. ksi	Elongation % Uniform	Elongation % Total	Area Red. %
Cr-.5Ta-1B-.05Y	A	276	500	---	47.8[1]	0	0	0
	A		500	89.4	89.8	<1	<1	0
Cr-.5Ta-.5C-.05Y	A	202	300	---	65.3[1]	0	0	0
	A		500	62.2	76.5	5.9	11.4	39.0
Cr-.5Ti-.5C-.05Y	A	180	300	44.9	47.3[2]	0.9	0.9	1.2
	A		300	53.7	57.4[2]	1.1	1.1	1.2
	A		500	43.7	57.3[2]	8.0	17.1	57.6
	C	173	300	27.5	43.4[2]	2.6	2.6	4.3
	C		500	26.5	49.1	12.4	15.5	26.0
Cr-.5Hf-1B-.05Y	A	145	300	39.8	64.8	9.1	12.1	21.4
	A		500	33.5	54.3	11.8	18.1	46.4
Cr-.5Cb-.5C-.05Y	A	203	300	---	70.0[1]	0	0	1.0
	A		500	66.4[3]	74.6[2]	6.7	11.0	34.4
	C	193	700	38.0	53.8[2]	2.9	2.9	3.9
	C		800	37.0	58.5	7.4	10.4	23.6
Cr-.25Cb-.25C-.05Y	A	193	500	---	54.0[1]	0	0	0
	A		700	63.7[3]	71.7	5.2	14.0	51.6
Cr-.25Ta-.25C-.05Y	A	201	500	68.6[3]	70.8	3.4	4.0	4.8
	A		700	66.2[3]	75.1	4.9	13.0	58.5
Cr-.5Zr-.5C-.05Y	A	154	75	44.8	48.4[2]	1.6	1.6	1.3
	A		300	22.7	42.8	18.6	24.0	22.5
Cr-.5Hf-.5C-.05Y	A	151	300	30.1	32.5[2]	0.5	0.5	1.3
	A		500	31.3	42.1	14.8	24.0	54.8
Cr-.5Cb-.5B-.05Y	A	222	500	73.6	77.2[2]	0.6	0.6	1.4
	A		700	71.8	87.7	7.5	14.2	46.8
Cr-.5Ta-.5B-.05Y	A	256	700	78.4	88.2[2]	3.5	3.5	1.6
	A		900	76.6	89.8	6.7	12.9	47.9

[1] Specimen fractured during elastic loading.

[2] Specimen fractured before reaching ultimate strength.

[3] Upper yield point.

[4] A - As fabricated C - Annealed .25 hr./2800°F + 3 hr./2100°F

Table 6. Low Temperature Tensile Behavior of Carbide and Boride Strengthened Alloys (SI Units)

Nominal Composition a/o	Condition[4]	Hardness DPH	Test Temp. °K	.2% Yield MN/m^2	U.T.S. MN/m^2	Elongation % Uniform	Elongation % Total	Area Red. %
Cr-.5Ta-1B-.05Y	A	276	532	---	330[1]	0	0	0
	A		532	616	619	<1	<1	0
Cr-.5Ta-.5C-.05Y	A	202	420	---	451[1]	0	0	0
	A		532	430	528	5.9	11.4	39.0
Cr-.5Ti-.5C-.05Y	A	180	420	310	326[2]	0.9	0.9	1.2
	A		420	370	396[2]	1.1	1.1	1.2
	A		532	320	395[2]	8.0	17.1	57.6
	C	173	420	190	299[2]	2.6	2.6	4.3
	C		532	183	339	12.4	15.5	26.0
Cr-.5Hf-1B-.05Y	A	145	420	275	446	9.1	12.1	21.4
	A		532	231	375	11.8	18.1	46.4
Cr-.5Cb-.5C-.05Y	A	203	420	---[3]	483[1]	0	0	1.0
	A		532	458[3]	514[2]	6.7	11.0	34.4
	C	193	644	272	370[2]	2.9	2.9	3.9
	C		700	255	404	7.4	10.4	23.6
Cr-.25Cb-.25C-.05Y	A	193	532	---[3]	373[1]	0	0	0
	A		644	438[3]	494	5.2	14.0	51.6
Cr-.25Ta-.25C-.05Y	A	201	532	262[3]	487	3.4	4.0	4.8
	A		644	255[3]	519	4.9	13.0	58.5
Cr-.5Zr-.5C-.05Y	A	154	297	309	334[2]	1.6	1.6	1.3
	A		420	157	295	18.6	24.0	22.5
Cr-.5Hf-.5C-.05Y	A	151	420	208	224[2]	0.5	0.5	1.3
	A		532	216	291	14.8	24.0	54.8
Cr-.5Cb-.5B-.05Y	A	222	532	508	533[2]	0.6	0.6	1.4
	A		644	495	605	7.5	14.2	46.8
Cr-.5Ta-.5B-.05Y	A	256	644	541	610[2]	3.5	3.5	1.6
	A		755	529	618	6.7	12.9	47.9

[1] Specimen fractured during elastic loading.

[2] Specimen fractured before reaching ultimate strength.

[3] Upper yield point.

[4] A - As fabricated C - Annealed .25 hr./1811°K + 3 hr./1422°K

Table 7. Impact Behavior of Carbide and Boride Strengthened Alloys

Nominal Composition a/o	Condition[2]	Hardness DPH	Test Temp. °F (°K)	Energy Absorbed in-lb	Energy Absorbed Joules	Specimen[1] Appearance
Cr-.5Ta-1B-.05Y	A	276	700 (644)	11.5	(186)	a
Cr-.5Ta-.5C-.05Y	A	202	550 (560)	37.9	(615)	b
	A		500 (532)	5.8	(94)	a
	B	150	550 (560)	85.0	(1380)	c
	B		500 (532)	15.0	(243)	b
Cr-.5Ti-.5C-.05Y	A	180	700 (644)	90.2	(1460)	c
	A		600 (588)	93.0	(1510)	c
	A		550 (560)	92.0	(1490)	c
	A		500 (532)	7.7	(125)	b
	B	141	550 (560)	87.0	(1410)	c
	B		500 (532)	88.0	(1425)	c
	B		500 (532)	8.6	(149)	b
Cr-.5Hf-1B-.05Y	A	145	450 (504)	62.4	(1015)	b
	A		400 (476)	53.8	(870)	b
	A		350 (448)	45.1	(731)	b
	B	130	400 (476)	88.0	(1425)	c
	B		350 (448)	19.0	(306)	b
Cr-.5Cb-.5C-.05Y	A	203	850 (728)	124.8	(2020)	c
	A		750 (672)	5.8	(94)	a
	A		750 (672)	108.5	(1750)	c
	A		600 (588)	2.9	(46.8)	a
	B	146	750 (672)	80.6	(1310)	c
	B		500 (532)	3.4	(54)	a
	B		400 (476)	2.9	(47)	a
Cr-.25Cb-.25C-.05Y	A	203	750 (672)	112.3	(1820)	c
	A		600 (588)	12.5	(202)	a
	B	147	750 (672)	82.6	(1340)	c
	B		400 (476)	2.9	(46.8)	a
Cr-.25Ta-.25C-.05Y	A	201	850 (728)	104.6	(1700)	c
	A		700 (644)	12.5	(202)	b
	A		600 (588)	8.5	(138)	a
	B	144	850 (728)	64.3	(1010)	c
Cr-.5Zr-.5C-.05Y	A	154	550 (560)	49.0	(793)	c
	A		400 (476)	16.5	(267)	a
	B	135	500 (532)	73.9	(1200)	c
	B		400 (476)	76.8	(1240)	c
	B		400 (476)	29.8	(484)	b
Cr-.5Hf-.5C-.05Y	A	151	550 (560)	70.1	(1135)	c
	A		400 (476)	3.8	(62)	a
	B	136	550 (560)	66.7	(1080)	c
	B		400 (476)	13.9	(225)	a
	B		400 (476)	5.3	(86)	a
Cr-.5Cb-.5B-.05Y	A	222	1000 (811)	108.5	(1760)	c
	A		700 (644)	126.7	(2050)	c
	A		600 (588)	18.2	(295)	a
	A		500 (532)	8.6	(138)	a
	B	165	700 (644)	86.4	(1400)	c
	B		500 (560)	100.8	(1640)	c
	B		400 (476)	109.4	(1770)	c
	B		300 (420)	17.3	(280)	a
Cr-.5Ta-.5B-.05Y	A	256	900 (755)	135.4	(2190)	c
	A		800 (700)	56.6	(915)	—
	A		800 (700)	31.7	(513)	—
	A		700 (644)	20.2	(327)	—
	B	167	700 (644)	96.7	(1560)	c
	B		600 (588)	15.4	(250)	a
	B		400 (476)	4.8	(78)	a

1. a - fractured without bending
   b - fractured with some bending
   c - bent without fracturing

2. A - As fabricated
   B - Annealed 1 hr./2400°F (1589°K)

Table 8. Estimated Ductile-Brittle Transition Temperatures of Carbide and Boride Strengthened Alloys[1]

Nominal Composition a/o	Condition[2]	Temperature, °F (°K), where Ductility & Toughness are: 5% Elongation		5% Area Red.		20 in-lb (32.4J)		Hardness DPH
Cr-.5Ta-1B-.05Y	A	>500	(>532)	>500	(>532)	>700	(>644)	276
Cr-.5Ta-.5C-.05Y	A	400	(476)	340	(442)	520	(543)	202
	B	---	---	---	---	500	(532)	150
Cr-.5Ti-.5C-.05Y	A	360	(454)	320	(431)	500	(532)	180
	B	---	---	---	---	510	(538)	141
	C	340	(442)	250	(392)	---	---	173
Cr-.5Hf-1B-.05Y	A	125	(322)	125	(322)	220	(375)	145
	B	---	---	---	---	350	(448)	130
Cr-.5Cb-.5C-.05Y	A	400	(476)	340	(442)	620	(599)	203
	B	---	---	---	---	550	(560)	146
	C	725	(658)	700	(644)	---	---	193
Cr-.25Cb-.25C-.05Y	A	575	(574)	520	(543)	620	(599)	203
	B	---	---	---	---	500	(532)	147
Cr-.25Ta-.25C-.05Y	A	525	(546)	500	(532)	710	(650)	201
	B	---	---	---	---	750	(672)	144
Cr-.5Zr-.5C-.05Y	A	110	(314)	110	(314)	320	(431)	154
	B	---	---	---	---	400	(476)	135
Cr-.5Hf-.5C-.05Y	A	350	(448)	310	(426)	450	(504)	151
	B	---	---	---	---	400	(476)	136
Cr-.5Cb-.5B-.05Y	A	575	(574)	525	(546)	600	(588)	222
	B	---	---	---	---	300	(420)	165
Cr-.5Ta-.5B-.05Y	A	730	(661)	720	(655)	700	(644)	256
	B	---	---	---	---	620	(599)	167

[1] Based upon temperatures at which total tensile elongation and reduction of area each fall to 5%, and impact energy to 20 inch-lbs (32.4 joules)

[2] A - As fabricated
B - Annealed 1 hr./2400°F (1589°K)
C - Annealed .25 hr./2800°F + 3 hr./2100°F (.25 hr/1811°K + 3 hr/1422°K)

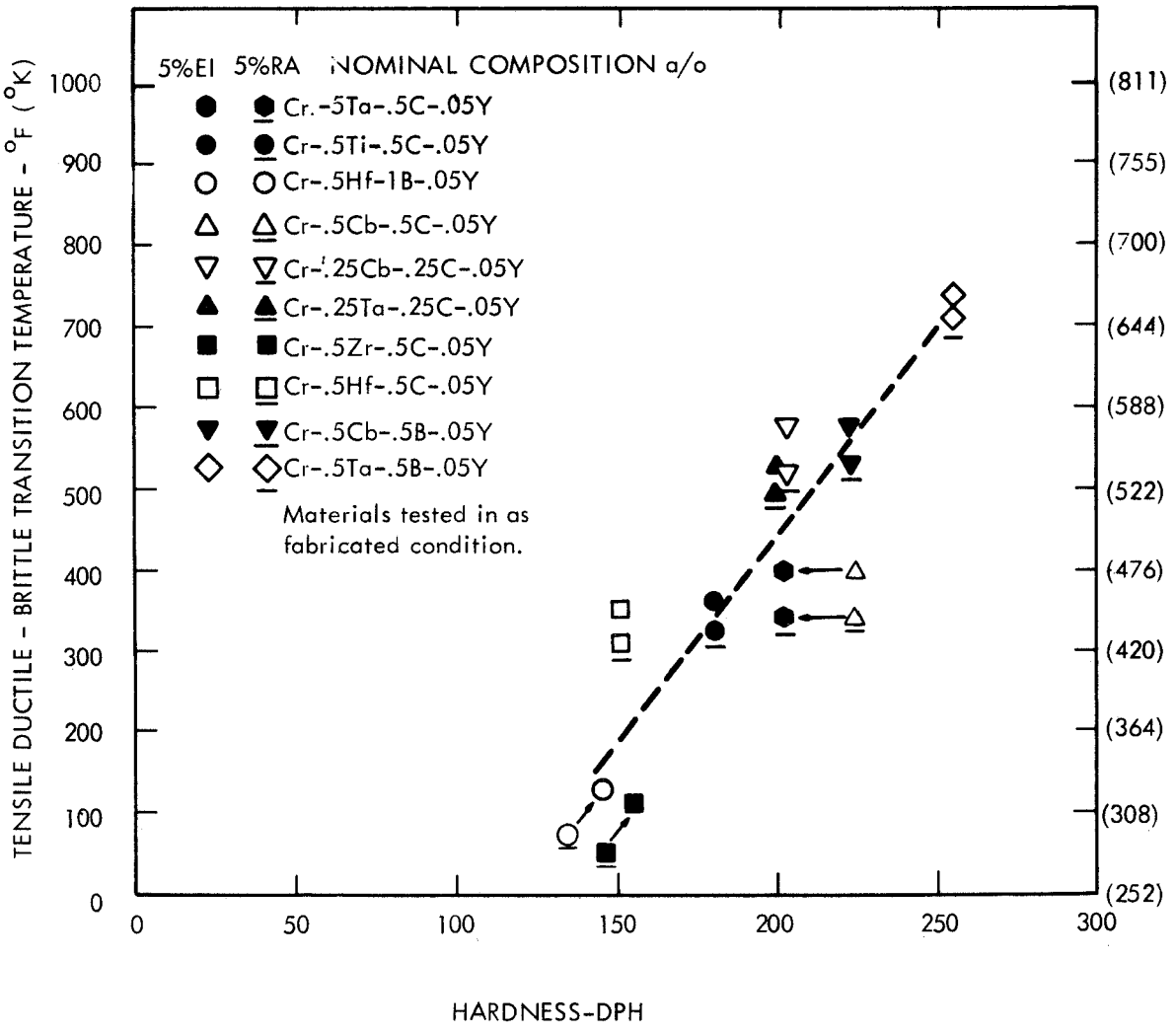

Figure 29. Correlation of Hardness and Temperature of Transition in Tensile Ductility of Carbide and Boride Strengthened Alloys

Heat treatment for 3 hours at 2100°F (1422°K) to effect partial carbide interchange to TiC after $Cr_{23}C_6$ formation by .25 hr/2800°F (1811°K) treatment had little effect on the tensile DBTT of the Cr-.5Ti-.5C alloy by comparison to that measured for the as fabricated condition (DBTT ~ 350°F). Similar heat treatment of the Cr-.5Cb-.5C alloy, however, resulted in a tensile DBTT of approximately 700°F (644°K), approximately 300°F (420°K) higher than the level measured for the as fabricated condition.

Little significant change in DBTT from that determined in tension, to an increase of approximately 200°F (364°K) was measured for the alloys impact tested in the as fabricated condition. An average increase of roughly 100°F (56°K) above the tensile value is characteristic of impact tested material.

A consistent response of impact DBTT to 1 hr/2400°F (1589°K) heat treatment was not observed. This heat treatment resulted in little change of impact DBTT from that noted for the as fabricated condition on a few alloys, while on others the DBTT either increased or decreased. The most significant change occurred on the Cr-.5Cb-.5B alloy where a decrease of DBTT from 600°F to 300°F (588 to 420°K) resulted from 1 hr/2400°F (1589°K) heat treatment. Except for this response, the influence recrystallization heat treatment had on impact DBTT could be characterized as a change of approximately $\pm$ 10°F to $\pm$ 130°F ($\pm$ 5.6 $\pm$ 72°K) from the as fabricated value. This amount of DBTT change is probably well within the range of experimental error associated with defining the property.

Tensile Properties

Tensile strengths of the study alloys tested at low temperatures in the as fabricated condition, reported in Table 6, reflect the microstructural condition of the materials. Lowest strengths were measured on the Cr-.5Hf-1B and Cr-.5(Zr or Hf)-.5C alloys which were recrystallized as fabricated. The strongest alloys, Cr-.5Ta-1B and Cr-.5(Ta or Cb)-.5B, had wrought microstructures as fabricated, while the remaining alloys, which displayed intermediate strengths, had partially recrystallized microstructures. Discussion of microstructure is covered in the first part of Experimental Program and Discussion. Hardness of the alloys, a measure of

microstructural conditions, is plotted against yield strength at 500°F (532°K) in Figure 30 to exemplify this point. Tensile data were obtained at 500°F (532°K) on eight of the eleven alloys studied, and sufficient information was gathered at nearby temperatures on the others to accurately estimate their strength at this temperature.

Tensile properties of the study alloys at 1900°F and 2100°F (1311 and 1422°K) are reported in Table 9. Data were gathered at these temperatures for a majority of alloys in the 1 hr/2400°F (1589°K) heat treated condition, and at 2100°F (1422°K) in the as fabricated condition. Tensile behavior at 2100°F (1422°K) was also measured on the Cr-.5(Ta, Ti or Cb)-.5C and Cr-.5(Ta or Cb)-.5B compositions heat treated .25 hr/2800°F* (1811°K) + 3 hr/2100°F (1422°K) and on the Cr-.5Hf-.5C alloy heat treated .25 hr/3050°F (1950°K) + 3 hr/2100°F (1422°K). Heat treatment at 2800°F (1811°K) forms $Cr_{23}C_6$ in the Cr-.5(Ta, Ti or Cb)-.5C alloys and Cr_4B in the Cr-.5(Ta or Cb)-.5B alloys. Aging for 3 hours at 2100°F (1422°K) causes partial solutioning of the $Cr_{23}C_6$ and Cr_4B phases and precipitation of TaC, TiC and CbC in the respective carbide alloys, and tantalum and columbium rich borides in the respective boride compositions. Classical aging and overaging occurs in these alloys as the carbide and boride interchange processes proceed at 2100°F (1422°K). Tensile behavior was measured at 2100°F (1422°K) to judge what effect the carbide and boride interchange reactions might have on strength. A higher initial heat treatment temperature, 3050°F (1950°K), was used for the Cr-.5Hf-.5C alloy. It was known that HfC was stable in the alloy up to at least 2850°F (1839°K). Heat treatment at 3050°F (1950°K) represented an attempt to solution treat the alloy, or, if carbide stability changes as noted for the Cr-(Ta, Ti or Cb)-C alloys, to form the $Cr_{23}C_6$ phase. Heat treatment effects and stability of carbide and boride phases in the study alloys are discussed in the first and third parts of Experimental Program and Discussion.

Yield strengths of the alloys measured at 1900°F and 2100°F (1311 and 1422°K) after the 1 hr/2400°F (1589°K) heat treatment are plotted in Figure 31. Highest strength was displayed by the Cr-.5(Ta or Cb)-.5B and Cr-.5Ta-1B alloys (> 18 ksi at 2100°F and >24 ksi at 1900°F) - (>124 MN/m^2 at 1422°K and >164 MN/m^2 at 1311°K). The Cr-.5(Zr or Hf)-.5C alloys were weakest, both displaying less than 10 ksi (69 MN/m^2) yield strength at these temperatures.

* Initial heat treatment of the Cr-.5Ta-.5C-.05Y alloy was performed at 2850°F (1839°K)

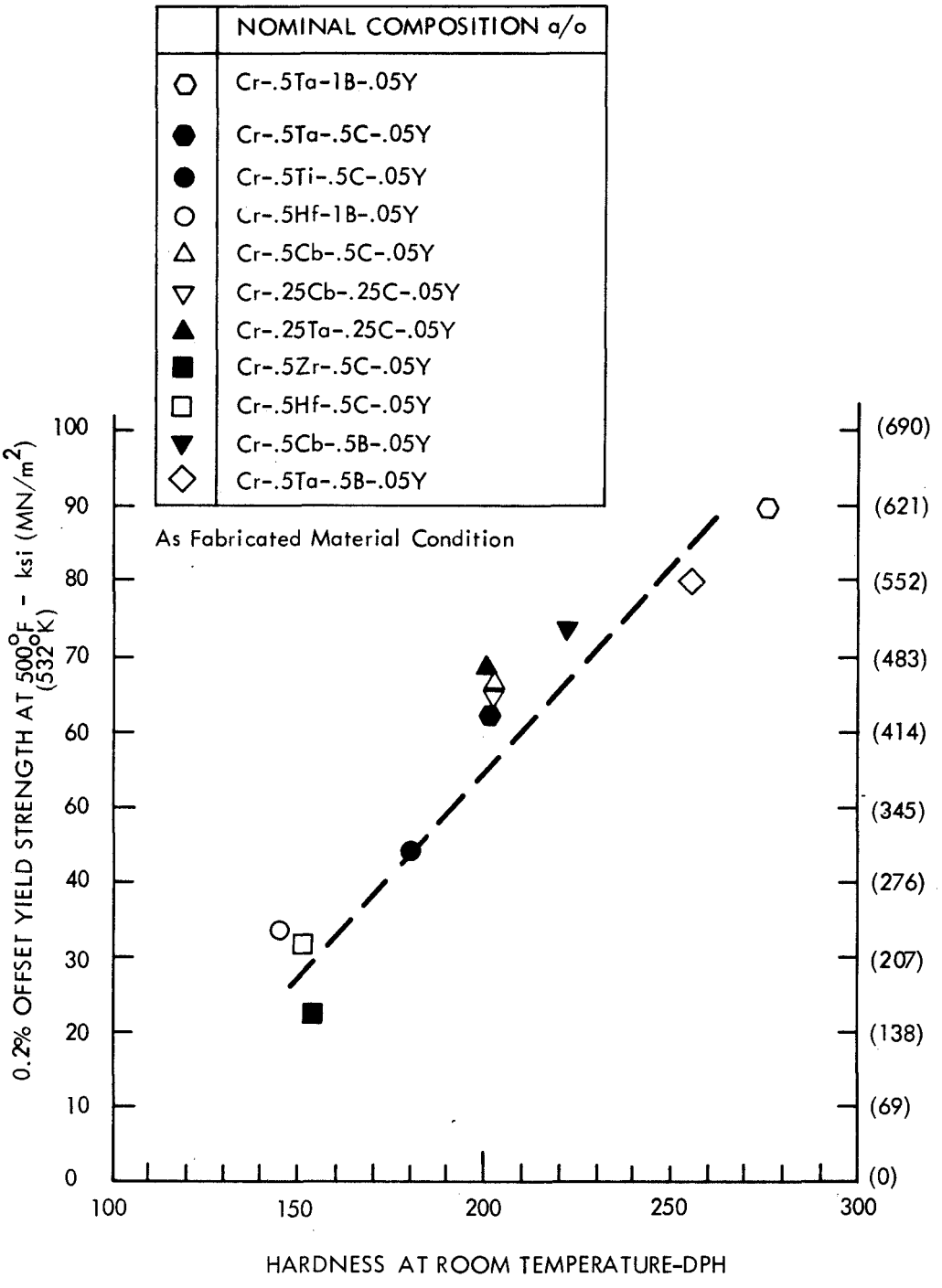

Figure 30. Correlation of Hardness and Yield Strength at 500°F for Carbide and Boride Strengthened Alloys

Table 9. Tensile Properties of Boride and Carbide Strengthened Alloys at 1900°F and 2100°F

Nominal Composition a/o	Condition[1]	Hardness DPH	Test Temp. °F	0.2% Yield ksi	0.2% Yield (MN/m²)	U.T.S. ksi	U.T.S. (MN/m²)	El. %	Area Red. %
Cr-.5Ta-1B-.05Y	B	159	2100[2]	18.6	(128)	26.0	(179)	41.7	78.0
Cr-.5Ta-.5C-.05Y	B	150	1900	20.5	(142)	25.4	(175)	30.0	87.0
	B	150	2100	13.6	(95)	16.6	(114)	36.5	88.0
	A	202	2100	27.2	(188)	28.3	(195)	16.5	75.7
	C	197	2100	30.1	(208)	32.1	(221)	18.3	81.0
Cr-.5Ti-.5C-.05Y	B	141	1900	11.8	(82)	19.5	(135)	40.0	88.0
	B	141	2100	12.1	(84)	14.9	(103)	46.6	91.3
	A	180	2100	20.9	(144)	21.4	(147)	21.0	81.8
	C	173	2100	18.3	(126)	20.4	(141)	28.0	88.0
Cr-.5Hf-1B-.05Y	B	130	2100	13.5	(93)	21.2	(146)	22.8	75.8
	A	145	2100	16.6	(114)	19.4	(134)	24.0	78.9
Cr-.5Cb-.5C-.05Y	B	146	1900	18.3	(126)	29.8	(199)	32.7	72.4
	B	146	2100	13.1	(91)	17.7	(122)	46.0	87.0
	A	203	2100	26.1	(180)	28.2	(195)	18.0	72.0
	C	197	2100	28.2	(188)	29.9	(206)	10.5	42.0
Cr-.25Cb-.25C-.05Y	B	147	1900	21.0	(145)	30.9	(220)	28.0	66.0
	B	147	2100	17.2	(118)	19.2	(132)	31.0	74.0
	A	193	2100	28.3	(195)	29.3	(202)	18.0	64.0
Cr-.25Ta-.25C-.05Y	B	144	1900	17.6	(122)	27.6	(191)	31.0	85.0
	B	144	2100	16.3	(112)	16.9	(117)	47.0	90.0
	A	201	2100	29.3	(203)	31.0	(215)	15.0	68.0
Cr-.5Zr-.5C-.05Y	B	135	2100	6.2	(43)	9.1	(63)	48.0	96.0
	A	154	2100	10.8	(75)	11.1	(76)	13.0	53.0
Cr-.5Hf-.5C-.05Y	B	136	1900	8.2	(57)	12.3	(85)	51.0	90.0
	B	136	2100	6.7	(46)	9.1	(63)	45.0	90.0
	A	151	2100	9.4	(65)	10.3	(71)	36.0	89.0
	C	---	2100	10.1	(70)	11.6	(80)	34.0	86.0
Cr-.5Cb-.5B-.05Y	B	165	1900	24.4	(168)	38.9	(268)	34.5	76.5
	B	165	2100	19.1	(132)	26.6	(184)	46.0	88.5
	A	222	2100	53.5	(369)	55.6	(384)	16.5	72.0
	C	198	2100	31.8	(220)	36.7	(254)	23.0	74.0
Cr-.5Ta-.5B-.05Y	B	167	1900	27.4	(189)	38.3	(265)	31.0	80.0
	B	167	2100	18.2	(126)	25.2	(174)	46.0	87.0
	A	256	2100	54.0	(372)	57.0	(393)	18.0	68.0
	C	179	2100	28.2	(194)	32.6	(226)	30.0	83.0

[1] A - As fabricated

B - Annealed 1 hr./2400°F (1589°K)

C - Annealed .25 hr./2850°F + 3 hr./2100°F for Cr-.5Ta-.5C-.05Y (.25 hr/1839°K + 3 hr/1422°K)
.25 hr./3050°F + 3 hr./2100°F for Cr-.5Hf-.5C-.05Y (.25 hr/1950°K + 3 hr/1422°K)
.25 hr./2800°F + 3 hr./2100°F for other compositions. (.25 hr/1811°K) + 3 hr/1422°K)

[2] 1900°F = 1311°K
2100°F = 1422°K

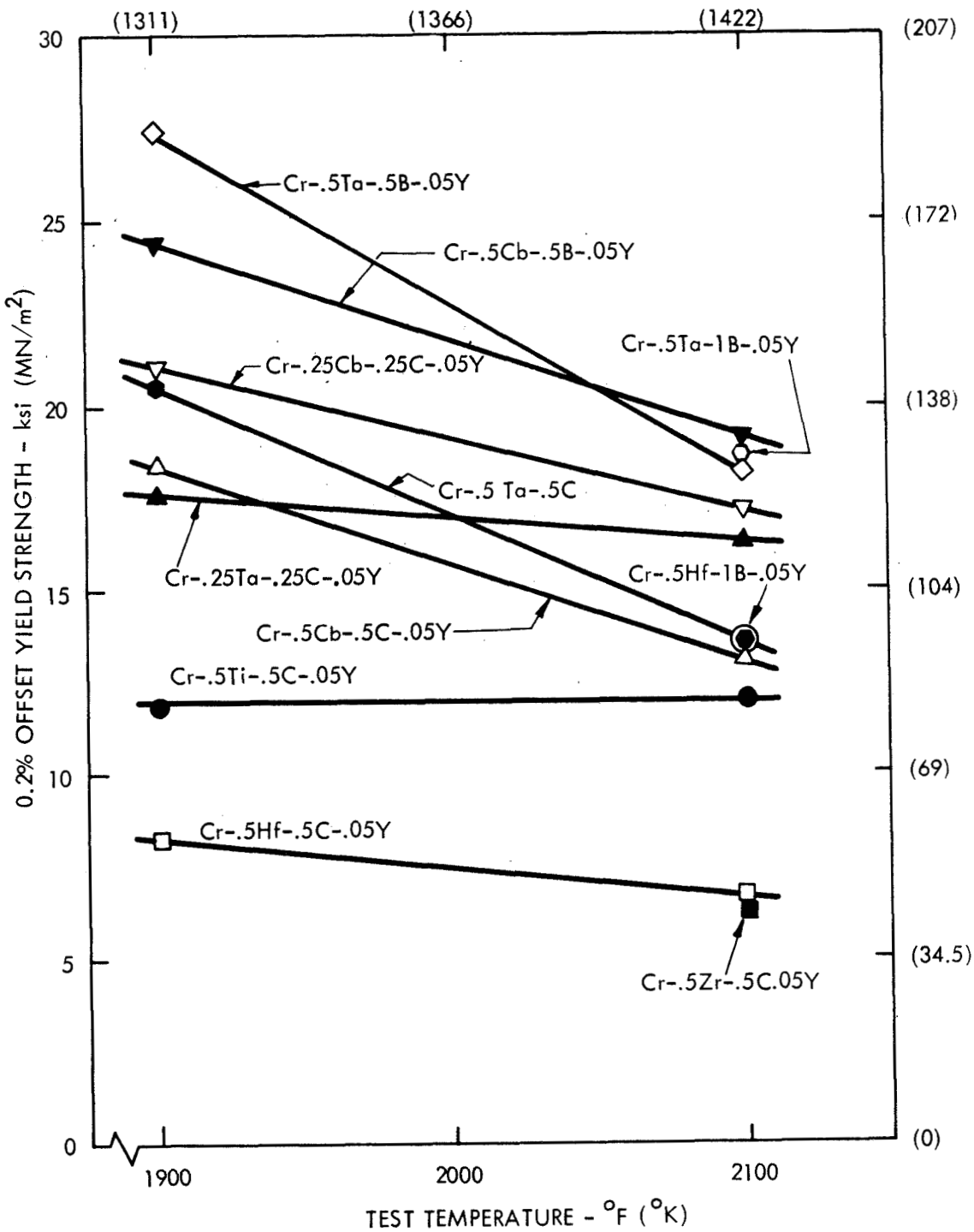

Figure 31. Yield Strengths at 1900°F and 2100°F of the Carbide and Boride Strengthened Alloys Heat Treated 1 Hour at 2400°F Prior to Testing

Yield strengths between 12 ksi and 17 ksi at 2100°F (83 and 117 MN/m^2 at 1422°K), and 12 ksi and 21 ksi at 1900°F (83 and 145 MN/m^2 at 1311°K, were measured on the other alloys given 1 hr/2400°F (1589°K) heat treatment.

After heat treatment to stabilize the $Cr_{23}C_6$ and Cr_4B phases then bring about partial carbide and boride interchange, i.e., .25 hr/2800°F + 3 hr/2100°F (.25 hr/1811°K + 3 hr/1422°K), yield strengths of the Cr-.5(Ta, Ti or Cb)-.5C and Cr-.5(Ta or Cb)-.5B alloys ranged from 18 to 32 ksi (124 to 211 MN/m^2) and were 50 to 130 percent higher than measured for the 1 hr/2400°F (1589°K) recrystallized condition (see Table 9). Comparing these conditions for the Cr-.5Hf-.5C alloy shows a 25% higher yield strength for .25 hr/3050°F + 3 hr/2100°F (.25 hr/1950°K + 3 hr/1422°K) heat treated material. Apparently, annealing at 3050°F (1950°K) did result in at least partial solutioning of the HfC phase allowing subsequent aging at 2100°F (1422°K) to effect some strengthening. Strength of this alloy in the .25 hr/3050°F + 3 hr/2100°F (.25 hr/1950°K + 3 hr/1422°K) condition was slightly greater than that measured for the as fabricated condition, 10.1 vs 9.4 ksi at 2100°F (70 vs 65 MN/m^2 at 1422°K) which is not surprising since the Cr-.5Hf-.5C alloy was recrystallized in the latter condition. However, higher yield strengths in the .25 hr/2800°F + 3 hr/2100°F (.25 hr/1811°K + 3 hr/1422°K) condition compared to that measured for the as fabricated materials were also observed on the Cr-.5(Ta or Cb)-.5C alloys, compositions which were partially cold worked in the as fabricated condition.

Strength at 2100°F (1422°K) was highest in the as fabricated condition for the Cr-.5Ti-.5C and Cr-.5(Ta or Cb)-.5B alloys, the latter two alloys displaying $\sim$54 ksi ($\sim$374 MN/m^2) yield strength. Overall, strength at 2100°F (1422°K) correlated roughly with room temperature hardness as shown in the plot of these properties given in Figure 32.

Stress-Rupture Behavior

Stress-rupture properties measured on the study alloys at 2100°F (1422°K) are reported in Table 10. The majority of data were gathered at 12 ksi and 15 ksi (83 and 104 MN/m^2). The two alloys which displayed tensile strengths lower than 12 ksi (83 MN/M^2), Cr-.5(Zr or Hf)-.5C, were not tested.

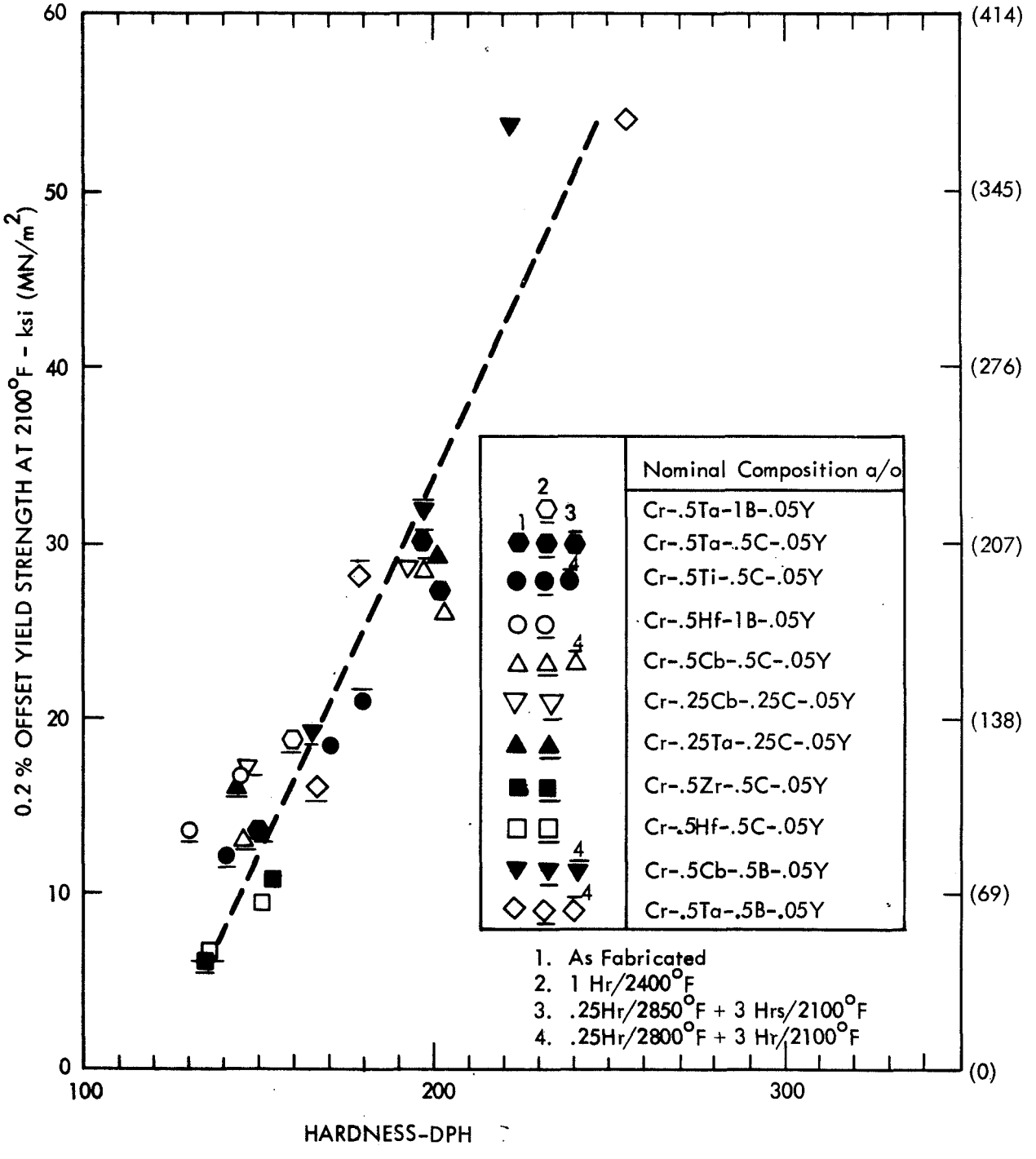

Figure 32. Correlation of Hardness and Yield Strength at 2100°F for the Carbide and Boride Strengthened Alloys

Table 10. Stress-Rupture Behavior of Carbide and Boride Strengthened Alloys at 2100°F

Nominal Composition a/o	Condition[1]	Test Stress ksi[6]	Creep Rate %/Hr.	Rupture Life Hrs.	Ductility % El.	Ductility % R.A.	3rd Stage Start Hrs.	3rd Stage Start % El.
Cr-.5Ta-1B-.05Y	A	15	----	25.4	34.2	68.0	----	----
	B	15	1.5	15.1	34.8	69.2	5.8	8.8
Cr-.5Ta-.5C-.05Y	A	15	2.0	4.0	25.0	80.3	1.3	4.2
	B	15	---	F.O.L.[2]	38.8	90.5	----	----
	C	15	0.0008	185.7[3]	12.5	66.0	130.0	1.8
	C	12	0.0025	164.5[4]	12.5	81.0	120.0	0.9
	C	12	0.0006	752.2[5]	14.0	60.3	435.0	1.2
Cr-.5Ti-.5C-.05Y	A	15	----	0.7	26.9	87.2	----	----
	B	12	----	0.2	40.4	88.0	----	----
	C	12	0.010	65.6	21.0	88.5	37.0	2.0
Cr-.5Hf-1B-.05Y	A	15	----	0.1	30.0	78.2	----	----
	B	12	5.1	2.8	33.7	76.4	>1.5	>9.4
Cr-.5Cb-.5C-.05Y	A	15	1.8	4.1	27.5	68.0	1.3	3.7
	B	12	20.5	1.0	43.0	88.5	.63	13.0
	C	15	0.08	10.0	2.7	5.3	7.8	1.4
	C	15	0.04	17.6	4.0	12.1	13.7	1.3
Cr-.25Cb-.25C-.05Y	A	15	3.0	2.7	27.5	76.0	1.1	4.2
	B	12	2.6	3.0	24.5	63.0	1.2	4.3
	C	15	0.23	2.5	9.5	25.0	2.0	1.8
	C	12	0.12	12.4	4.5	7.5	9.0	1.7
Cr-.25Ta-.25C-.05Y	A	15	1.3	5.8	26.5	77.5	2.4	4.6
	B	12	11.3	0.5	48.5	93.5	----	----
	C	12	0.0044	172.7	4.0	26.0	154.0	2.6
Cr-.5Cb-.5B-.05Y	A	15	0.51	21.6	55.0	80.5	5.8	3.6
	A	12	0.29	37.4	37.0	80.7	16.5	6.3
	B	12	0.27	46.2	48.0	88.0	11.0	4.5
	C	15	0.0014	117.3	28.0	80.0	50.0	1.8
	C	15	0.0086	84.7	20.0	78.4	44.5	1.0
Cr-.5Ta-.5B-.05Y	A	15	0.22	24.3	56.0	80.7	4.0	1.5
	A	12	0.15	36.7	32.0	80.5	10.3	2.4
	B	12	0.90	21.3	48.0	85.4	6.0	7.0
	C	15	0.0006	381.7	18.8	79.6	175.0	2.0
	C	17	0.0029	296.7	16.0	72.5	185.0	1.3

[1] A - As Fabricated
B - Annealed 1 hr./2400°F
C - Annealed .25 hr./2850°F + 3 hr./2100°F for Cr-.5Ta-.5C-.05Y
Annealed .25 hr./2900°F + 3 hr./2100°F for Cr-.25Ta-.25C-.05Y and Cr-.25Cb-.25C-.05Y
Annealed .25 hr./2800°F + 3 hr./2100°F for other compositions

[2] Failed on Loading

[3] Hardness before testing RB 82

[4] Hardness before testing RB 74

[5] Hardness before testing RB 86

[6] 12, 15 & 17 ksi = 83, 104 & 118 MN/m^2

Rupture life of the boride alloys tested in the as fabricated condition at 15 ksi and 2100°F (104 MN/m^2 and 1422°K) ranged from 0.1 hour for the Cr-.5Hf-1B alloy to 20-25 hours for the Cr-.5Ta-1B and Cr-.5(Ta or Cb)-.5B compositions. Lowering the test stress to 12 ksi (83 MN/m^2) only increased the rupture life in this material condition to ~37 hours for the Cr-.5(Ta or Cb)-.5B alloys. As fabricated, the carbide compositions failed at 2100°F and 15 ksi (1422°K and 104 MN/m^2) in 5.8 hours or less. Annealing the carbide strengthened alloys for 1 hour at 2400°F (1589°K) further weakened them, and rupture typically occurred in 3 hours or less at 12 ksi (83 MN/m^2). A similar weakening effect of annealing at 2400°F (1589°K) was noted for the Cr-.5Ta-1B and Cr-.5Ta-.5B compositions. Recrystallization of the Cr-.5Cb-.5B alloy had an opposite effect, the alloy displaying at 12 ksi (83 MN/m^2) a 46.2 hour rupture life compared to 37.4 hours as fabricated.

Major improvement in stress-rupture behavior was brought about for several compositions by carbide and boride interchange heat treatments. A rupture life of 185.7 hours was measured for the Cr-.5Ta-.5C alloy at 15 ksi and 2100°F (104 MN/m^2 and 1422°K) after heat treating at 2850°F (1839°K) to form the $Cr_{23}C_6$ carbide, then aging at 2100°F (1422°K) for 3 hours to effect partial carbide interchange and TaC formation. A second similarly heat treated sample of this alloy resisted failure for 752.2 hours at 12 ksi and 2100°F (83 MN/m^2 and 1422°K), while another specimen failed after 165.4 hours at these test conditions. The discrepancy in rupture life measured on these samples was likely associated with their hardness levels prior to testing (see bottom of Table 10). After heat treatment a much lower hardness, R_B74, was measured on the 165 hour rupture life sample, compared to R_B86 for the 752 hour life sample. This hardness difference indicates that perhaps heat treatment was not identical for both samples.

Rupture times of 65.6 hours and 172.7 hours were measured respectively at 12 ksi (83 MN/m^2) for the Cr-.5Ti-.5C and Cr-.25Ta-.25C compositions after heat treating to form $Cr_{23}C_6$ then aging for 3 hours at 2100°F (1422°K). Rupture behavior of the CbC strengthened alloys, however, did not respond to this type of heat treatment. This is somewhat surprising since both displayed a hardening response to carbide interchange heat treatment similar to that observed on the Cr-(Ta or Ti)-C alloys (see Figure 19). Furthermore, tensile properties of the Cr-.5Cb-.5C

alloy responded to this heat treatment (see Table 9). Generally, lower overall ductility was measured on samples of the CbC strengthened alloys rupture tested in the carbide interchange heat treated condition as compared to the similarly annealed and tested samples of other compositions. Examination of rupture tested specimens of these alloys revealed that failure occurred completely through grain boundaries. Furthermore, grain boundary separation occurred on the Cr-.25Cb-.25C alloy samples at several locations along their gauge sections. Grain boundaries are a natural site for weakness at high temperatures in those carbide alloys which can be heat treated through an interchange cycle. The $Cr_{23}C_6$ phase formed by the initial high temperature anneal employed for this heat treatment develops as an essentially continuous grain boundary network. Aging for 3 hours at 2100°F (1422°K) prior to testing at this temperature was used to partially solution the $Cr_{23}C_6$ phase, reducing its continuity and any effect it might have on high temperature grain boundary strength. Experiments on the Cr-.5(Ta or Ti)-.5C alloys showed the $Cr_{23}C_6$ phase to be discontinuous after only 1 hour of aging at 2100°F (1422°K) (see Figures 16 and 17). However, 3 hours aging at 2100°F (1422°K) may not have been sufficient to avoid serious grain boundary weakness in the Cr-Cb-C compositions. Also, out of the alloys studied in this heat treated condition, oxygen contamination was most severe in these compositions, and at approximately 2 to 3 times the level in the next most contaminated alloy (see Table 2). This contaminant may have had a deleterious effect on rupture life.

The Cr-.5Cb-.5B alloy heat treated .25 hour at 2800°F (1811°K) to form Cr_4B then aged 3 hours at 2100°F (1422°K) to effect partial boride interchange displayed an average 100 hour rupture strength at 2100°F of 15 ksi (1422°K of 104 MN/m^2). The Cr-.5Ta-.5B alloy similarly heat treated, however, was much stronger at 2100°F (1422°K) displaying 381.7 hours life at 15 ksi (104 MN/m^2) and 296.7 hours at 17 ksi (117 MN/m^2).

Stress-rupture behavior at 2100°F (1422°K) is summarized in Figures 33 and 34. Also included in these figures are yield and ultimate strengths of the alloys at this temperature. It is clear from these summaries that the best combination of tensile and stress-rupture properties is displayed by the Cr-.5Ta-.5B alloy. The Cr-.5Ta-.5C alloy appears to be second best on this basis principally due to its somewhat superior stress rupture strength in comparison to the

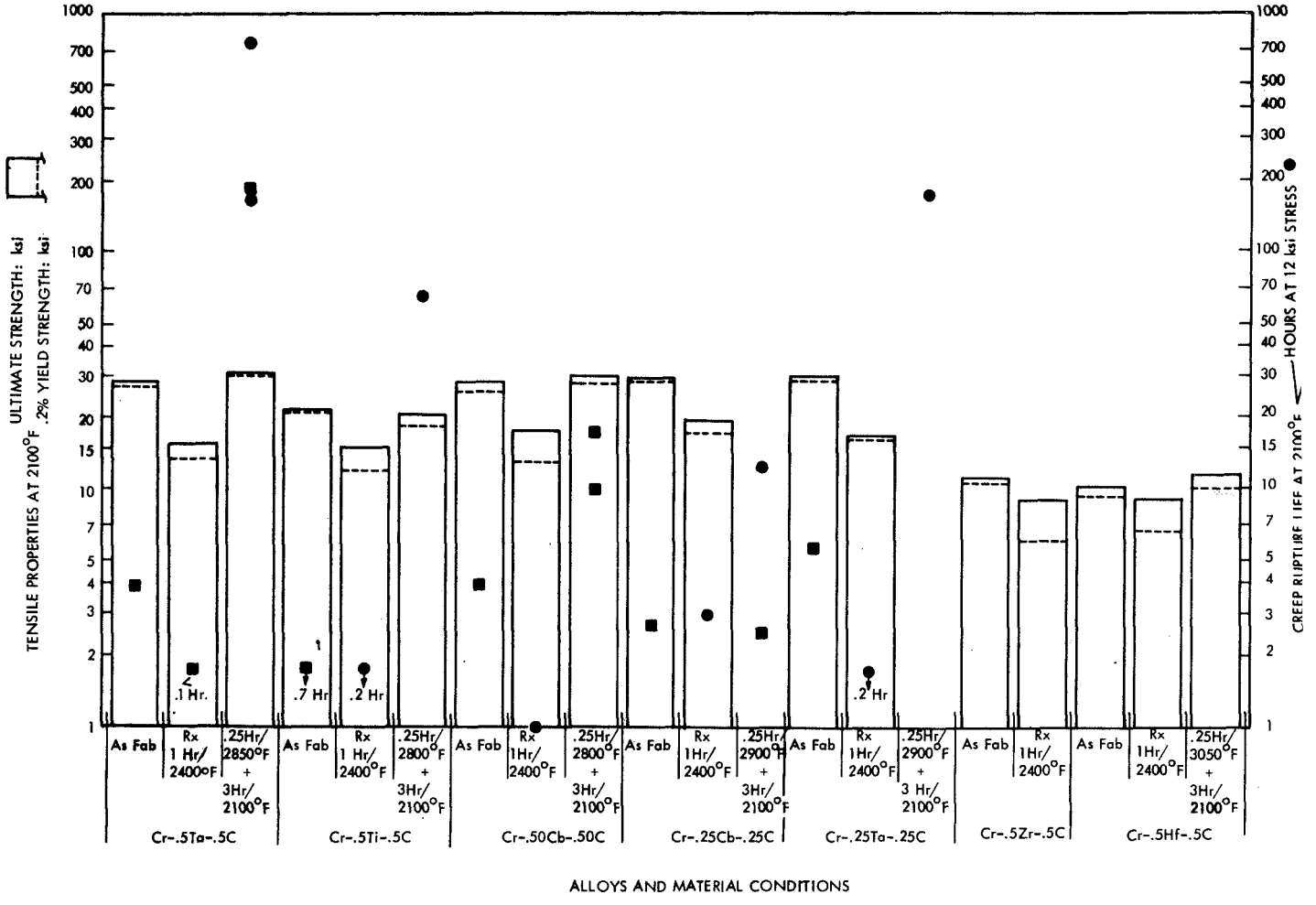

Figure 33. A Summary of Tensile and Stress-Rupture Properties of the Carbide Strengthened Compositions at 2100°F (1422°K)

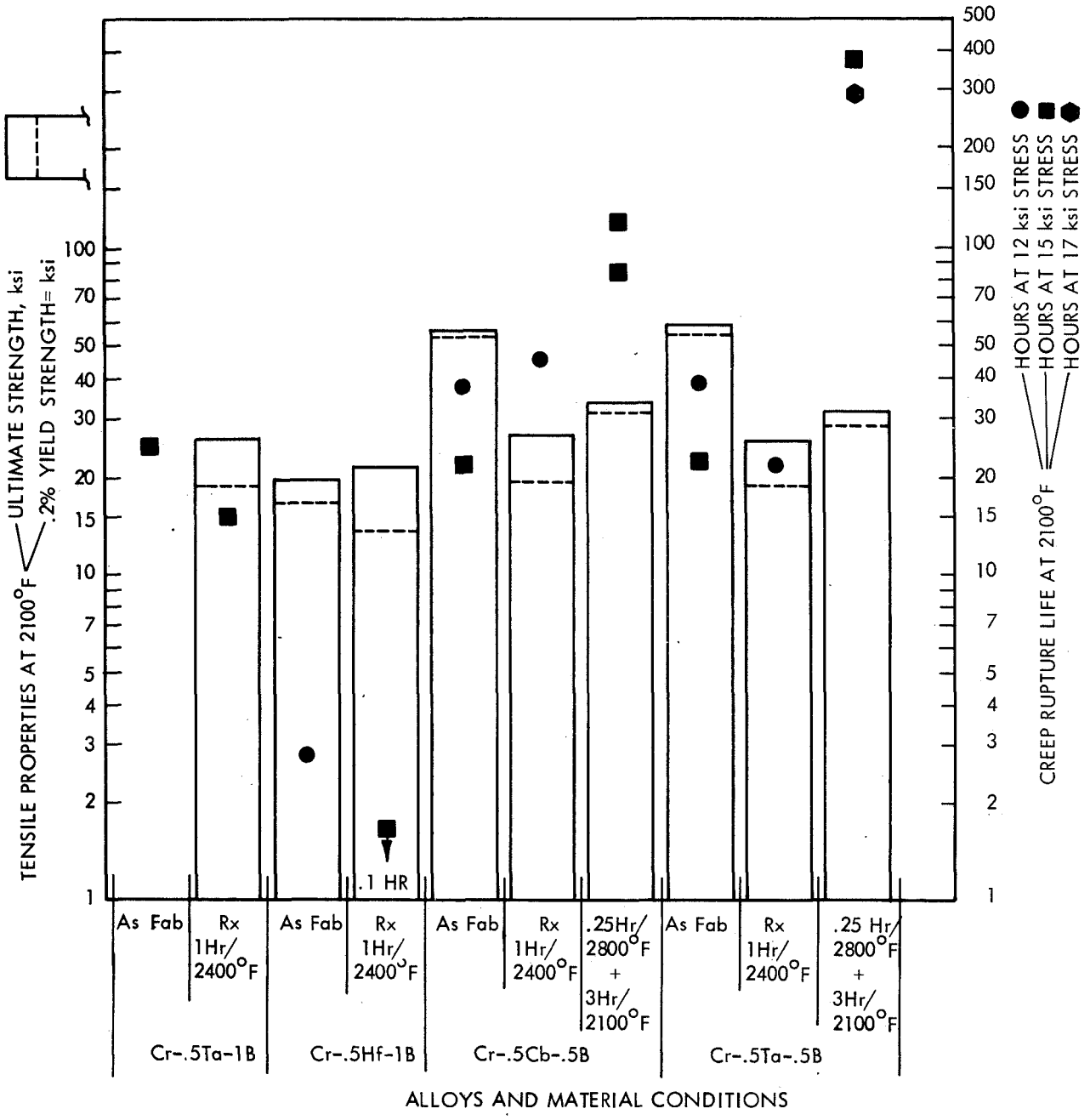

Figure 34. A Summary of Tensile and Stress-Rupture Properties of the Boride Strengthened Compositions at 2100°F (1422°K)

Cr-.5Cb-.5B alloy. The Cr-.25Ta-.25C and Cr-.5Ti-.5C compositions, respectively, rank fourth and fifth.

Stress-rupture behavior is plotted on the Larson-Miller basis for these five compositions in their optimum condition in Figure 35. Stress to cause failure in 100 hours, estimated from this plot, is reported for the two best high temperature alloys, Cr-.5Ta-.5(C or B), in Table 11 along with tensile strength data. Included for comparison in this table are data for two other chromium-base alloys. The two comparison alloys, developed on NASA sponsored work by Clark[4], Cr-4Mo-.6(Ta or Cb)-.4C, display the highest 100 hour rupture strengths of any composition developed to date. Strengthening is obtained in the compositions by solid solution molybdenum addition and dispersed phase carbide formation. Rupture strength at 2100°F (1422°K) comparable or better than reported for the strongest alloys can be obtained from the Cr-.5Ta-.5(C or B) compositions, alloys which do not contain any high melting temperature solid solution addition such as molybdenum.

The question arises as to why the Cr-4Mo-.6(Ta or Cb)-.4C alloys display optimum rupture behavior in the as fabricated condition, the condition in which the solely dispersion strengthened alloys were extremely weak. Some rupture strength benefit is undoubtedly derived directly from the molybdenum solid solution addition in the Cr-4Mo-.6(Ta or Cb)-.4C compositions. However, in addition, the molybdenum content of these alloys may have had a potent indirect effect on rupture behavior as a result of its influence on fabricability. Molybdenum seriously impairs fabricability requiring use of high fabrication temperatures. As an example, Clark extruded the Cr-4Mo-.6(Ta or Cb)-.4C alloys at 2750°F (1783°K), then swaged test rod starting at 2600°F (1700°K) and finishing at 2250°F (1505°K)[4]. Judging from the carbide stability information generated on this program, extrusion at 2750°F (1783°K) probably results in formation and retention of the $Cr_{23}C_6$ carbide. If so, subsequent swaging at lower temperatures would cause carbide interchange to TaC and CbC in the respective compositions with possible benefit to rupture properties.

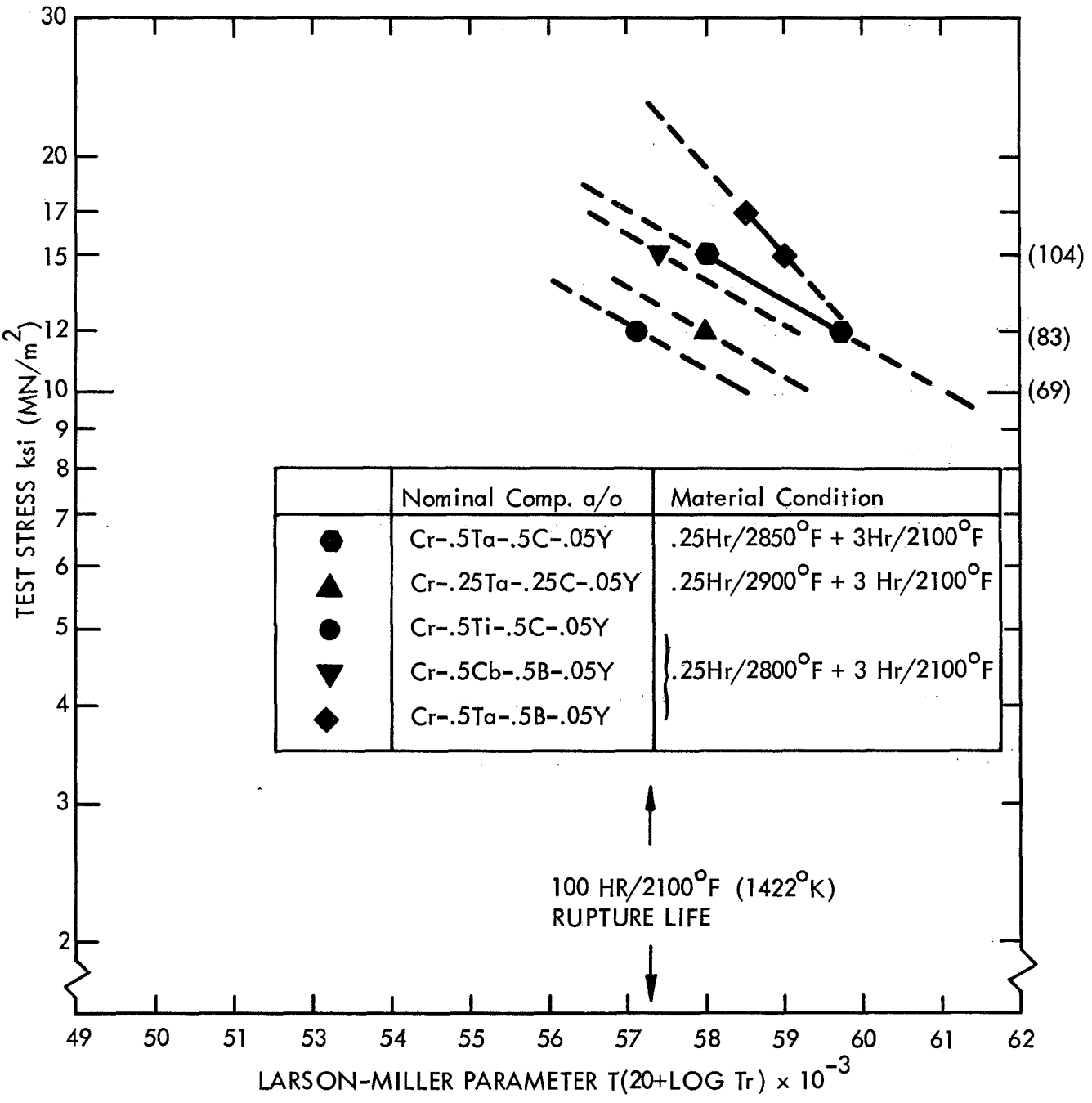

Figure 35. Stress-Rupture Properties of Five Superior Study Alloys Presented in Larson-Miller Form

Table 11. Stress-Rupture and Tensile Properties of Four Chromium-Base Alloys at 2100°F

Nominal Composition a/o	Material Condition[1]	100 Hr. Rupture Strength ksi (MN/m^2)	Yield Strength ksi	Ultimate Strength ksi
Cr-.5Ta-.5C-.05Y	.25 hr/2850°F + 3 hr/2100°F	16.5 (114)	30.1	32.1
Cr-.5Ta-.5B-.05Y	.25 hr/2800°F + 3 hr/2100°F	23.0 (159)	28.2	32.6
Cr-4Mo-.6Ta-.4C-.05Y	As Fabricated[2]	16.0 (110)	>38	>42
Cr-4Mo-.6Cb-.4C-.05Y	As Fabricated[2]	18.0 (124)	46.3	49.6

[1]Optimum condition reported for stress-rupture properties.

[2]Extruded at 2750°F (1783°K) + swaged at 2600 to 2250°F (1700 to 1505°K)

The Cr-4Mo-.6(Ta or Cb)-.4C alloys do excel in short time strength at high temperatures, i.e., tensile strength. This undoubtedly reflects a direct effect of the 4 a/o molybdenum solid solution addition. It may be possible, however, to properly combine carbide and boride interchange aging and processing of the solely dispersed phase strengthened alloys to obtain classically dispersion hardened products, i.e., ones in which stability of the dispersoid-substructure network is maintained for long times at elevated temperatures. In this manner, both improved high temperature tensile strength as well as the rupture strength potential derived from the interchange processes might be realized. Heat treatment alone should not be considered as the only means for strengthening the alloys studied on this program.

The Effect of Temperature and Composition on Boride Stability

Ten Cr-(Ti, Zr, Cb or Ta)-B alloys were prepared on this study by nonconsumable arc melting. Samples of each were then equilibrated for 20 to 24 hours in the temperature range 2100 to 2700°F (1422°K to 1755°K) and water quenched to retain the elevated temperature condition. A small, .05 a/o, yttrium addition was made to each alloy to serve as a getter. Boride phases formed in the alloys were released by matrix dissolution in a 10% methanol-bromine solution, then collected and examined by x-ray diffraction to identify phases, and x-ray fluorescence to measure the level of metals present. Compositions studied and results of boride phase identification and metal content analysis are summarized in Table 12.

With exception of the Cr-1Ti-.5B alloy equilibrated at 2100°F (1422°K), only Cr_4B was observed as a boride phase in the alloys containing titanium heat treated in the temperature range 2100 to 2700°F (1422 to 1755°K). Some diffraction lines which could not be indexed were obtained in addition to those identifying Cr_4B from the boride residue extracted after 2100°F (1422°K) equilibration of the Cr-1Ti-.5B alloy. A major amount of titanium was detected by x-ray fluorescent analysis of this sample implying the unindexed lines characterize a compound or compounds rich in this metal, presumably a boride or borides of high titanium content. By comparison, x-ray fluorescent analysis for titanium content of the extraction obtained from this alloy after 2700°F (1755°K) equilibration which was identified as Cr_4B

Table 12. X-Ray Data Characterizing High Temperature Precipitate Formation in Ten Boride Strengthened Alloys

Composition a/o	Equilibration Temperature, X-Ray Diffraction & Fluorescence Results: 2100°F (1422°K) Diffraction	2100°F (1422°K) Fluorescence[1]	2500°F (1644°K) Diffraction	2500°F (1644°K) Fluorescence	2700°F (1755°K) Diffraction	2700°F (1755°K) Fluorescence
Cr-1Ti-.5B-.05Y	Cr_4B + Unindexed lines	Ti(s) Cr (m) Y (w)	Cr_4B		Cr_4B	Ti (w) Cr (s) Y (w)
Cr-.5Ti-.5B-.05Y	Cr_4B		Cr_4B		Cr_4B	Ti (w) Cr (s) Y (w)
Cr-.5Ti-.25B-.05Y	Cr_4B		Cr_4B		Cr_4B	
Cr-.5Zr-.5B-.05Y	ZrB_2[2] + FCC a=?		ZrB_2[2] + FCC a=4.691		ZrB_2[2] + FCC a=4.692	
Cr-.5Zr-.25B-.05Y	ZrB_2[2] + FCC a=?		ZrB_2[2] + FCC a=4.698	Zr (s) Cr (w) Y (w)	ZrB_2[2] + FCC a=4.686	
Cr-1Cb-.5B-.05Y	X	Cb (s) Cr (w) Y (w)	X	Cb (s) Cr (w) Y (w)	X	Cb (s) Cr (w) Y (w)
Cr-.5Cb-.5B-.05Y	X + Cr_4B		X + Cr_4B	Cb (s) Cr (m) Y (w)	Cr_4B	Cb (zero) Cr (s) Y (w)
Cr-.5Cb-.25B-.05Y	X		X	Cb (s) Cr (w) Y (w)	X + Cr_4B	
Cr-.5Ta-.5B-.05Y	X + Cr_4B		X + Cr_4B		X + Cr_4B	
Cr-.5Ta-.25B-.05Y	X + Cr_4B		X	Ta (s) Cr (m) Y (w)	X + Cr_4B	Ta (m-s) Cr (m) Y (w)

[1] (s) strong (m) moderate (w) weak

[2] c = 3.169 a = 3.530 c/a = 1.11

revealed only a low level of this element. It should be understood that where Cr_4B was identified the intensity and spacing of diffraction lines obtained were sufficiently close to that for pure Cr_4B to yield this conclusion, but in all cases differed enough to indicate some deviation from stoichiometry or solid solution substitution. Detection by x-ray fluorescence of the low concentration of metals present other than chromium in residues identified as Cr_4B suggests solid solution substitution.

The x-ray patterns characterizing the phases extracted from the Cr-.5Zr-.5B and Cr-.5Zr-.25B alloys after quenching from 2100°F to 2700°F (1422 to 1755°K) were all similar, and the diffraction lines could be separated into FCC and CPH sets. A typical pattern is reported in Table 13. The CPH diffraction lines indexed exactly with the standard for ZrB_2: a = 3.169Å, c = 3.530Å, c/a = 1.11. Where the FCC diffraction line set was of suitable quality to permit a parameter estimate results from 4.686Å to 4.698Å were obtained depending upon the alloy and heat treat condition. The monoboride of zirconium, ZrB, is reported as being of FCC structure with a 4.668Å parameter[8], but an ASTM diffraction standard has not been cataloged. As a result, it is concluded that the FCC phase is ZrB containing some substitutional elements causing enlargement of the lattice parameter. Weak amounts of yttrium and chromium were detected in the boride residue extracted from the Cr-.5Zr-.25B alloy after equilibration at 2500°F (1644°K) suggesting substitution in the phases. A few extremely weak lines which could not be indexed were also observed in the diffraction patterns obtained on extractions from the Cr-.5Zr-.5B and Cr-.5Zr-.25B alloys.

Extractions from the Cr-1Cb-.5B alloy representing equilibration from 2100°F to 2700°F (1422 to 1755°K) gave identical diffraction patterns which could not be indexed and are designated X in Table 12. X-ray fluorescent analysis of these extractions revealed that columbium was present as the principal metallic component.

Extractions from the Cr-.5Cb-.5B alloy representing equilibration at 2100°F and 2500°F (1422 and 1644°K) gave identical diffraction patterns. A set of diffraction lines in these patterns indexed with Cr_4B and when separated from the total pattern left the same X diffraction pattern obtained on the extractions from the Cr-1Cb-.5B alloy. The extraction obtained from the

Table 13. X-Ray Diffraction Data Obtained on Borides Extracted from Compositions Alloyed with Zirconium and Boron after Equilibration at 2100°F to 2700°F[1] (1422 to 1755°K)

Diffraction Patterns				
Cr-.5Zr-.5B-.05Y and Cr-.5Zr-.25B-.05Y Alloys		ZrB_2 Standard[3]		Lines Matching FCC Phase
d	I	d	I	
3.53	70[2]	3.53	44	
2.98	5			
2.75	80	2.74	65	
2.70	25			*
2.56	10			
2.35	15			*
2.17	100	2.16	100	
2.09	5			
1.77	20	1.764	13	
1.725	5			
1.66	15			*
1.59	25	1.585	19	
1.485	40	1.484	22	
1.45	25	1.445	18	
1.42	15			C**
1.415	5			
1.395	5			
1.375	10	1.372	10	
1.355	5			*
1.280	30	1.278	17	
1.18	30	1.179	16	
1.085	30	1.083	8	
1.050	5			C**
1.040	10	1.037	6	
1.000	30	.994	14	

Diffraction lines of d < .994 not reported

[1] Samples Equilibrated 20 to 24 hours at temperature before water quenching.

[2] Intensity values estimated visually.

[3] c = 3.530 a = 3.169 c/a = 1.11

Cr-.5Cb-.5B alloy after 2700°F (1755°K) equilibration gave the Cr_4B diffraction pattern only.

The X pattern of diffraction lines was obtained on the extraction residues representing 2100°F and 2500°F (1422 and 1644°K) equilibration of the Cr-.5Cb-.25B alloy. A diffraction pattern containing lines matching the Cr_4B phase plus the X pattern was obtained from the extraction representing 2700°F (1755°K) equilibration of this alloy.

Diffraction patterns separable into X and Cr_4B were observed for extractions obtained from the Cr-.5Ta-.5B alloy after 2100°F to 2700°F (1422 to 1755°K) equilibration. It is not surprising that behavior similar to that observed on the alloys containing columbium was noted for this alloy since the atomic sizes of tantalum and columbium, their valences, and reactivities are all similar, and they form isomorphous compounds.

The patterns X and Cr_4B were found for the samples representing equilibration of the Cr-.5Ta-.25B alloy at 2100°F and 2700°F (1422 and 1755°K), but only X was observed in the sample representing 2500°F (1644°K) equilibration. Since the bulk of the information on the columbium and tantalum alloys suggests stabilization of X phase (or phases) at low temperatures, with transition to X + Cr_4B and subsequently Cr_4B only as temperature is increased, the result of X + Cr_4B stable at 2100°F (1422°K) in this alloy is thought to be incorrect. Instead, X phase (or phases) alone is probably stable at this temperature, and the detection of Cr_4B is likely a result of insufficient equilibration time to solution this phase formed during the casting process.

Detection of a large amount of tantalum in the sample representing 2500°F (1644°K) equilibration of the Cr-.5Ta-.25B alloy which gave the X diffraction pattern only is consistent with the detection of high columbium in the X pattern extractions obtained from alloys containing this metal.

Although X patterns where observed on alloys containing columbium or tantalum were similar they were not identical in all respects. For example, significant differences in line position in the back reflection region were noted in comparing the X diffraction patterns obtained from alloys containing columbium with those from alloys containing tantalum. This indicates, if the X pattern truly represents a single phase, that the lattice parameters of the phase differ depending upon whether it is columbium or tantalum rich.

Spacings and intensities of the diffraction patterns observed and identified as X, Cr_4B, and X + Cr_4B for extractions obtained from alloys containing columbium and tantalum are reported in Table 14. The Cr_4B pattern standard is also shown in this table.

The X pattern could not be indexed with any ASTM catalogued tantalum, columbium, or chromium boride, or Cr-Ta or Cr-Cb intermetallic compound. Possible impurity related compounds were included in the examination, e.g., oxides, nitrides, or carbides of the alloy constituents, but matching was not obtained. An ASTM computer analysis of the X pattern was also made. In it, logically possible compounds were compared with the X pattern as measured, and with the d spacings ranging both ± 0.04Å and ± 0.08Å from the measured values. The likelihood that solid solution substitution might have sufficiently altered the diffraction pattern from that which could be matched with catalogued standards was taken into account by allowing variation in d spacings. In spite of this, identification was not obtained.

If it is assumed that the alloys containing columbium and tantalum can be represented as simple ternary compositions, i.e., if the small, .05 a/o, yttrium addition can be assumed isomorphous in one or more of the stable ternary system phases, it follows that the X diffraction pattern must characterize a single phase. Liquation was not observed in the microstructure of these alloys indicating that only solid phases were stable in the 2100°F to 2700°F (1422 to 1755°K) study range. With a ternary system assumed, a maximum of only three solid phases can be in equilibrium if temperature freedom is permitted. Since one of the solid phases in this study was the metal matrix it follows that at most two boride phases can be stable, further implying, because the Cr_4B and X diffraction patterns occurred together in several instances, that the X pattern must represent a single boride phase. The

Table 14. X-Ray Diffraction Data Obtained on Borides Extracted from Compositions Alloyed with Columbium or Tantalum and Boron after Equilibration at 2100°F to 2700°F (1422 to 1755°K)

Diffraction Patterns Observed[1]					Cr_4B Standard Calculated Pattern[3]	
X		Cr_4B		X + Cr_4B		
d ± .01	I	d	I	d ± .01	d	I
					3.678	3
		3.55	1[2]		3.579	6
3.25	60[2]			3.25		
2.96	20	2.95	5	2.95	2.949	5
2.66	80			2.66		
2.57	60			2.57		
		2.30	70	2.30	2.300	36
2.20	90			2.20		
		2.12	80	2.12	2.108	72
2.10	30			2.10		
2.06	100	2.04	100	2.05	2.044	97
		1.96	25	1.96	1.953	20
1.88	60			1.88		
1.83	5	1.83	50	1.83	1.826	30
1.65	5	1.65	60	1.65	1.649	56
1.63	50			1.63		
1.44	50			1.44		
1.43	10			1.43		
Diffraction lines of d < 1.43 not reported						

[1] Alloy compositions and conditions given in Table 12.

[2] Intensity values estimated visually

[3] E. A. Brandes, B. A. Hatt, Monthly Technical Progress Narrative, Nov. 1969, Contract NASW 1720

columbium or tantalum rich character of the extractions which gave the X pattern suggests that it represents a boride of these elements. Major structural distortion by the solid solution presence of some chromium and yttrium is a possible explanation for the inability to index the phase.

Evidence that the X diffraction pattern does indeed represent a tantalum or columbium rich boride was obtained by electron microprobe analysis of the Cr-1Cb-.5B alloy in the 2700°F (1755°K) equilibrated condition. A photomicrograph of the structure developed by 2700°F (1755°K) equilibration of the alloy is presented in Figure 36. Also given in this figure is a photomicrograph showing the structure of the Cr-.5Cb-.5B alloy in the 2700°F (1755°K) equilibrated condition. The size of particles present in the microstructures differ. Except for this, other particle differences are unapparent. However, x-ray diffraction analysis of the particles extracted from the Cr-1Cb-.5B alloy gave the X pattern, while the diffraction pattern obtained on those particles extracted from the Cr-.5Cb-.5B alloy indexed with Cr_4B (see Table 12).

Electron microprobe examinations were performed on the particles present in the 2700°F (1755°K) equilibrated microstructures of these alloys. Particles in the Cr-1Cb-.5B alloy were found to contain major amounts of boron and columbium. Electron microprobe evidence of this is given in Figure 37. This information supports the conclusion that the X diffraction pattern characterizes a single boride phase containing a major amount of columbium or tantalum, depending upon which of these elements is in the specific alloy.

Electron microprobe data obtained on particles in the 2700°F (1755°K) equilibrated microstructure of the Cr-.5Cb-.5B alloy are presented in Figure 38. The particles were found to be chromium rich at a level almost equivalent to the matrix. Boron was also found concentrated in the particles, but not to the degree noted in the X phase particles studied on the Cr-1Cb-.5B alloy (compare photographs of boron concentration in Figures 37 and 38). These results are consistent with the particles in the Cr-.5Cb-.5B alloy being Cr_4B since this phase contains a relatively large amount of chromium and a small amount of boron. Furthermore, it follows that

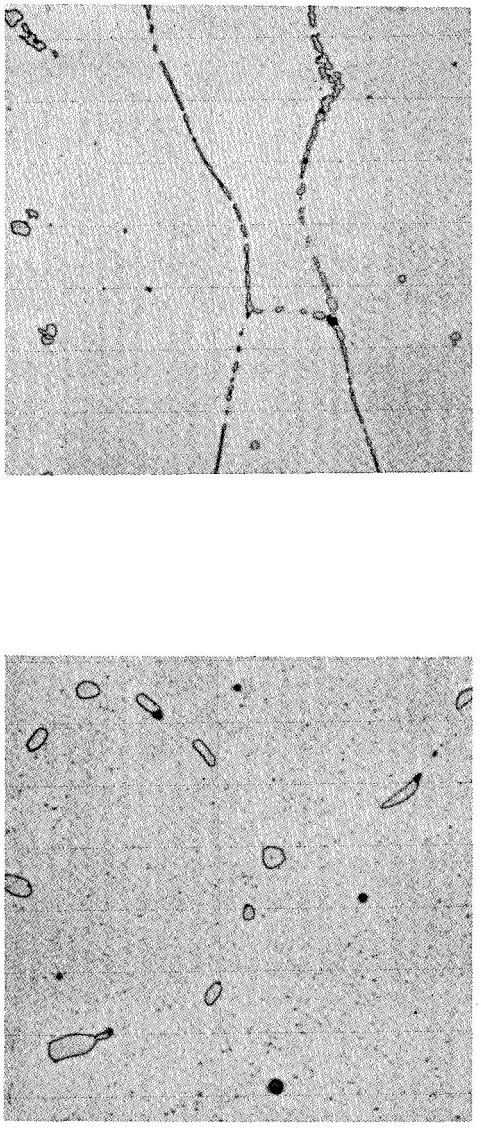

Figure 36. Microstructures of Cr-1Cb-.5B-.05Y (top) and Cr-.5Cb-.5B-.05Y Developed by 20 Hour Equilibration at 2700°F (1755°K) 500X

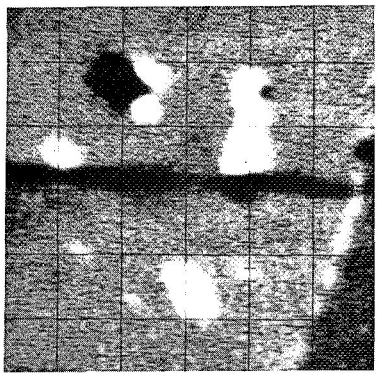

Back Scattered
Electronmicrograph

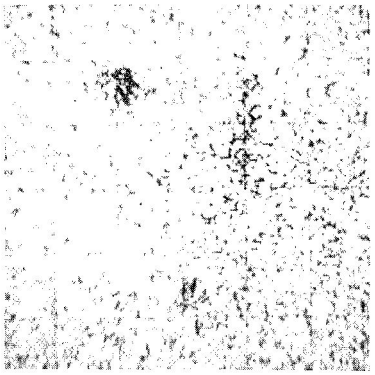

Cr

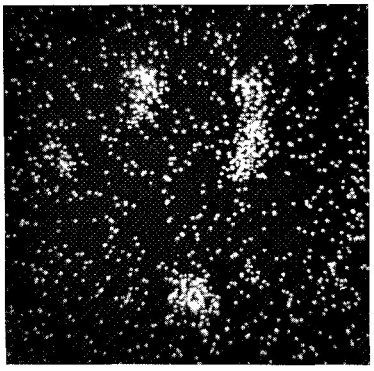

Cb

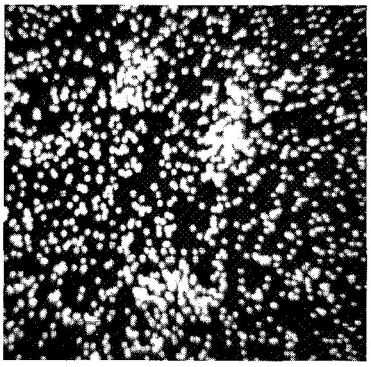

B

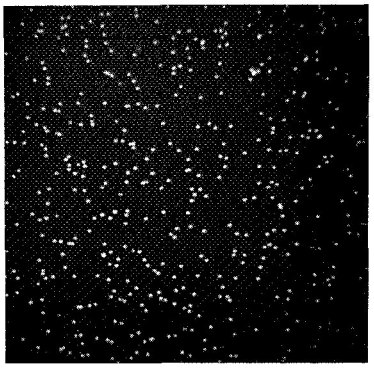

Y

Figure 37. Concentration of Elements in Particles and Matrix Formed by 2700°F (1755°K) Equilibration of the Cr-1Cb-.5B-.05Y Alloy 800X

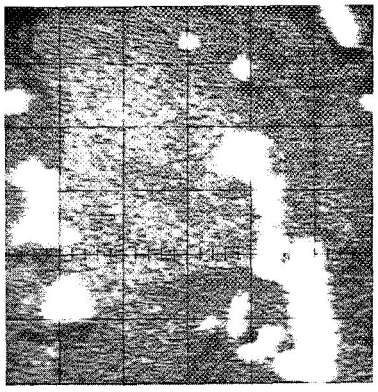

Back Scattered Electronmicro-graph

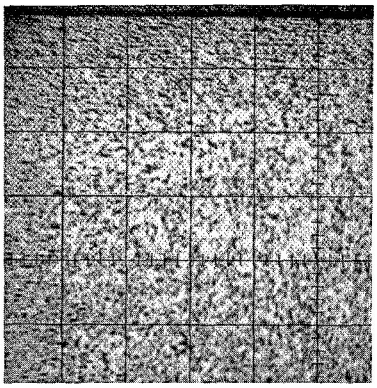

Cr

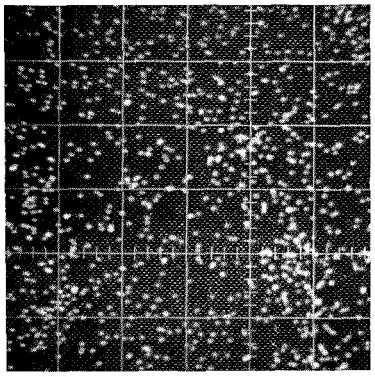

B

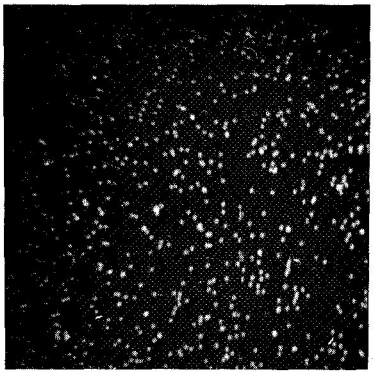

Cb

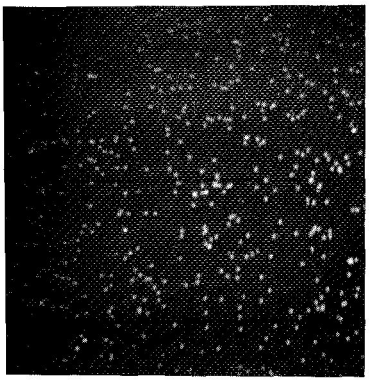

Y

Element	Intensity of Characteristic Radiation CPS	
	Precipitate	Matrix
Cr	17,000	18,000
Cb	50	50
B	50	17
Y	30	30

Figure 38. Concentration of Elements in Particles and Matrix Formed by 2700°F (1755°K) Equilibration of the Cr-.5C-.5B-.05Y Alloy 800X

well above 20 a/o boron must be present in the X phase since the 20 a/o level of boron in the Cr_4B phase is barely distinguishable by electron microprobe analysis as compared to the strong indication of boron obtained by the technique on particles of the X phase (again compare photographs of boron concentration in Figures 37 and 38).

Conclusions can also be extracted from the phase stability data concerning changes in precipitate phases observed as a function of composition and temperature. Change of precipitate phase stability from X to X + Cr_4B and finally to Cr_4B alone as temperature is increased is an obvious trend seen in the data for those alloys containing columbium and tantalum (see Table 12). Actual composition governs whether X, X + Cr_4B, or Cr_4B are stable at a specific temperature in the 2100°F to 2700°F (1422 to 1755°K) study range. It appears that higher alloying metal content and alloying metal to boron ratio both increase the temperatures at which transitions from X to X + Cr_4B and X + Cr_4B to Cr_4B are developed.

With exception of the Cr-1Ti-.5B alloy, the compositions containing titanium displayed only Cr_4B precipitate stability over the 2100°F to 2700°F (1422 to 1755°K) study range. Only Cr_4B precipitate stability was found after 2500°F and 2700°F (1644 to 1755°K) heat treatment in the Cr-1Ti-.5B composition. A titanium rich phase (or phases) was observed in addition to Cr_4B in this alloy after 2100°F (1422°K) heat treatment, a conclusion arrived at from the observation of unindexed diffraction lines and a high titanium level in the extraction. The Cr-1Ti-.5B composition had the highest titanium content and titanium-to-boron ratio of the study containing this metal addition. As a result, analogy with the alloys containing columbium or tantalum indicates a titanium rich phase should be stable to the highest temperature in this composition. Further analogy with these alloys implies a transition of boride phase formation from X' + Cr_4B to Cr_4B probably occurs between 2100°F to 2500°F (1422 to 1644°K) in the Cr-1Ti-.5B composition, where X' represents a boride rich in titanium. Transition from X' + Cr_4B to Cr_4B must occur below 2100°F (1422°K) in the other two study compositions alloyed with titanium. Apparently, borides of titanium are not stable in chromium to as high a temperature as are borides of columbium or tantalum, in compositions containing comparable metal and boron levels.

The boride phase stability transition behavior observed on alloys containing tantalum, columbium, and titanium is quite similar to that observed for the carbide alloys containing these metal additions which are discussed in the first two parts of Experimental Program and Discussion. Carbide strengthened alloys studied on the program, Cr-.25(Ta or Cb)-.25C, Cr-.5(Ta, Cb or Ti)-.5C, compositions in which the monocarbides TaC, CbC or TiC were concluded to be stable at least up to 2200°F (1477°K), all displayed a change to $Cr_{23}C_6$ stability at approximately 2800°F (1811°K). The $Cr_{23}C_6$ compound is obviously similar to Cr_4B.

Most interestingly, Cr_4B formation after heat treatment to 2700°F (1755°K) was not observed for the alloys Cr-.5Zr-.5B or Cr-.5Zr-25B, but neither was $Cr_{23}C_6$ formed in Cr-.5Zr-.5C by heat treatment up to 2850°F (1839°K). Transition to $Cr_{23}C_6$ stability was not found on the Cr-.5Hf-.5C alloy heat treated up to 2850°F (1839°K), but Cr_4B was observed in the Cr-.5Hf-1B alloy after heat treatment at 2600°F and 2800°F (1700 and 1811°K). The boron and carbon levels of these alloys, however, are not comparable, and the higher boron content would be expected to lower the temperature at which Cr_4B formed. At comparable metal and boron or carbon levels, borides and carbides of zirconium and hafnium are likely stable in chromium to higher temperatures than are borides or carbides of tantalum or columbium.

IV. CONCLUSIONS

Chromium-base alloys strengthened by a group IV B or V B metal carbide or boride were studied to define phase stability and mechanical properties. Conclusions generated from this work are:

1. Elevated temperature strength adequate for advanced air breathing engine application can be developed in chromium solely by dispersion strengthening.

2. Tantalum carbide and boride were the most effective strengthening phases studied. Of these the boride was most potent. Carbides and borides of zirconium and hafnium were least effective strengtheners, and those of columbium and titanium displayed an effect somewhat between the extremes.

3. High tensile strengths at elevated temperatures can be achieved in dispersion hardened chromium alloys as exemplified by the Cr-.5Ta-.5B (a/o) and Cr-.5Cb-.5B compositions which, warm worked and stress relieved, display ~55 ksi yield strength at 2100°F (~380 MN/m^2 at 1422°K).

4. The rupture strength of several alloys improved markedly when aged at 2100°F to precipitate the stable group IV B or V B metal carbide or boride following higher temperature heat treatment to form and retain the $Cr_{23}C_6$ or Cr_4B phases.

5. When heat treated to bring about the phase interchange reactions $Cr_{23}C_6 \rightarrow TaC$ and $Cr_4B \rightarrow TaxBy$, rupture strengths of the alloys Cr-.5Ta-.5C (a/o) and Cr-.5Ta-.5B at 2100°F (1422°K) compare to or exceed the highest values reported for chromium-base alloys.

6. A rough ranking of group IV B and V B metal carbide and boride stability in chromium would place the compounds of zirconium and hafnium as most stable, compounds of titanium as least stable, and compounds of tantalum and columbium somewhat between these extremes.

V. REFERENCES

1. N. E. Ryan, "The Formation, Stability and Influence of Carbide Dispersions in Chromium," J. Less-Common Metals, Vol. II, 1966.

2. A. M. Filippi, "Arc Melting and Properties of Two Chromium-Base Alloys," Contract NAS 3-10485, Report NASA-CR-72525, Dec. 22, 1968.

3. D. J. Maykuth, A. Gilbert, "Chromium and Chromium Alloys," DMIC Report 234, Oct. 1966.

4. J. W. Clark, "Development of High-Temperature Chromium Alloys," Contract NAS 3-7260 Final Report NASA CR-72731, Nov. 4, 1970.

5. E. Rudy, "Ternary Phase Equilibria in Transition Metal-Boron-Carbon-Silicon Systems," Part V Compendium of Phase Diagram Data, AFML-TR-65-2.

6. R. A. Perkins, "Effect of Processing Variables on the Structure and Properties of Refractory Metals," Technical Report AFML-TR-65-234, Part II May 1967.

7. R. P. Elliott, "Constitution of Binary Alloys, First Supplement," McGraw-Hill, Inc., 1965.

8. W. B. Pearson, "A Handbook of Lattice Spacings and Structures of Metals and Alloys -2," Pergamon Press, 1967.

DISTRIBUTION LIST

NASA Headquarters
600 Independence Avenue
Washington, D. C. 20546
Attn: RLC/N. F. Rekos

NASA Headquarters
600 Independence Avenue
Washington, D. C. 20546
Attn: RW/G. C. Deutch

NASA Headquarters
600 Independence Avenue
Washington, D. C. 20546
Attn: RRM/R. H. Raring

NASA-Ames Research Center
Moffett Field, California 94035
Attn: Library

NASA-Flight Research Center
P. O. Box 273
Edwards, California 93523
Attn: Library

NASA-Goddard Space Flight Center
Greenbelt, Maryland 20771
Attn: Library

Jet Propulsion Laboratory
4800 Oak Grove Drive
Pasadena, California 91102
Attn: Library

NASA-Langley Field, Virginia 23365
Attn: 214/Irvin Miller

NASA-Langley Research Center
Langley Field, Virginia 23365
Attn: Library

NASA-Manned Space Flight Center
Houston, Texas 77058
Attn: Library

NASA-Marshall Space Flight Center
Huntsville, Alabama 35812
Attn: Library

Air Force Office of Scientific Research
Propulsion Research Division
USAF Washington, D. C. 20525
Attn: Library

Defense Documentation Center (DDC)
Cameron Station
5010 Duke Street
Alexandria, Virginia 22314

NASA-Lewis Research Center
21000 Brookpark Road
Cleveland, Ohio 44135
Attn: 105-1/G. M. Ault

NASA-Lewis Research Center
21000 Brookpark Road
Cleveland, Ohio 44135
Attn: 3-19/Technology Utilization Office

NASA-Lewis Research Center
21000 Brookpark Road
Cleveland, Ohio 44135
Attn: 49-1/S. Grisaffe

NASA-Lewis Research Center
21000 Brookpark Road
Cleveland, Ohio 44135
Attn: 105-1/N. T. Saunders

NASA-Lewis Research Center
21000 Brookpark Road
Cleveland, Ohio 44135
Attn: Library (60-3) (3)

NASA-Lewis Research Center
21000 Brookpark Road
Cleveland, Ohio 44135
Attn: 5-5/Report Control Office

DISTRIBUTION LIST

(Continued)

NASA-Lewis Research Center
21000 Brookpark Road
Cleveland, Ohio 44135
Attn: 105-1/J. R. Stephens (2)

NASA-Lewis Research Center
21000 Brookpark Road
Cleveland, Ohio 44135
Attn: 49-1/J. P. Merutka

NASA-Lewis Research Center
21000 Brookpark Road
Cleveland, Ohio 44135
Attn: 77-3/L. W. Schopen

NASA-Lewis Research Center
21000 Brookpark Road
Cleveland, Ohio 44135
Attn: 105-1/W. D. Klopp (12)

NASA-Lewis Research Center
21000 Brookpark Road
Cleveland, Ohio 44135
Attn: 105-1/R. W. Hall

NASA-Lewis Research Center
21000 Brookpark Road
Cleveland, Ohio 44135
Attn: 49-1/J. C. Freche

NASA-Lewis Research Center
21000 Brookpark Road
Cleveland, Ohio 44135
Attn: 49-1/H. B. Probst

NASA Scientific & Tech. Information
P. O. Box 33 Fac.
College Park, Maryland 20740 (6)

General Electric Company
Attn: Mr. Michael Toth
51000 West 164th Street
Cleveland, Ohio 44142

Industrial Materials Technology, Inc.
Attn: Mr. Robert Widmer
127 Smith Place
West Cambridge Industrial Park
West Cambridge, Massachusetts 02138

U. S. Atomic Energy Commission
Washington, D. C. 20545
Attn: Technical Reports Library

Oak Ridge National Laboratory
Oak Ridge, Tennessee 37830
Attn: Technical Reports Library

Department of the Navy
ONR
Code 429
Washington, D. C. 20525

Headquarters
Wright-Patterson AFB, Ohio 45433
Attn: MAMP

Headquarters
Wright-Patterson AFB, Ohio 45433
Attn: MATB

Headquarters
Wright-Patterson AFB, Ohio 45433
Attn: MAAM/Technical Library

Headquarters - Attn: AFSC-FTDS
Wright-Patterson AFB, Ohio 45433

DISTRIBUTION LIST
(Continued)

Headquarters
Wright-Patterson AFB, Ohio 45433
Attn: AFML:MAM

Headquarters
Wright-Patterson AFB, Ohio 45433
Attn: MAG/Directorate of Materials

U. S. Army Aviation Materials Laboratory
Port Eustis, Virginia 23604
Attn: SMOFE-APG/John White, Chief

Bureau of Naval Weapons
Department of the Navy
Washington, D. C. 20525
Attn: RRMA-2/T. F. Kearns, Chief

Army Materials Research Agency
Watertown Arsenal
Watertown, Massachusetts 02172
Attn: Director

Battelle Memorial Institute
505 King Avenue
Columbus, Ohio 43201
Attn: Defense Metals Information
Center (DMIC)

Battelle Memorial Institute
505 King Avenue
Columbus, Ohio 43201
Attn: Dr. R. I. Jaffe

Aerospace Corporation
Reports Acquisition
P. O. Box 95085
Los Angeles, California 90045

Advanced Metals Research Corporation
149 Middlesex Turnpike
Burlington, Massachusetts 01804
Attn: J. T. Norton

Allegheny Ludlum Steel Corporation
Research Center
Alabama and Pacific Avenues
Brackenridge, Pennsylvania 15014
Attn: Library

American Society for Metals
Metals Park
Novelty, Ohio 44073
Attn: Library

Avco Space Systems Division
Lowell Industrial Park
Lowell, Massachusetts 01851
Attn: Library

The Bendix Corporation
Research Laboratories Division
Southfield, Michigan 48075
Attn: Library

Boeing Company
P. O. Box 733
Renton, Washington 98055
Attn: SST Unit Chief, W. E. Binz

Case Institute of Technology
University Circle
Cleveland, Ohio 44106
Attn: Library

Chromalloy Corporation
169 Western Highway
West Nyack, New York 10994
Attn: Mr. L. Maisel

Denver Research Institute
University Park
Denver, Colorado 80210
Attn: Library

DISTRIBUTION LIST
(Continued)

Douglas Aircraft Company MFSD
3000 Ocean Park Boulevard
Santa Monica, California 90406
Attn: Library

Fansteel Metallurgical Corporation
Number One Tantalum Place
North Chicago, Illinois 60064
Attn: Library

Ford Motor Company
Materials Development Dept.
20000 Rotunda Drive
P. O. Box 2053
Dearborn, Michigan 48123
Attn: Mr. Y. P. Telang

Firth Sterling, Inc.
Powder Metals Research
P. O. Box 71
Pittsburgh, Pennsylvania 15230
Attn: Library

General Electric Company
Advanced Technology Laboratory
Schenedtady, New York 12305
Attn: Library

General Electric Company
Materials Development Lab. Oper.
Advance Engine and Tech. Dept.
Cincinnati, Ohio 45215
Attn: Mr. L. P. Jahnke

General Motors Corporation
Allison Division
Indianapolis, Indiana 46206
Attn: Mr. D. K. Hanink,
Materials Laboratory

General Technologies Corporation
708 North West Street
Alexandria, Virginia 22314
Attn: Library

E. I. DuPont de Nemours and Co., Inc.
Pigments Dept. Metal Products
Wilmington, Delaware 19898
Attn: Library

IIT Research Institute
Technology Center
Chicago, Illinois 60616
Attn: Mr. V. Hill

IIT Research Institute
Technology Center
Chicago, Illinois 60616
Attn: Library

Ilikon Corporation
Natick Industrial Center
Natick, Massachusetts
Attn: Library

International Nickel Company
P. D. Merica Research Laboratory
Sterling Forest
Suffern, New York 10901
Attn: Library

Arthur D. Little, Inc.
20 Acorn Park
Cambridge, Massachusetts
Attn: Library

Lockheed Palo Alto Research Labs.
Materials and Science Lab. 52-30
3251 Hanover Street
Palo Alto, California 94304
Attn: Roger Perkins

DISTRIBUTION LIST
(Continued)

Lockheed Palo Alto Research Labs.
Materials and Science Lab. 52-30
3251 Hanover Street
Palo Alto, California 94304
Attn: Mr. E. C. Burke

Massachusetts Institute of Technology
Metallurgy Dept., RM-8-305
Cambridge, Massachusetts 02139
Attn: Library

Narmco Research & Development Div.
Whittaker Corporation
3540 Aero Court
San Diego, California 92123
Attn: Library

AFML (MAMP)
Wright-Patterson AFB, Ohio 45433
Attn: Mr. N. Geyer

Bureau of Naval Weapons
Department of the Navy
Washington, D. C. 20525
Attn: Mr. I. Machlin

Alloy Surfaces, Inc.
100 South Justison Street
Wilmington, Delaware 19899
Attn: Mr. George H. Cook

Battelle Memorial Institute
505 King Avenue
Columbus, Ohio 43201
Attn: Mr. E. Bartlett

City College of New York
Department of Chemical Engineering
New York, New York 10031
Attn: Mr. R. A. Graff

City College of New York
Department of Chemical Engineering
New York, New York 10031
Attn: Mr. M. Kolodney

E. I. DuPont de Nemours and Company
1007 Market Street
Wilmington, Delaware 19898
Attn: Dr. Warren I. Pollack

General Electric Company
Materials Development Lab. Oper.
Advance Engine and Tech. Dept.
Cincinnati, Ohio 45215
Attn: Mr. M. Levinstein

General Electric Company
Materials Development Lab. Oper.
Advance Engine and Tech. Dept.
Cincinnati, Ohio 45215
Attn: Mr. J. W. Clark

Howmet Corporation
Misco Division
One Misco Drive
Whitehall, Michigan 49461
Attn: Mr. S. Wolosin

Pratt & Whitney
Division of United Aircraft Corp.
Manufacture Engineering
Aircraft Road
Middletown, Connecticut 06457
Attn: Mr. Frank Talboom

Sylvania Electric Products
Sylcor Division
Cantiague Road
Hicksville L. I., New York 11802
Attn: Mr. L. Sama

DISTRIBUTION LIST
(Continued)

Texas Instruments, Inc.
Materials and Controls Division
P. O. Box 5474
Dallas, Texas 75222
Attn: Mr. Gene Wakefield

U.S.A.F.
San Antonio Air Material Area
Kelley Air Force Base, Texas 78241
Attn: SANEPJ/A. E. Wright, Chief
Jet Engine Section

University of Dayton
Research Institute
300 College Park Avenue
Dayton, Ohio 45409
Attn: Library

University of Illinois
Department of Ceramic Engineering
Urbana, Illinois 61801
Attn: Mr. J. Wurst

Nuclear Materials Company
West Concord, Massachusetts 01781
Attn: Library

Ohio State University
Columbus, Ohio 43210
Attn: Library

Rensselaer Polytechnic Institute
Troy, New York 12180
Attn: Library

Sherritt Gordon Mines, Ltd.
Research and Development Div.
Fort Saskatchewan, Alberta, Canada
Attn: Library

Spartan Aviation, Inc.
Aviation Services Division
P. O. Box 51239
Dawson Station
Tulsa, Oklahoma 07052
Attn: Mr. M. Ortner

Stanford Research Institute
Menlo Park, California
Attn: Library (Technical)

Stanford University
Palo Alto, California 94305
Attn: Library

Union Carbide Corporation
Stellite Division
Technology Department
Kokomo, Indiana 46901
Attn: Library (Technical)

United Aircraft Corporation
400 Main Street
East Hartford, Connecticut 06108
Attn: Research Library

United Aircraft Corporation
400 Main Street
East Hartford, Connecticut 06108
Attn: E. F. Bradley, Chief
Materials Engineering

United Aircraft Corporation
Prate and Whitney Division
West Palm Beach, Florida 33402
Attn: Library

Universal-Cyclops Steel Corporation
Bridgeville, Pennsylvania 15017
Attn: Library

DISTRIBUTION LIST
(Continued)

Wah Chang Corporation
Albany, Oregon 97321
Attn: Library

University of Pittsburgh
Center for Study of Thermodynamic
Properties of Materials
409 Engineering Hall
Pittsburgh, Pennsylvania 15213
Attn: Dr. G. R. Fitterer

University of Washington
Ceramics Department
Seattle, Washington 98101
Attn: Dr. J. Mueller

Westinghouse Electric Corporation
Research Laboratories
Beulah Road, Churchill Buro.
Pittsburgh, Pennsylvania 15235
Attn: Mr. R. Grekila

Whitfield Laboratories
P. O. Box 287
Bethel, Connecticut 06801